FACULDADE DE ENGENHARIA DA UNIVERSIDADE DO PORTO

Protocol of Communications for VORSat Satellite

Carlos Jorge Rodrigues Capela

Master Degree in Electrical Engineering
Major in Telecommunications

Supervisor: Sérgio Reis Cunha (PhD)

September 2012

U.PORTO

FEUP FACULDADE DE ENGENHARIA UNIVERSIDADE DO PORTO

MIEEC - MESTRADO INTEGRADO EM ENGENHARIA ELETROTÉCNICA E DE COMPUTADORES 2011/2012

A Dissertação intitulada

"Protocol of Communications for VORSat Satellite"

foi aprovada em provas realizadas em 11-10-2012

o júri

Presidente Professor Doutor Henrique Manuel de Castro Faria Salgado
Professor Associado do Departamento de Engenharia Eletrotécnica e de Computadores da Faculdade de Engenharia da Universidade do Porto

Professor Doutor Armando Carlos Domingues Rocha
Professor Auxiliar do Departamento de Eletrónica, Telecomunicações e Informática da Universidade de Aveiro

Professor Doutor Sérgio Reis Cunha
Professor Auxiliar do Departamento de Engenharia Eletrotécnica e de Computadores da Faculdade de Engenharia da Universidade do Porto

O autor declara que a presente dissertação (ou relatório de projeto) é da sua exclusiva autoria e foi escrita sem qualquer apoio externo não explicitamente autorizado. Os resultados, ideias, parágrafos, ou outros extratos tomados de ou inspirados em trabalhos de outros autores, e demais referências bibliográficas usadas, são corretamente citados.

Autor - Carlos Jorge Rodrigues Capela

Faculdade de Engenharia da Universidade do Porto

Resumo

A exploração espacial é uma área de investigação cada vez mais vasta. Desde a exploração do espaço profundo até às proximidades da Terra, a ciência não para de evoluir.

O desenvolvimento de satélites, independentemente da base para o que são construídos, é um meio muito usado para atingir este fim.

O caso particular dos CubeSats insere-se na política de abrir as portas da exploração espacial à investigação feita também nas universidades de todo o mundo. Assim, o projeto VORSat nasceu a partir de alguma experiência trazida de um grupo de professores e alunos de outro projeto anterior, o STRAPLEX (Stratospheric Platform Experiment), e da vontade de continuar o trabalho nesta área. O projeto evoluiu, mas o fundamento mantém-se.

Esta dissertação encerra em si a complexidade de um projeto que abarca várias áreas. A definição do protocolo de comunicações do VORSat é o grande objetivo, mas isso obriga a que várias metas sejam estabelecidas. Uma dessas metas é procurar determinar a atitude de um satélite em órbita, usando para isso o sinal enviado pelas suas antenas. Normalmente, os satélites possuem dispositivos que permitem controlar a sua atitude, mas neste caso isso existe apenas parcialmente, e para efeitos de controlo do efeito de arrasto, pelo que a determinação da atitude do VORSat se reveste de especial importância. Primeiramente, pensou-se usar a diferença de fase dos seus sinais na receção, e o recurso a sequências de bits pseudoaleatórias foi a solução final implementada neste trabalho.

A definição da estrutura da mensagem e dos dados a enviar decorre da definição do esquema de transmissão, e é um dos objetivos a atingir. Outros objetivos, passíveis de serem testados dentro do tempo de realização desta dissertação, incluem garantir que a transmissão é possível no pior caso possível e, como já foi referido, mostrar que é possível determinar a rotação do VORSat recorrendo a sequências pseudoaleatórias.

Abstract

Space exploration is an area of research increasingly vast. Since the exploration of deep space to the vicinity of Earth, science is constantly evolving.

The development of satellites, regardless of the basis for what they are built, is a much used means to reach this end.

The particular case of CubeSats is part of the policy of opening the doors of space exploration also to the research in universities worldwide. Thus, VORSat project was born from the experience brought by a group of teachers and students from other previous project, STRAPLEX (Stratospheric Platform Experiment), and from the will to continue to work in this area. The project evolved, but its foundation remains.

This dissertation contains within itself the complexity of a project that spans several areas. The definition of the protocol of communications of VORSat is the ultimate goal, but it requires the establishment of multiple targets. One of these goals is to try to achieve attitude determination of a satellite in orbit, using the signals sent by their antennae. Typically, satellites have devices that allow for attitude control, but in this case it exists only partially, for effects of drag control, whereat attitude determination of VORSat is very important. Firstly it was thought to use the phase difference at the reception of its signals, and the use of pseudorandom bit sequences have been the final solution to implement.

The definition of the message structure and outgoing data flows from the definition of the transmission scheme, and is one of the objectives to be achieved. Other milestones, which can be tested in time of accomplishment of this dissertation, include ensuring that the transmission is possible in the worst case scenario and, as already mentioned, to show that it is possible to determine the rotation of VORSat using pseudorandom bit sequences.

Acknowledgements

First of all, I must thank Prof. Sérgio Cunha for all his unmatchable support not only during this dissertation, but also in the final years of my course. It is a privilege for me to have his friendship and to learn from him. For all his efforts with me, I know that in my professional life I'll prove it was worth it.

I must also thank my parents for all their patience and for the love and trust they keep giving me. I'll prove that everything was worth it.

To my co-worker Serafim Ferreira, I thank all the good moments we've had in the last few years. Fighting for making dreams come true is worth it.

For all of my friends, colleagues and family that directly or indirectly have contributed to my work during this dissertation I extend my sincere thanks.

I could never write this page without a special word to Nádia Moreira. They say love and belief makes you stronger. All words seem short to me to describe how much I have to thank you for my strength. We are worth it.

Finally, I reserve some lines to myself. For the simple meaning that the writing of this page has to me and for all the reasons that lie in my heart, I thank myself for being here. I know I'm worth it.

Carlos Jorge Rodrigues Capela

“The heavens revolve over you showing you their eternal glory,
but your eyes merely stare at the ground.”

Dante

Table of Contents

1. Introduction 1
1.1 – Objectives 1
1.2 – VORSat Project 2
1.2.1 – CubeSat concept 2
1.2.2 – Project structure 2
1.2.3 – Mission 3
1.3 – Structure 8
2. State of the Art and Theoretical Background 11
2.1 – Satellites 11
2.1.1 – History 11
2.1.2 – Orbits 12
2.2 – CubeSat Missions 16
2.2.1 – Protocols and communication procedures 17
2.3 – Inter-Satellite Links 19
2.4 – Satellite Communication Losses 21
2.5 – Definition of Spread Spectrum 29
2.5.1 – Frequency Hopping vs. Direct Sequence 30
2.5.2 – Basic features of DSSS 31
2.6 – Pseudo Noise Sequences 32
2.7 – Two-Line Elements 36
2.8 – Time Difference of Arrival Antennas 37
2.9 – Ongoing Studies on Attitude Measurement 38
2.10 – Summary 38
3. Attitude Determination 41
3.1 – Transmission Scheme 41
3.2 – Sequences and Basic Features 42
3.3 – Modulation 46
3.4 – Peak Definition 47
3.5 – Synchronism 52
3.6 – System Noise 53
3.7 – Link Budget 55
3.8 – Summary 60
4. Message Definition 61

4.1 – TLE 61
4.2 – Frame Structure 62
4.3 – Word Structure 66
4.4 – Code Correction Techniques 67
4.5 – Link Budget for Encoding 67
4.6 – Summary 71
5. Tests and Results 73
5.1 – Equipment and Setup 73
5.2 – Procedures 75
5.3 – Conclusions 84
5.4 – Summary 85
6. Conclusions 87
6.1 – Summary of the Performed Work 87
6.2 – Accomplishments 88
6.3 – Future Work 88
References 91

List of Figures

Figure 1.1 – VOR Principle. 4
Figure 1.2 – Measurement of the 3 Angles of Attitude as in the Primary Idea. 5
Figure 1.3 – New Layout of VORSat. 6
Figure 1.4 – Capsule Position Inside VORSat, according to the Primary Idea. Courtesy of João Gomes. 7
Figure 1.5 – Capsule Position Inside VORSat, according to the New Constraints. 7
Figure 1.6 – De-orbiting Process. 8
Figure 2.1 – Different orbits. From left to right: GEO, HEO, MEO and LEO. 13
Figure 2.2 – GEO Satellite Footprint and Trajectory (Eutelsat W3A). 13
Figure 2.3 – HEO Satellites Footprints and Trajectories (Molniya 1-86 and 3-45). 14
Figure 2.4 – MEO Satellite Footprint and Trajectory (Globalstar m019). 14
Figure 2.5 – LEO Satellite Footprint and Trajectory (CanX-1 CubeSat). 15
Figure 2.6 – Orbital Altitudes. 15
Figure 2.7 – Inter-Satellite Link: GEO – LEO in the left and LEO – LEO in the right. 19
Figure 2.8 – GEO – LEO ISL Lead-Ahead Angle. 20
Figure 2.9 – Ionospheric scintillation fading depth. 24
Figure 2.10 – Attenuation vs. Frequency. 25
Figure 2.11 – Galaxy noise influence in noise temperature. 27
Figure 2.12 – Noise temperature variation with frequency. 28
Figure 2.13 – Dates and duration of eclipses. 29
Figure 2.14 – Frequency Hopping modulator scheme. 30
Figure 2.15 – Direct Sequence modulator scheme. 31
Figure 2.16 – Reception scheme for recovery of original data. 32
Figure 2.17 – Autocorrelation of an m-sequence. 33
Figure 2.18 – A TDOA antenna. 37
Figure 3.1 – M-sequence-1 (u) and m-sequence-2 (v). 43
Figure 3.2 – Crosscorrelation of sequences *u* and *v*. 44
Figure 3.3 – Modulation Scheme. 47
Figure 3.4 – Crosscorrelation between *uu* and *vv*. 48
Figure 3.5 – Peak 1. 50
Figure 3.6 – Peak 2. 50
Figure 3.7 – Peak 3. 50
Figure 3.8 – Peak 1 with Tukey Window. 51

Figure 3.9 – Peak 2 with Tukey Window. 51
Figure 3.10 – Peak 3 with Tukey Window. 52
Figure 3.11 – One face of VORSat, with the determination process of $\Delta\Phi_V$ and $\Delta\Phi_H$. 53
Figure 3.12 – Reception scheme of GS at FEUP. 54
Figure 3.13 – Variation of the distance VORSat – GS with the elevation angle. 56
Figure 3.14 – Variation of the Lfs with the distance, considering f = 2.45 GHz. 57
Figure 3.15 – Variation of the attenuation with the variation of the elevation angle of the satellite. 58
Figure 4.1 – Frame Sequence. 63
Figure 4.2 – Structure of Frames 1 to 3. 63
Figure 4.3 – Structure of Frame 4. 64
Figure 4.4 – Clock drift. 64
Figure 4.5 – Structure of the Data Word. 66
Figure 4.6 – Structure of Telemetry Word. 66
Figure 4.7 – Structure of Handover Word. 67
Figure 5.1 – Experiment Setup. 74
Figure 5.2 – Tx Antennas Setup. 74
Figure 5.3 – Antennas are distanced 9 cm from each other. 74
Figure 5.4 – Test for I/Q phases in I/Q Modulator 1. 75
Figure 5.5 – Test for I/Q phases in I/Q Modulator 2. 76
Figure 5.6 – QPSK in the received signal. 76
Figure 5.7 – Spectrogram of the first test. 77
Figure 5.8 – Time in each face is visited. 77
Figure 5.9 – Transmission of 1 sec, with 48 000 samples. 78
Figure 5.10 – Transmission of 3 antennas. 78
Figure 5.11 – Peak definition. 79
Figure 5.12 – Rotation of the antennas. 79
Figure 5.13 – Interpolation of data during rotation. 80
Figure 5.14 – Transmission for 500 km. 81
Figure 5.15 – Peak Definition at 500 km. 81
Figure 5.16 – Transmission for 1 500 km. 82
Figure 5.17 – Peak Definition at 1 500 km. 83
Figure 5.18 – Frequency Spectrum at the Reception. 83

List of Tables

Table 2.1 – Orbit Characteristics. 16
Table 2.2 – Summary of CubeSat transmitters (1). 17
Table 2.3 – Summary of CubeSat transmitters (2). 18
Table 2.4 – Frequency Bands / Wavelengths for ISL. 21
Table 2.5 – Major losses in satellite communications. 22
Table 2.6 – Polarization losses for different polarizations in antennas. 27
Table 2.7 – Number of subsequences of a given length in each m-sequence. 33
Table 2.8 – TLE Format. 36
Table 3.1 – Characteristics of the solution to implement. 45
Table 3.2 – Number of Information Bits available depending on each modulation and the number of chip delays used, with face decoding. 46
Table 3.3 – Number of Information Bits available depending on each modulation and the number of chip delays used, without face decoding, with 3 PRBS and 2 PRBS for information transmission in the left and in the right respectively. Marked in grey it is the final solution. 47
Table 3.4 – Phase shifts of the signal to be transmitted in the new base for each antenna. 49
Table 3.5 – Phase shifts of the signal to be transmitted with the generic message “1231231”. . 49
Table 3.6 – Calculation of EIRP. 56
Table 3.7 – Calculation of the propagation loss. 59
Table 3.8 – Calculation of reception antenna gain. 59
Table 3.9 – Calculation of the system noise temperature. 60
Table 4.1 – Coding of characters to be sent. 62
Table 4.2 – Orbital Elements and Number of Bits necessary to their transmission. 62
Table 4.3 – Calculation of P_r/N_0 68
Table 5.1 – Phase Differences in I/Q Modulators 1 and 2. 75
Table 5.2 – Error and standard deviation for the several time intervals of the test of rotation of antennas. 80

Acronyms and Abbreviations

ASK – Amplitude Shift Keying
AFSK – Audio Frequency Shift Keying
BER – Bit Error Ratio
BPSK – Binary Phase Shift Keying
CDMA – Code Division Multiple Access
CNR – Code to Noise Ratio
CW – Continuous Wave
DOF – Degrees of Freedom
DS – Direct Sequence
DSSS – Direct Sequence Spread Spectrum
EIRP – Equivalent Isotropic Radiated Power
ERC – Earth Re-entry Capsule
ESA – European Space Agency
FEC – Forward Error Correction
FEUP – Faculty of Engineering of University of Porto
FFH – Fast Frequency Hopping
FH – Frequency Hopping
FHSS – Frequency Hopping Spread Spectrum
FM – Frequency Modulation
FSK – Frequency Shift Keying
GEO – Geosynchronous Earth Orbit
GNSS – Global Navigation Satellite System
GPS – Global Positioning System
GS – Ground Station
HEO – Highly Elliptical Earth Orbit
HOW – Handover Word
HOW_ref – Handover Word of reference
HPA – High Power Amplifier
HWN – Half Week Number
HWN_ref – Half Week Number of reference
IoDC – Issue of Data, Clock
IoDE – Issue of Data, Ephemeris

IOL – Inter-Orbital Link
ISL – Inter-Satellite Link
ISM – Industrial, Scientific and Medical
ISS – International Space Station
ITU-R – International Telecommunication Union – Recommendation Sector
LEO – Low Earth Orbit
LFSR – Linear Feedback Shift Register
LHCP – Left Hand Circular Polarization
LPF – Low Pass Filter
MEO – Medium Earth Orbit
NASA – National Aeronautics and Space Administration
NORAD – North American Aerospace Defense Command
P-POD – Poly-Picosatellite Orbital Deployer
PG – Processing Gain
PN – Pseudo Random Noise Code
PRBS – Pseudo Random Bit Sequence
PSD – Power Spectral Density
PSK – Phase Shift Keying
QPSK – Quadrature Phase Shift Keying
RF – Radio Frequency
RFL – Receiver Feeder Losses
RHCP – Right Hand Circular Polarization
SDR – Software Defined Radio
SF – Spreading Factor
SFH – Slow Frequency Hopping
SIS – Signal in Space
SNR – Signal to Noise Ratio
SS – Spread Spectrum
SSETI – Student Space Exploration and Technology Initiative
TLE – Two-Line Elements
TLM – Telemetry Word
TNC – Terminal Node Controller
TOW – Time of Week
UHF – Ultra High Frequency
USB – Upper Side Band
USSR – Union of Soviet Socialist Republics
USA – United States of America
UTC – Coordinated Universal Time
VHF – Very High Frequency
VKI – Von Karman Institute
VOR – VHF Omni Directional Radio Range
VORSat – VHF Omni Directional Radio Range Satellite
WN – Week Number
XOR – Exclusive Or
XPD – Cross Polarization Discrimination

Chapter 1

Introduction

Satellites are unavoidably part of our world since their value was understood some decades ago.

From communication satellites to education oriented ones, passing by satellites with military purposes or scientific studies, they form a major area of development and society growth. Several tests have been made in space in search for new technologies that not only allow mankind to explore outer space but also to understand better our world and consequently improve our quality of life.

1.1 – Objectives

All the work behind this dissertation aims to demonstrate the theoretical and practical viability to measure attitude of a satellite from the ground and to elaborate the protocol of communications of VORSat.

The signals will be transmitted in Radio Frequency (RF) band from multiple antennas forming a RF front end with a carrier frequency of 2.45 GHz. The transmitted signals from each antenna will be multiplied by Pseudo Random Bit Sequences (PRBS) with given properties of length, autocorrelation and crosscorrelation and will be sent in Spread Spectrum.

Transmitted signal will be composed by synchronism, attitude and data sequences, which also must allow transmission of satellite telemetry.

Signal will be received by a radio that is able to decode Upper Side Band (USB) and by an audio card, what makes that the bandwidth of baseband is 20 kHz at the most.

VORSat attitude determination in space and its tumbling rate will be accomplished by computing the phase shift of the received signal. It has great importance to assure the reception of the signal even in the worst case scenario, in lower elevation angles and in greater distances, so that time of reception of VORSat signals can be maximized.

This will imply a profound study of each PRBS to use because a bad lead up may have severe consequences on the quality of the attained results.

The project of the whole protocol of communications includes the project of the frame structure of the signals to be sent by VORSat. That's why a good study of the Two-Line Elements (TLE) has to be done, in order to be as efficient as possible in message codification.

The calculation of the link budget of any satellite is unavoidable and it is also one of the objectives of this work.

1.2 – VORSat Project

This dissertation is focused in VORSat project, an ongoing project of the Faculty of Engineering of the University of Porto (FEUP), in a partnership with the European Space Agency (ESA).

It is impossible to refer to VORSat separately because it is part of a greater project. Also, the full comprehension of its educational purposes will only be achieved if it is previously mentioned how CubeSats were born.

1.2.1 – CubeSat concept

The CubeSat concept was born in the late 20th century, in the USA universities California Polytechnic State University (Cal Poly) and Stanford University. Bob Twiggs and Jordi Puig-Suari were the forerunners of this new idea for satellite technology. Initially devoted for academic exploration, soon companies started to develop their own CubeSats to exploit the huge scope of study for the technological progress that these satellites possess.

CubeSats are included in the category of picosatellites. Initially they were cubes with 10 x 10 x 10 cm (1U), weighing no more than 1 kg. Some changes in the specifications have been made in order to fulfill other needs, and now the weight can go up to 1.33 kg. What remain unchanged are the basic dimensions of the cube. They must be 10 x 10 cm regardless of its length, which can be 20 cm (2U) or 30 cm (3U). They are carried into space in a Poly-Picosatellite Orbital Deployer (P-POD) which is developed also by Cal Poly that, depending on CubeSats dimensions, can carry up to 3 satellites. P-POD travels on board of a launch vehicle that orders the deployment of the cubes [1].

The technologies applied in standard satellites may also be applied in CubeSats. It provides uplink/downlink communications and attitude control and/or determination in a self-powered spacecraft within its own limits, obviously. Other functions may be implemented in each satellite, varying with each project's purpose, never forgetting the lack of space these satellites have.

Despite all these setbacks and the harsh restrictions CubeSat designers face during the development of each cube, this side of aerospace industry is in a visible growth.

1.2.2 – Project structure

This is not an isolated project. On the contrary, it is embedded in a much larger program with a few other entities. Altogether, they allow the birth and development of VORSat.

Once a single CubeSat is too small to transport as much sensors as required for relevant scientific research, the combination of several CubeSats operating in network and carrying the same payload allows the achievement of the main goal. This kind of network is an old issue that

has received the attention of companies and space agencies along the time, but only recently it has been proved feasible.

Therefore, in order to study in situ the characteristics of the lower thermosphere, the least explored layer of the atmosphere, which ranges from 90 km to 320 km, Von Karman Institute (VKI), ESA and National Aeronautics and Space Administration (NASA) took the initiative to give birth the QB50 Project. In this network, 50 CubeSats will be separated for a few hundred kilometres and will communicate with each other in order to measure predefined parameters, for the analysis of the re-entry process. Due to high costs of other kinds of satellites, it is not even a hypothesis to use other equipment than CubeSats for this study. Even if some cubes fail, this mission can be entirely successful.

One essential requirement QB50 respects is the lifetime of space debris. CubeSats have 3 months maximum and the international rules point out 25 years as the limit. This mission is being prepared to launch 50 CubeSats in the middle of 2013, in Murmansk, Northern Russia, at an orbit of 320 km and an inclination of 79º. The ceiling of 320 km is related to the altitude of the International Space Station (ISS). Many CubeSats launched above the ISS could endanger the space station due to the altitude decay of the cubes [2].

A partnership has been established with Tekever, a Portuguese firm which is entering also in space programs. Main goals are to use Software Defined Radio (SDR) to establish Inter-Satellite Links (ISL) with other satellites, in order to calculate the differential evolution of atmospheric drag between CubeSats. This will be achieved by considering an ad-hoc network of CubeSats where each one is a node. Satellites must be capable to calculate the distance between them and determine each other's attitude. These features are going to be implemented in parallel to the VORSat features as well.

This partnership with Tekever gave birth to GAMA-Sat and to a Brazilian Satellite, 14BISat. These satellites will carry similar payload and will be linked in space. GAMA-Sat team will design and develop an innovator CubeSat transceiver module based on SDR technology, which will perform communications and navigation by Global Navigation Satellite System (GNSS). This module is going to be at the same time a telecommunications transceiver and a GNSS receiver and it will support several applications [3]:

1. VHF, S-band and GNSS waveforms in a single hardware platform;
2. Inter-satellite ad-hoc networking capabilities, transforming each cube in a node of that network;
3. GNSS, in order to receive both GPS and Galileo Signal in Space (SIS);
4. Range and attitude determination through VOR principle (VORSat).

Once the initial goals of the VORSat project remain untouched, in this text the only designation used is, precisely, VORSat. Some dissertations have also been developed under this project, each of them with its own milestones to achieve.

1.2.3 – Mission

This mission has as primary objective proving the feasibility of measuring the satellite attitude from the ground based on a set of RF signals transmitted from orbit. The original idea is to combine multiple signals and antennas, so that given modulated information, encoded as signal phases, depends on the direction from which the signals are received. This will allow the

determination of satellite attitude with just one degree of expected accuracy. This approach is similar to the VOR principle, as will be seen later.

The second objective lies on controlled de-orbiting and re-entry for later retrieval of an inner capsule the satellite is going to carry in it. In order to do so, controlled de-orbiting is necessary, the exact point for capsule release must be determined and the study of atmospheric drag is being carried out.

Both these objectives will be explained with more detail later on during this text. Although, once this dissertation is focused especially on the first one, more emphasis will be given to VORSat attitude rather than its re-entry.

During its lifetime, satellite signals will be received at the Ground Station (GS) placed in FEUP. The GS characteristics are quite enough for this purpose:

1. 2 Degrees of Freedom (DOF) and 3 m parabolic dish with 2.45 GHz horizontal and vertical feeds;
2. LNA (Low Noise Amplifier);
3. Down-converter;
4. Computer with a sound card running the software to demodulate the signals.
5. Yagi antennas (1.2 GHz, 433 MHz, 145 MHz) with circular polarization;
6. 400º azimuth rotation and 100º elevation;
7. 0.5º accuracy.

VORSat is being designed with simplicity and testability prior to launch as major cornerstones. It is an objective to build it free of required actions before or during its launch.

The acronym VOR, as in VORSat, means VHF Omnidirectional Radio Range. It is a radio navigation system used in aviation for the exact determination of the position of an aircraft. Its modus operandi is easy to understand (figure 1.1). A VOR GS broadcasts a radio signal in VHF band (30 – 300 MHz), composed by the station identifier in Morse code and by the navigation signal, which will enable the receiver aircraft to know the direction from the GS in relation to the Earth's magnetic north. Voice is also possible if allowed by the equipment. VOR GS in areas where magnetic compass are not reliable are oriented to the true north. This line of position is the radial from the VOR. The intersection of two radials from two GS provides the intended position.

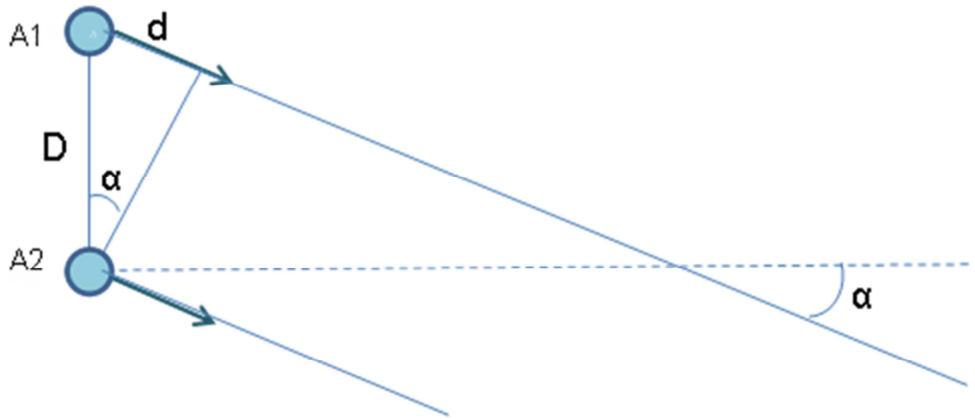

Figure 1.1 – VOR Principle.

Without diving in usual VOR technical details, the same principle is to be applied in VORSat. In this case, the satellite will be tumbling in its orbit at nearly 300 km from the Earth, emitting signals in all directions. Knowing its position relatively to the GS will enable the computation of its attitude, after the determination of the radial. VOR uses only one signal in this calculation, but this specific case requires three signals, which won't be in VHF band, but in UHF (300 MHz – 3 GHz), specifically 2.45 GHz, an ISM (Industrial, Scientific and Medical) band. The superior frequency is due to the littleness of the satellite, using a free frequency for RF scientific purposes. It is also justified with the needs for quick phase measurements originated by the tumbling rate of VORSat.

The primary idea was to determine attitude using Radio Frequency (RF) signals emitted by three antennas per face, transmitting two at a time, in a frequency of 2.45 GHz and its operation behaviour was intended to be the following. Antenna A_1 transmits frequencies f_1 and f_2. A_2 transmits frequency f_3. Both antennas are separated from a distance D. The three frequencies represent three sinusoidal waves, observed by a distant point with a relative orientation to the antennas characterized by the angle α. Considering that:

- A_1, A_2 and A_3 → Antennas 1, 2 and 3 of each face (18 in total);
- Φ_1, Φ_2 and Φ_3 → Phases of the three frequencies as received at Ground Station (GS), in cycles;
- f_0 = 2.45 GHz.

Antennas 1 and 3 would transmit alternately, while A_2 transmits permanently. From GS, the phase difference between the pairs of antennas will be detected and calculated, according to:

$$\begin{cases} A_1 \begin{cases} f_1 = f_0 + \Delta f \\ f_2 = f_0 \end{cases} \\ A_2 \{ f_3 = f_0 - \Delta f \end{cases}$$

The phase difference between each pair of antennas provides two angles of attitude being the third one given by the change of the angle of sight (figure 1.2).

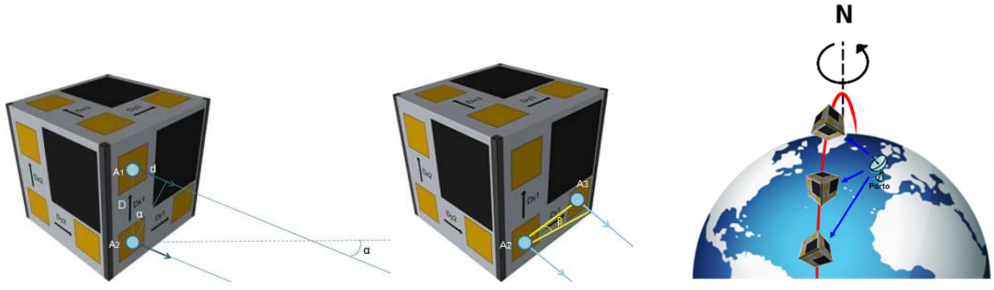

Figure 1.2 – Measurement of the 3 Angles of Attitude as in the Primary Idea.

The received signal would then suffer down-conversion to baseband and the angle α would be computed.

Meanwhile, although the attitude measurement remains as the primary objective not only of this project but also of this dissertation, the way to achieve it suffered some changes.

The transmission scheme has changed. They include attitude determination achieved by 12 antennas, placed 3 in each of the 4 faces along the major axes of VORSat. The fourth antenna of each of these 4 faces is destined for GPS. The other 2 faces are destined to ISL and other purposes. Also, the signals now will include a multiplication by a PRBS that will provoke the spreading of the signal by the entire available bandwidth, in the true meaning of Code Division Multiple Access (CDMA). In the reception, the original signal will take the place of the spread signal due to a new multiplication by the same PRBS. It will be possible to calculate then the phase shift of each signal and therefore VORSat attitude.

The attitude will be determined according to the expression

$$\theta = arcsin\left(\frac{\lambda.\Delta\phi}{D.2\pi}\right)$$

where θ is the attitude angle, ϕ represents the effective movement of rotation of antennas and D the distance they are apart from each other.

Figure 1.2 shows VORSat as it was planned in first hand. It was a 1U satellite, according to the specifications of Cal Poly. The project's evolution dictated that the two satellites to be sent will be 2U and 3U, where VORSat is the 3U. Also, the display of the antennas and the solar panels suffered obvious modifications, as figure 1.3 illustrates.

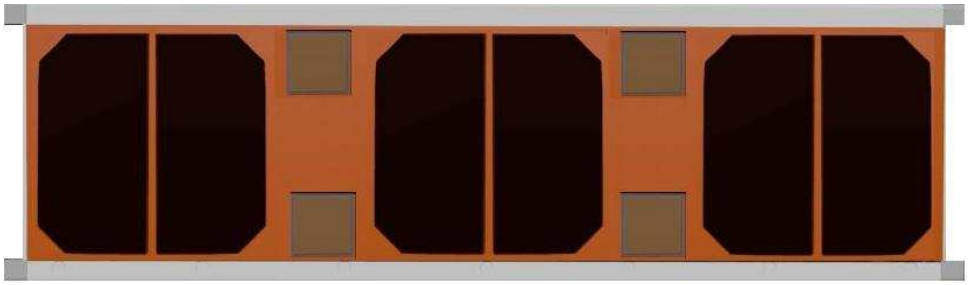

Figure 1.3 – New Layout of VORSat.

The new constraints and requirements of this project include the insertion of partial attitude control. The need to establish ISL between both satellites involved in this project forces attitude control over one of the axes so that the faces with smaller dimensions (or the tops of the prism, if one considers 2U and 3U satellites as prisms) may become permanently aligned with an error not exceeding 5º.

The second major objective lies on the re-entry. VORSat will orbit Earth in a Low Earth Orbit (LEO), which corresponds to approximately 300 km of altitude. It has a predicted lifetime of about one or two months, time that marks the onset of the de-orbiting process. It will carry an Earth Re-entry Capsule (ERC) that is going to be released in an advanced phase of de-orbiting. The capsule will be built in a robust material (Carbon Fiber Reinforced Polymer), so it can resist to the several hard tests it's going to be exposed to after its release, such as air friction at very high speed and its predictable splashdown. Necessarily, it must be very small in order to fit inside VORSat (figure 1.4).

Figure 1.4 – Capsule Position Inside VORSat, according to the Primary Idea. Courtesy of João Gomes.

As figure 1.4 illustrates, the first idea was to perform drag control with the mechanical opening of the faces of VORSat. However, changes in the project and in the basic structure of the satellite force some modifications not only in the capsule position inside it (figure 1.5) but also in the adjustment of drag control. None of the faces will open to obtain drag control. It will be accomplished using attitude control in one of the axes by turning and causing some apparent wind that will allow the deceleration of the satellite.

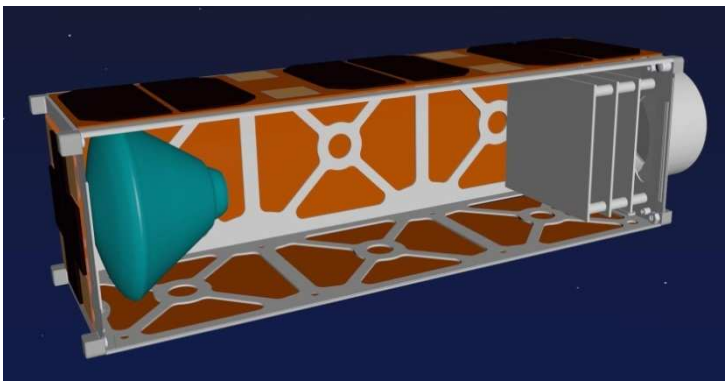

Figure 1.5 – Capsule Position Inside VORSat, according to the New Constraints.

For the de-orbiting process, three main goals are to be achieved:

1. Adjust drag coefficient regardless VORSat attitude;
2. Adjust drag using control loop with feedback from GPS;
3. Capsule release soon before significant deceleration (1/10 g).

This process can be described by figure 1.6, which relates variations of drag and atmosphere density with predicted number of orbits before the splashdown.

Spoilers act around 240 km, when gravity really starts to make effect in the satellite decay, and consequently in the number of orbits it takes. Below 120 km it is impossible to attain control over the capsule, due to its high speed and to the superior mesosphere density. After atmospheric re-entry it takes nearly ten minutes to the splashdown to happen. Calculations are being made so that it may occur in the North Atlantic Ocean.

Through a transmitter inserted in the capsule operating at 433 MHz using Argos system, which enables the geographic localization of any data source that operates at its required conditions, the capsule recovery becomes possible.

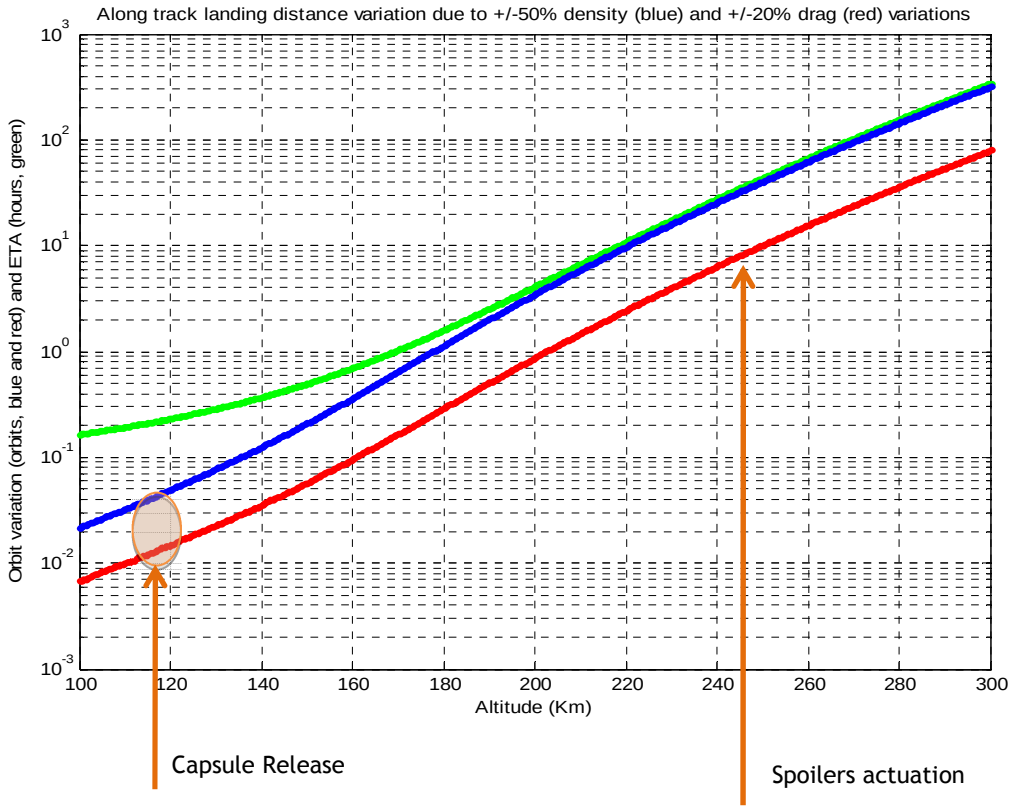

Figure 1.6 – De-orbiting Process.

1.3 – Structure

In this first chapter, the intention has been to provide the reader a general overview of the VORSat project as a whole, as well as introducing the objectives of this dissertation, without great technical details.

Chapter 2 has an introduction of all major issues that concern to the work to be done. After a brief description and comparison between the several kinds of orbits, a docket of the several CubeSat missions is presented. Afterwards, it is also shown a study of the major satellite communication losses that can harm the quality of transmission. It is also critical to provide a brief explanation of Spread Spectrum and PN sequences. This section ends with a brief overview of the TLE and Time Difference of Arrival (TDOA) antennas, and with a quite short view about the ongoing studies on attitude measurement.

Chapter 3 provides the explanation of how the transmission will be performed. Also, the chosen sequences for each satellite and their characteristics are described, as well as the way they help in the attitude determination. Afterwards, calculations for system noise and the link budget are presented.

Chapter 4 is dedicated to the data frame structure, in its composition and how the several fields fit in the frames. It is explained how error detection is thought to be and the link budget is completed.

In chapter 5 the results of the experiment are shown and analysed. They will provide some important conclusions about the feasibility of the proposed study.

Chapter 6 concludes this document with the author's view of the developed work. It is also discussed how significant are the results attained in the scope of the entire project, as well as the developments to be made.

Chapter 2

State of the Art and Theoretical Background

In this chapter the intention is to supply to the reader the basic necessary information for the full comprehension of this dissertation.

In order to do so, a brief introduction to satellite history is presented so that evolution of technologies may be better understood. Then, a detailed description of satellite orbits is conducted, because there are some features that can only be understood if one comprehends the specific case of LEO.

Then, a brief list of missions is shown, as well as a more detailed table with several characteristics that CubeSat missions have been using.

Even though the work this dissertation is aimed for does not include ISL, this project is. That is why it is made a prelude to this subject afterwards.

An exhaustive analysis to satellite communication losses is performed next, trying to mention all the important aspects.

Some considerations about Spread Spectrum are then given, oriented to the use of Direct Sequence, the technique that is going to be used in this project. The use of Direct Sequence Spread Spectrum forces an explanation about Pseudo Noise Sequences.

In this particular case, it is mandatory to provide also some theoretical background about the Two Line Elements and about TDOA antennas.

2.1 – Satellites

For a better embedding of the reader in this work, a brief description of history of satellites and a short description of its kinds of orbits are made next.

2.1.1 – History

Various sources attribute to Arthur C. Clarke, the author of "*2001: A Space Odyssey*", the credits for the original idea of a communication satellite orbiting the earth in a geosynchronous

orbit. In 1945, he made the quite correct assumption that a satellite in a circular equatorial orbit with a radius of 42 242 km would have the same angular velocity the Earth has, allowing the permanent coverage of more than a hemisphere. Thus, with only three satellites placed 120º apart from each other, the whole planet could be covered through relaying of signals. The idea had been born, but technology hadn't.

The first satellite to be placed in orbit was Sputnik 1, on October 4, 1957, built in the USSR, what put the United States behind, in the newborn space race. The following year, the answer came with the first relay equipment in space. U. S. Air Force launched SCORE (Signal Communicating by Orbiting Relay Equipment) in low elliptical orbit with a period of 101 min. It represented the first "bent pipe in the sky" satellite repeater, broadcasting a message of President Eisenhower, uplinked when passing over a ground station and transmitted at another station's request. It had even scarcer resources than today's spacecrafts, obviously. The message to transmit couldn't be longer than 4 minutes and it had to be transmitted through the only voice channel available. The alternative was seventy 60-words-per-minute teletype channels. The transmission power was 8 W maximum, and the uplink/downlink frequencies were 150/132MHz. The batteries lasted for 35 days.

However, only when Echo 1 and 2 were launched in 1960 people's interest arose, because they were visible to the naked eye. Although they showed some improvements in technology used, they kept being too demanding in other aspects such as power and antenna requirements. Both ends had 10 kW transmitters and antenna dishes with no less than 18 meters.

Telstar 1 and 2 were the first satellites with broadband real-time transponders. Their launch occurred in 1962 and 1963 and had a low orbit, as all satellites launched till then. They used FM (Frequency Modulation) analog signals in a 50 MHz bandwidth. Uplink/downlink frequencies were 6389.58/4169.72 MHz, the ancestor frequencies of C-Band (4/6 GHz).

As technologies evolved, companies and governments realized this was a quite lucrative business, with gigantic rooms for improvement. Digital modulation appeared in the form of PSK in the Syncom series. By that time, geosynchronous communications satellites allowed full duplex operation due to its transponder's ability to support two carriers at a time.

In 1965, the USA and Europe established protocols for frequent operations. The "Early Bird", as Intelsat 1, the first communication satellite, was formerly named, marked the beginning of a new era of satellite communications. It had two transponders with a 25 MHz bandwidth and operated in C-Band [4].

Since then, endless scientific advances were made and the know-how increased exponentially. Different types of modulation, frequency bands and communication protocols are used, depending on the functions each satellite has to fulfill. Although they are heavier and larger, they have much larger radio and power resources. Satellite usage is widespread due to its high reliability at a fairly low cost when compared to other communication systems and to its low transmission delays.

2.1.2 – Orbits

It wouldn't be possible to think about satellites without associating them to the various functions they may have. From military operations to simple TV broadcasts, from Earth observation to satellites with educational purposes, they all play an essential role today. Depending on the service to be implemented, several variables must be defined.

For instance, for television broadcasting service, geostationary orbits are required, so that costs can be minimized enhancing the quality of service, making a permanent coverage of the intended area. Examples of satellite systems that provide this service are Astra, Eutelsat and Intelsat. Mobile communications require a lower orbit, so, other satellite systems are used, like Iridium, Globalstar and Inmarsat, which offer a more adequate service.

Not only mobile communications and television broadcasting have special requirements. Satellites are used in other applications, such as military, business and civil services. They offer advantages, like access in remote areas and secure communications, as well as worldwide coverage. They also make it possible to control sea areas, where no other means of communication is possible.

Scientific oriented satellites include Earth observation, space exploration and education satellites. It is in this last category VORSat is included.

The purpose for which each satellite is intended affects its features and characteristics, mainly its orbit. There are 4 main kinds of orbit: GEO, HEO, MEO and LEO (figure 2.1).

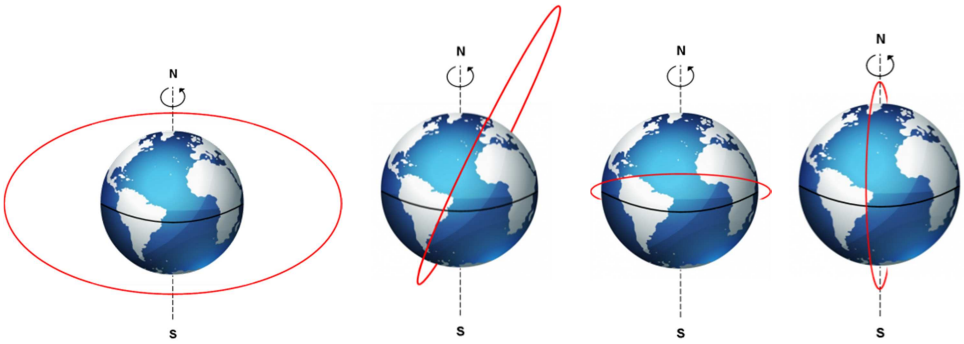

Figure 2.1 – Different orbits. From left to right: GEO, HEO, MEO and LEO.

Satellites in Geosynchronous Earth Orbit have always the same sub-satellite point over the Equator, with very light differences, corrected by mechanisms already incorporated in them (figure 2.2 [5]). Therefore, they don't need tracking or any constellation for local permanent coverage because their time of passage is virtually unlimited. Their period of revolution corresponds to the sidereal day, with 23 h 56 m 4.091 s.

Each satellite footprint has an area of about 1/3 or 1/2 of Earth surface, with some safety overlap between them, but not covering North and South poles. Because they are at an average altitude of 35 786 km, free space losses are high and propagation delay (Earth – satellite – Earth) is large, around 250 ms, yet the Doppler effect is hardly felt.

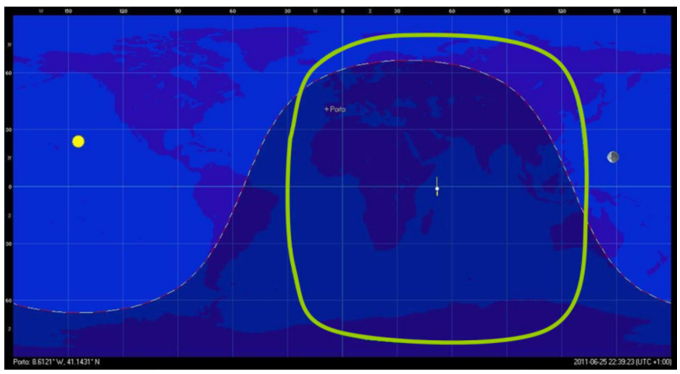

Figure 2.2 – GEO Satellite Footprint and Trajectory (Eutelsat W3A).

Highly Elliptical Orbits are used in pretty particular cases, mostly in countries of high latitudes, such as Russia, USA or Canada. Since this orbit is characterized for a great difference between perigee (~1 000 km) and apogee (~39 000 km), satellites using it suffer long dwell times over the same spot, according to Kepler's Law. Obviously, by the same law they pass over other spots at very high speeds, what causes huge differences in propagation delays (nearly 150 ms in the best case, but possibly extending until 300 ms) and also very strong Doppler effect. Unavoidably, it causes great free space losses. In order to achieve a permanent coverage over the same spot, three satellites are required. Each satellite covers from 1/3 to 1/2 of the Earth and has a time of passage of approximately 8 to 12 hours. Tracking is necessary but not complex. Molniya and Tundra orbits are the most notable cases of these elliptical orbits. Its inclination rounds the 63.4º. In figure 2.3 [5] it is possible to observe the differences between the footprint when a HEO satellite is close to the Earth (on the left) and when it is in half of its trajectory. If it were in the apogee, its highest peak, the footprint would focus almost entirely in the North Pole.

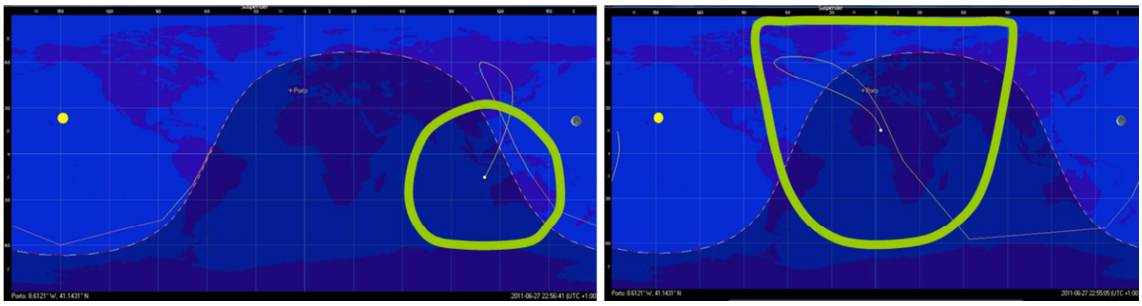

Figure 2.3 – HEO Satellites Footprints and Trajectories (Molniya 1-86 and 3-45).

Satellites operating in Medium Earth Orbit (figure 2.4 [5]) are able to provide full terrestrial coverage when they are part of a satellite system of not less than 10 satellites. Their time of passage over each spot rounds 2 h. Once their elevation at the reception point varies with its passage, Doppler effect is moderately felt, and propagation delays are not constant, oscillating between 70 ms when the satellite is near the zenith and 100 ms when it is closer to the horizon. This also provokes some free space losses. Tracking is mandatory, except when wide beam antennas are used. The period of revolution varies mostly between 6 h and 12 h at average altitudes of 10 400 km or 21 000 km, even though other orbits and altitudes are used.

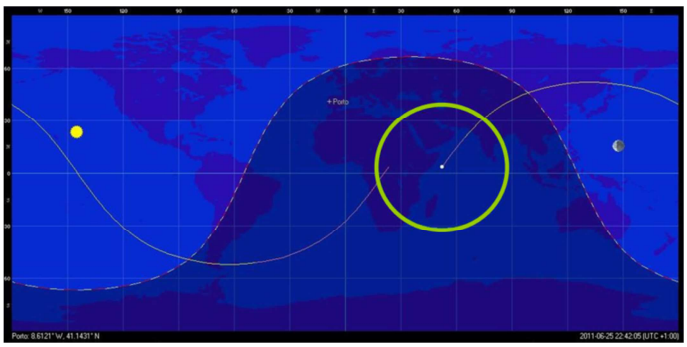

Figure 2.4 – MEO Satellite Footprint and Trajectory (Globalstar m019).

Low Earth Orbits are the specific case of this dissertation, for being the ones used by CubeSats. They are a very special case, because the majority of the satellites that use LEO have polar, or nearly polar, orbits. All latitudes are covered by each satellite in its very fast trajectory

of almost 8 000 ms^{-1}, but the time of passage over each point is not longer than 15 minutes, even less if the satellite is farther from the zenith. This implies a significant Doppler effect and great differences in elevation during the passage of the satellite. Permanent coverage is achieved with no less than 48 satellites, because the closer they are from Earth, smaller the footprint is (figure 2.5 [5]). Tracking is indispensable. Free space losses are very low, also due to the very slim propagation delay these communications suffer. Considering the particular case of a CubeSat orbiting Earth at less than 400 km, a round-trip transmission takes less than 5 ms and high data rates are allowed due to small transmission distance. The period of revolution of a CubeSat is approximately 90 min.

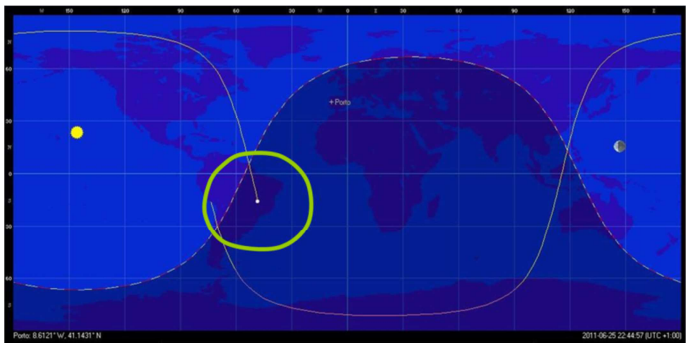

Figure 2.5 – LEO Satellite Footprint and Trajectory (CanX-1 CubeSat).

All kinds of orbit have different usages, according to the advantages they offer to the satellites and consequently to the communication needs they serve. Due to its lifetime lasting fixedness over the same spot, GEO has the great advantage to provide permanent local coverage with only one satellite, which supplies communications with very low Doppler effect. Polar regions are better covered with satellites using HEO, because in MEO and LEO the time of passage of each satellite is much reduced, although Doppler effect is worse. MEO are mostly used for navigation constellation satellites, like GPS, Glonass or Galileo, because, among many other factors, the relationship between Earth coverage and losses is quite acceptable. LEO presents many other advantages when compared to other types of orbit. In spite any satellite with a polar orbit may cover all latitudes, the quite reduced free space losses and the minimal propagation delays are the most prominent characteristics. These orbits are also much used for education satellites because there are much smaller costs in placing a satellite at a lower orbit than in a higher one. LEO for CubeSats is also optimal, because the CubeSat concept itself prevents the accumulation of space debris. Table 2.1 [6] summarizes the characteristics of each orbit.

Figure 2.6 allows a clear comparison of the different orbital altitudes.

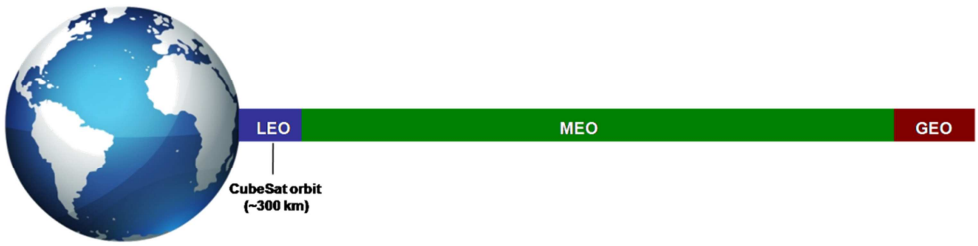

Figure 2.6 – Orbital Altitudes.

Table 2.1 – Orbit Characteristics.

CHARACTERISTICS	TYPE OF ORBIT			
	GEO	HEO	MEO	LEO
Earth Coverage (1 sat)	1/2 - 1/3 Earth (poles not covered)	1/2 - 1/3 Earth	global	global
Time of Passage (1 sat)	unlimited	~ 8 h	~ 2 h	< 15 min
Permanent Local Coverage	-	3 sat	> 10 sat	> 48 sat
Free Space Loss	high	high	average	low
Propagation Delay (round-trip time)	250 ms	150 - 300 ms	70 - 100 ms	< 5 ms (CubeSats) 10 - 25 ms (other)
Doppler Effect	very low	high	average	average
Satellite Elevation at Ground Station	high in the Equator	high in intermediate latitudes	variable with satellite's passage	variable with satellite's passage
Tracking	not necessary	necessary but not complex	mandatory	mandatory

2.2 – CubeSat Missions

CubeSat industry is developing because it has been proving to be profitable in the compromise between cost and final results. That's why companies and universities all over the world bet on it to take advantage of the new possibilities for scientific research. ESA and NASA already understand the paramount importance of CubeSats.

The launch attempts of CubeSats into space date back to 2003, when Eurorockot 2003 mission took place. However, it has been an unsuccessful launch. Meanwhile, other CubeSat launches have been made. Eurorockot 2003 was only succeeded in 2006. Since then, several other missions involving many CubeSats were carried out, with a good success rate. A list with some of the most important missions is presented next [7]:

1. SSETI Express 2005
2. M-V-8 2006
3. Eurorockot 2003
4. Falcon-1 Launch 3
5. DNEPR Launch 1
6. GeneSat-1
7. DNEPR Launch 2
8. TacSat-3
9. RAX and O/OREOS Minotaur IV
10. Taurus XL Launch

One must not forget the possibility of failure. As an example, it can be referred the particular case of the last mission. Taurus rocket carried a P-POD with three CubeSats built by universities of Colorado, Kentucky and Montana State, incorporated in NASA's first Education Launch of Nanosatellites. The attempt to put them in orbit took place in early March 2011 in California, but failure happened because the rocket failed to reach the proper altitude.

Other missions are planned. QB50 satellites will be launched in Vega Flight, scheduled for mid 2013 in French Guiana.

2.2.1 – Protocols and communication procedures

Since CubeSat era started, several different signal modulations and protocols have been used. Also, communications between space and Earth have been using different types of antennas. Generally speaking, each satellite designer has its own ideas and each purpose its own requirements. The following tables summarize most of CubeSats features and data launched until November 2008 [8]. Prior to its analysis, it's important to refer some important remarks:

- Mentioned frequencies only concern to downlink;
- The "Object" item refers to the spacecraft ID number at the NORAD database, available at [9];
- Baud-rate and data-rate may differ because they relate to symbols and bps, respectively;
- Downloaded data refer only to the amount of data received and downloaded by GS. They do not include beacon data due to its continuous transmission or protocol headers, or even forward error correction (FEC) bits;
- Lifetime defines the useful life of each spacecraft;
- Blank cells represent "information unknown".

As it possible to see in table 2.2, almost all CubeSats use amateur band frequencies around 437 MHz. Only two satellites use the frequency VORSat is being designed to, of 2.45 GHz. These spacecrafts need a superior power to operate, about 1 W or 2 W, and have their own communication protocol, unlike the majority of the others, which utilize AX.25 or CW.

Another fact the table provides is that a great share of the cubes present in the table use frequency modulations, like FSK and AFSK. Phase modulations like BPSK have been rarely used, in Delfi-C3 and CanX-2. The original idea is to apply BPSK or QPSK to VORSat communications.

Table 2.2 – Summary of CubeSat transmitters (1).

Satellite	Radio	Frequency	License	Power	Protocol	Baud Rate/Modulation
AAU1 CubeSat	Wood & Douglas SX450	437.475 MHz	amateur	500 mW	AX.25, Mobitex	9600 baud GMSK
DTUsat-1	RFMD RF2905	437.475 MHz	amateur	400 mW	AX.25	2400 baud FSK
CanX-1	Melexis	437.880 MHz	amateur	500 mW	Custom	1200 baud MSK
Cute-1	Maki Denki (Beacon)	436.8375 MHz	amateur	100 mW	CW	50 WPM
(CO-55)	Alinco DJ-C4 (Data)	437.470 MHz	amateur	350 mW	AX.25	1200 baud AFSK
QuakeSat-1	Tekk KS-960	436.675 MHz	amateur	2 W	AX.25[2]	9600 baud FSK
XI-IV	Nishi RF Lab (Beacon)	436.8475 MHz	amateur	80 mW	CW	50 WPM
(CO-57)	Nishi RF Lab (Data)	437.490 MHz	amateur	1 W	AX.25	1200 baud AFSK
XI-V	Nishi RF Lab (Beacon)	437.465 MHz	amateur	80 mW	CW	50 WPM
(CO-58)	Nishi RF Lab (Data)	437.345 MHz	amateur	1 W	AX.25	1200 baud AFSK
NCube-2		437.505 MHz	amateur		AX.25	1200 baud AFSK
UWE-1	PR430	437.505 MHz	amateur	1 W	AX.25	1200/9600 baud AFSK
Cute-1.7+APD	Telemetry Beacon	437.385 MHz	amateur	100 mW	CW	50 WPM
(CO-56)	Alinco DJ-C5	437.505 MHz	amateur	300 mW	AX.25/SRLL	1200 AFSK/9600 GMSK
GeneSat-1	Atmel ATA8402 (Beacon)	437.067 MHz	amateur	500 mW	AX.25	1200 baud AFSK
	Microhard MHX-2400	2.4 GHz	ISM	1 W	Proprietary	
CSTB1	Commercial[6]	400.0375 MHz	Experimental	<1 W	Proprietary	1200 baud AFSK
AeroCube-2	Commercial[6]	902-928 MHz	ISM	2 W	Proprietary	38.4 kbaud
CP4	TI CC1000	437.325 MHz	amateur	1 W	AX.25	1200 baud FSK
Libertad-1	Stensat	437.405 MHz	amateur	400 mW	AX.25	1200 baud AFSK
CAPE1	TI CC1020	435.245 MHz	amateur	1 W	AX.25	9600 baud FSK
CP3	TI CC1000	436.845 MHz	Experimental	1 W	AX.25	1200 baud FSK
MAST[10]	Microhard MHX-2400	2.4 GHz	ISM	1 W	Proprietary	15 kbps
Delfi-C3	Custom Beacon	145.870 MHz	amateur	400 mW	AX.25	1200 baud BPSK
(DO-64)	Custom Transponder	145.9-435.55 MHz	amateur	200 mW	Linear	40 kHz wide
Seeds-2	Musashino Electric (Beacon)	437.485 MHz	amateur	90 mW	CW	
(CO-66)	Musashino Electric (Data)	437.485 MHz	amateur	450 mW	AX.25	1200 baud AFSK
CanX-2	Custom S-Band	2.2 GHz	Space Research[12]	500 mW	NSP	16kbps-256kbps BPSK
AAUSAT-II	Holger Eckhardt (DF2FQ)	437.425 MHz	amateur	610 mW	AX.25	1200 baud MSK
Cute 1.7+APD II	Invax (Beacon)	437.275 MHz	amateur	100 mW	CW	50 WPM
(CO-65)	Alinco DJ-C5 (Data)	437.475 MHz	amateur	300 mW	AX.25/SRLL	1200 AFSK/9600 GMSK
Compass-1	BC549 (Beacon)	437.275 MHz	amateur	200 mW	CW	15 WPM
	Holger Eckhardt (Data)	437.405 MHz	amateur	300 mW	AX.25	1200 baud AFSK/MSK

Table 2.3 – Summary of CubeSat transmitters (2).

Satellite	Object	Size	Radio	TNC	Downloaded	Lifetime	Antenna
AAU1 CubeSat	27846	1U	Wood & Douglas SX450	MX909	1 kB	3 months	dipole
DTUsat-1	27842	1U	RFMD RF2905		0[1]	0 days	canted turnstile
CanX-1	27847	1U	Melexis		0[1]	0 days	crossed dipoles
Cute-1 (CO-55)	27844	1U	Maki Denki (Beacon) Alinco DJ-C4 (Data)	PIC16LC73A MX614	N/A >10 MB	65+ months	monopole monopole
QuakeSat-1	27845	3U	Tekk KS-960	BayPac BP-96A	423 MB	7 months	turnstile
XI-IV (CO-57)	27848	1U	Nishi RF Lab (Beacon) Nishi RF Lab (Data)	PIC16C716 PIC16C622	N/A >11 MB	65+ months	dipole dipole
XI-V (CO-58)	28895	1U	Nishi RF Lab (Beacon) Nishi RF Lab (Data)	PIC16C716 PIC16C622	N/A	36+ months	dipole dipole
NCube-2	28897[3]	1U			0[1]	0 days	monopole
UWE-1	28892	1U	PR430	H8S/2674R[4]		0.75 months	end-fed dipole
Cute-1.7+APD (CO-56)	28941	2U	Telemetry Beacon Alinco DJ-C5	H8S/2328[4] CMX589A	N/A <1 MB	2.5 months	dipole dipole
GeneSat-1	29655	3U+	Atmel ATA8402 (Beacon) Microhard MHX-2400	PIC12C617 Integrated[5]	N/A 500 kB	3 months	monopole patch
CSTB1	31122	1U	Commercial[6]	PIC	6.77 MB[7]	19+ months	dipole
AeroCube-2	31133	1U	Commercial[6]	Integrated[5]	500 kB	0.25 months	patch
CP4	31132	1U	TI CC1000	PIC18LF6720	487 kB	2 months	dipole
Libertad-1	31128	1U	Stensat		0[8]	1 month	monopole
CAPE1	31130	1U	TI CC1020	PIC16LF452	0[9]	4 months	dipole
CP3	31129	1U	TI CC1000	PIC18LF6720	2.0 MB[7]	19+ months	dipole
MAST[10]	31126	3U	Microhard MHX-2400	Intgrated[5]	>2 MB	0.75 months	monopole
Delfi-C3 (DO-64)	32789	3U	Custom Beacon Custom Transponder	PIC18LF4680 N/A	60 MB[11] N/A	7+ months	turnstile turnstile
Seeds-2 (CO-66)	32791	1U	Musashino Electric (Beacon) Musashino Electric (Data)		N/A 500 kB	7+ months	monopole monopole
CanX-2	32790	3U	Custom S-Band	Integrated	250 MB	7+ months	patch
AAUSAT-II	32788	1U	Holger Eckhardt (DF2FQ)	PIC18LF6680	8 MB[13]	7+ months	dipole
Cute 1.7+APD II (CO-65)	32785	3U+[14]	Invax (Beacon) Alinco DJ-C5 (Data)	H8S/2328 H8S/2328, CMX589A	N/A 21 MB[15]	7+ months	monopole monopole
Compass-1	32787	1U	BC549 (Beacon) Holger Eckhardt (Data)	PIC12F629 C8051F123, FX614	N/A <1 MB	7+ months	dipole dipole

Table 2.3 shows that almost all CubeSats are 1U. Only recently the idea of bigger spacecrafts is becoming generalized. It is also possible to hope VORSat can reach expected lifetime of 2 or 3 months, because that is the average so far. Only two spacecrafts used patch antennas until that date, the ones which operate at higher frequencies. The exception is MAST, with monopole antennas. There are cases of satellites that never signalled their presence in space, but on the other hand others have transmitted great amount of data during their lifetime.

Other explanations to allow a better understanding of the tables:

1. Satellite never heard from in space.
2. Used a modified Pacsat protocol on top of AX.25. Source code available upon request.
3. Object separated from SSETI Express months later and is presumed to be NCube-2.
4. This is also the main satellite processor.
5. The radio module accepts serial data and uses an internal TNC.
6. The manufacturer and model number is unknown.
7. As of April 2008.
8. No uplink commands received by spacecraft.
9. CAPE1 team knew the receiver was dead before integration but had no time to fix it.
10. One identical radio per satellite section, so three total radios onboard.
11. Since no on-board telemetry storage exists on this satellite, this figure is not for commanded data and cannot be directly compared to the other spacecraft. This figure is beacon data and includes duplicate beacons.

12. First CubeSat with a licensed frequency in the 2200 to 2290 MHz Space Research band. Internationally coordinated.
13. This figure includes all data from the spacecraft, including beacons, bad packets, and retransmissions.
14. This satellite does not technically count as a CubeSat, as the actual size is 11.5cm x 18cm x 22cm, but is based on the earlier CubeSat designs.
15. This includes 7 MB from the Tokyo Tech ground station, 5 MB from the Japanese GSN, and 9 MB from amateurs.

As it is easy to confirm, none of the CubeSats launched until November 2008 had the characteristics that VORSat is being designed to have. Also, none of them sought to prove attitude determination. In this aspect, VORSat possess a very significant amount of scientific innovation.

2.3 – Inter-Satellite Links

Inter-Satellite Links are a very useful method to enlarge and improve the quality of Earth coverage by satellites, because radio spectra for communications is suffering of overflow. Constellations of satellites, independently of their size, may be used to perform several scientific studies. Recent projects try to use these constellations to measure high latitude energy input due to Northern and Southern Lights, to achieve Earth observation or to monitor and guide maritime traffic. ISL provide added capacity to a communications system. Among several types of ISL, three of them are the most commonly used:

1. GEO – GEO link;
2. GEO – LEO link, also called inter-orbital links (IOL);
3. LEO – LEO link.

The first type will not be discussed here, for obvious reasons.

IOL already involve LEO satellites (figure 2.7). They are mostly used to combine the characteristics of both orbits. GEO satellites have very large footprint, reaching this way to several Earth areas. LEO satellites have very reduced path losses in their transmissions to and from Earth.

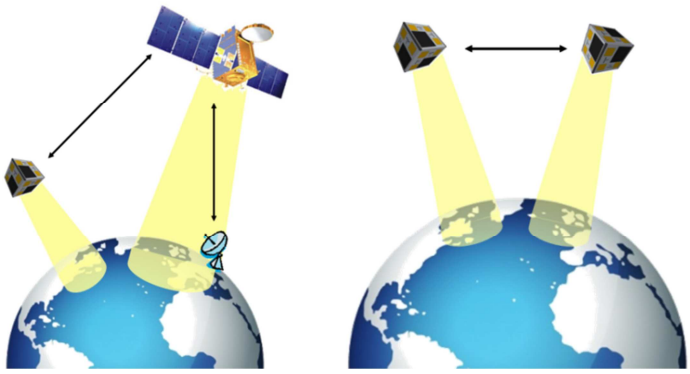

Figure 2.7 – Inter-Satellite Link: GEO – LEO in the left and LEO – LEO in the right.

In these cases, the variable relative velocity of two moving satellites leads to the variation of the lead-ahead angle, which is the angle between two satellites in motion (figure 2.8 [10]). In IOL's, this angle reaches its maximum value when the LEO satellite passes through the equatorial plane.

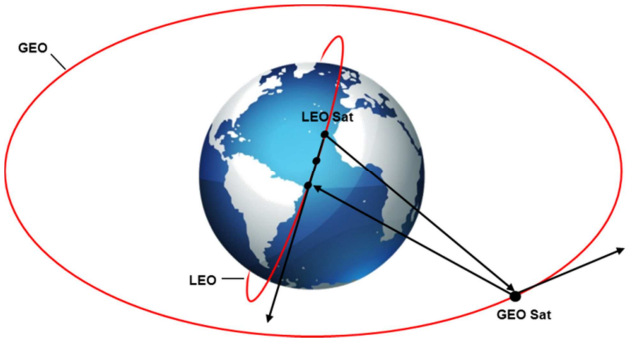

Figure 2.8 – GEO – LEO ISL Lead-Ahead Angle.

But ISL between LEO satellites is the case that matters the most for this specific analysis. Several LEO satellites already use an ISL to communicate with each other. This way, communications these satellites serve are significantly improved. Likewise, other services provided by them, such as voice and GPS system, which truly need an excellent real-time performance, become able to attain a higher quality of service. Proving ISL communication with CubeSats could open doors to different scientific and research studies.

There are two different ways to perform ISL communications, depending on the data to transmit and the characteristics of the used satellite. Those links may adopt communication via radio frequency or via optical links, as explained later. Frequencies used in Inter-satellite Links are specific, previously defined and ruled by the Radiocommunication Regulations. They correspond to frequencies that are absorbed by the lower layers of the atmosphere. This way, there are no interferences between space and terrestrial links. All the same, interferences between satellite links are to be avoided because these use shared frequencies.

Once signal doesn't propagate through the atmosphere, one ought to consider propagation losses only as free space losses. Nevertheless, in RF links, re-use of frequencies from one beam to another is mandatory. Antennas used for these purposes must be narrow beam antennas and must produce side lobes as reduced as possible, so interferences with other satellite systems can be avoided. Due to antenna size constraints forced by launchers and the technical harshness of developing deployable antennas, the use of high frequencies revealed to be the best option for this case. This is where the importance of optical links arises. Table 2.4 [10] illustrates frequencies used in Radio Frequency and in Optical Links.

Optical links have a big amount of technical characteristics that could be exhaustively described, though it is not the objective at this point, mainly because it is not feasible to implement this technology in a CubeSat.

First of all, the telescope used to data transmission is usually 30 cm diameter. What is considered small for other satellites is huge for CubeSats, because it represents the triple of a normal cube, or the whole face of a 3U. Also, typical optical beam width is 5 microradians. In satellites moving both at very high speeds, it is quite difficult to point in the correct direction. For VORSat it is even worse, once it will have a limited attitude control. Therefore, an optical link is not an option.

Table 2.4 – Frequency Bands / Wavelengths for ISL.

ISL SERVICE	FREQUENCY BANDS
Radio Frequency	22.55 - 23.55 GHz 24.45 - 24.75 GHz 32 - 33 GHz 54.25 - 58.2 GHz
Optical Links	0.8 - 0.9 μm (AlGaAs laser diode) 1.06 μm (Nd:YAG laser diode) 0.532 μm (Nd:YAG laser diode) 10.6 μm (CO2 laser)

Link establishment represents another problem for satellites this small. The first phase at this point is signal acquisition, which requires high power peaks. In a satellite with so meager resources, these peaks might exceed available power, supplied only by solar panels and secondary batteries. The other two phases, tracking and communications, clearly depend on the first one. Tracking wouldn't be an easy task as well.

The adoption of one of the two techniques depends on the mass and power consumed. Establishing a parallel between these two options, both are viable for bigger satellites in any orbit, including LEO. Notwithstanding, for CubeSats it is not possible to establish optical links. Even if it wasn't problematic, it wouldn't be the best choice for this specific purpose, because RF links are better for low throughputs.

2.4 – Satellite Communication Losses

In any satellite transmission, there are always losses from various sources. Some of those losses may be constant, others are dependent of statistical data and others vary with the weather conditions, especially with rain.

With table 2.5, it is intended to provide a clear view of the major impairments this kind of communication may suffer, as well as their origin. A detailed explanation will be given afterwards, in order to determine and justify all the values achieved in the calculations for VORSat.

Losses in the received signal may have their origin in its propagation from the satellite to the ground station or the opposite, although the uplink will not be studied in this case once VORSat will only have downlink signal for attitude determination. They also may appear in the ground station itself or in the satellite. There are three major issues to take into account as far as propagation losses concern.

- Free space losses
- Atmospheric losses
- Pointing losses

Free space loss (Lfs) is the dominant component in the loss of the strength of the signal. It doesn't refer to attenuation of signal, but to its spreading through space.

Table 2.5 – Major losses in satellite communications.

<table>
<tr><td rowspan="10">SATELLITE COMMUNICATION LOSSES</td><td rowspan="8">PROPAGATION LOSSES</td><td colspan="3">FREE SPACE LOSSES</td></tr>
<tr><td rowspan="7">ATMOSPHERIC LOSSES</td><td rowspan="2">Ionospheric effects</td><td>Faraday rotation</td></tr>
<tr><td>Scintillation effects</td></tr>
<tr><td rowspan="5">Tropospheric effects</td><td>Attenuation</td></tr>
<tr><td>Rain attenuation</td></tr>
<tr><td>Gas absorption</td></tr>
<tr><td>Depolarization</td></tr>
<tr><td>Sky noise</td></tr>
<tr><td colspan="2">Local effects</td></tr>
<tr><td colspan="3">POINTING LOSSES</td></tr>
<tr><td rowspan="3">LOCAL LOSSES</td><td rowspan="2">RECEPTION LOSSES</td><td colspan="2">Feeder losses</td></tr>
<tr><td colspan="2"></td></tr>
<tr><td colspan="3">ENVIRONMENT LOSSES</td></tr>
</table>

In order to perform all the mandatory calculations on the link power budget for any satellite, a key component must be taken into account, the Equivalent Isotropic Radiated Power (EIRP), which may be considered the input power in one end of the link. EIRP is also introduced precisely at the beginning of all calculations so it can be understood the source of each component and to allow the correct comprehension of all the deductions presented.

The maximum power flux density at a distance r is given by:

$$\psi_M = \frac{G_T . P_S}{4\pi r^2} \tag{2.1}$$

where:

ψ_M →maximum power flux density (dBW/m^2)
G_T →transmission antenna gain (dB)
P_S →radiated power from the antenna (W)
r →distance between the satellite and the receiving station (m)

Considering an isotropic radiator with an input power equal to $G_T.P_S$ the same flux density would be produced.

$$EIRP = G_T . P_S \tag{2.2}$$

Once EIRP is usually expressed in dBW, it is possible to write:

$$EIRP(dBW) = P_S(dBW) + G_T(dB) \tag{2.3}$$

The first step in the calculations for free space loss is to determine the losses in clear-sky conditions. These are the losses that remain constant with time. As said before, Lfs derive from the spreading of signal in space.

The received power is given by:

$$P_R = \Psi_M . A_{eff} \tag{2.4}$$

P_R → received power (W)

A_{eff} → effective aperture of the receiving antenna (m^2)

From the equations above, it is possible to write:

$$\psi_M = \frac{EIRP}{4\pi r^2} \tag{2.5}$$

The effective aperture of the antenna is provided by:

$$A_{eff} = \frac{\lambda^2 G_R}{4\pi} \tag{2.6}$$

So, the received power may also be calculated by:

$$P_R = \frac{EIRP}{4\pi r^2} \frac{\lambda^2 G_R}{4\pi} \tag{2.7}$$

$$P_R = EIRP . G_R . \left(\frac{\lambda}{4\pi r}\right)^2 \tag{2.8}$$

In dB, this equation can be rewritten as:

$$P_R = EIRP + G_R - 10 \log \left(\frac{4\pi r}{\lambda}\right)^2 \tag{2.9}$$

In this equation, EIRP refers to the transmitter, G_R to the receiver and the last term of the second member of the equation to the free space spreading losses.

Once $\lambda = c/f$ free space losses are given by the following expression:

$$L_{fs} = 10 \log \left(\frac{4\pi r f}{c}\right)^2 \tag{2.10}$$

When the frequency f is represented in MHz and the distance r in km, the above expression for free space loss comes as:

$$L_{fs} = 32{,}4 + 20 \log(r) + 20 \log(f) \tag{2.11}$$

Atmospheric losses derive from the absorption of energy by atmospheric gases. They can assume two different types:

- Atmospheric attenuation;
- Atmospheric absorption.

Attenuation is the reduction of signal amplitude and has two mechanisms: absorption and scattering. Likewise, these losses can be due to ionospheric, tropospheric and other local effects.

All radio waves transmitted by satellites to the Earth or vice versa must pass through the ionosphere, the highest layer of the atmosphere, which contains ionized particles, especially due to the action of sun's radiation. Free electrons are distributed in layers and clouds of electrons may be formed, originating what is known as travelling ionospheric disturbances, what provoke signal fluctuations that are only treated as statistical data [11]. The effects are:

- Polarization rotation;
- Scintillation effects;
- Absorption;
- Variation in the direction of arrival;
- Propagation delay;
- Dispersion;
- Frequency change.

These effects decrease usually with the increase of the square of the frequency and most serious ones in satellite communications are the polarization rotation and the scintillation effects, and those are the ones that will be treated in this dissertation.

When a radio wave passes through the ionosphere, it contacts the layers of ionized electrons that move according to the Earth's magnetic field. The direction these electrons move will no longer be parallel to the electric field of the wave and therefore the polarization is shifted, in what is called Faraday rotation (θ_F).

This is not a serious problem in frequencies above 10 GHz and in cases where linear polarization is used.

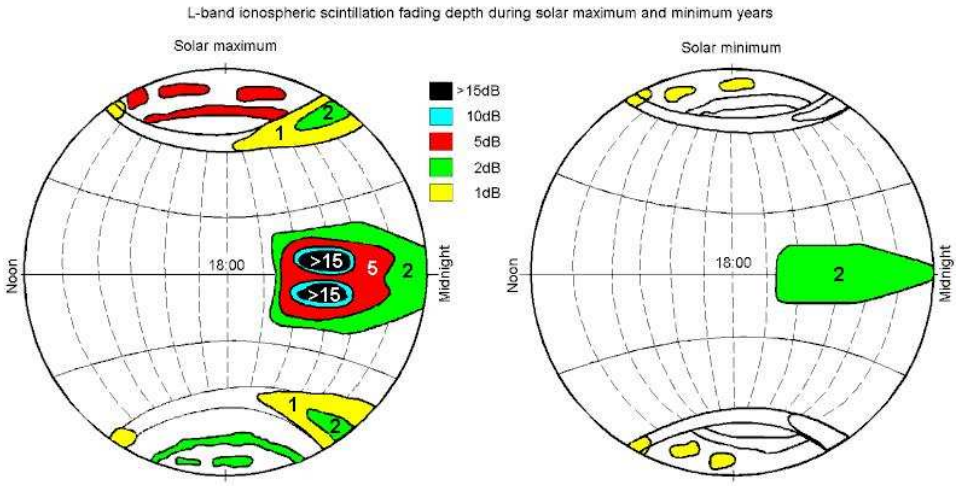

Figure 2.9 – Ionospheric scintillation fading depth.

In respect to scintillation effects, differences in the atmospheric refractive index may cause scattering and multipath effect, due to the different directions rays may take through the atmosphere. They are detected as variations in amplitude, phase, polarization and angle of

arrival of the radio waves. It is often recommended the introduction of a fade margin so atmospheric scintillation can be a tolerated phenomenon. Figure 2.9 [12] shows how ionospheric scintillation affects signals operating in the L-Band (1 GHz – 2 GHz). It is not exactly the frequency of VORSat, but it is quite close.

Troposphere is composed by a miscellany of molecules of different compounds, such as hail, raindrops or other atmospheric gases. Radio waves that pass by troposphere will suffer their effects and will be scattered, depolarized, absorbed and therefore attenuated.

It is necessary to analyze each effect on its own so that its respective contribution can be understood.

Signal attenuation comes from the radio waves that cross troposphere and their radio frequency energy is converted into thermal energy. They will also be scattered into various directions which means that there is a small percentage that doesn't reach the receiver antenna at the ground station. The main scatterer particles in troposphere are hydrometeors like raindrops, hail, ice, fog or clouds, and these particles represent a problem for frequencies higher than 10 GHz [11]. Both this kind of absorption and scattering rise with frequency.

Attenuation caused by rainfall is a concern for GEO satellites, once the satellite's position in relation to the GS is permanent. For LEO satellites the problem is much smaller, because the sub-satellite point is not permanent and the probability of crossing over an area under the influence of heavy rain is inferior.

Under normal conditions, only oxygen and water vapour have a significant contribution in gas absorption. Other atmospheric gases only become a problem in very dry air conditions above 70 GHz. Thereby, losses caused by atmospheric absorption vary with frequency and the collection of data already received allows the elaboration of figure 2.10 [14].

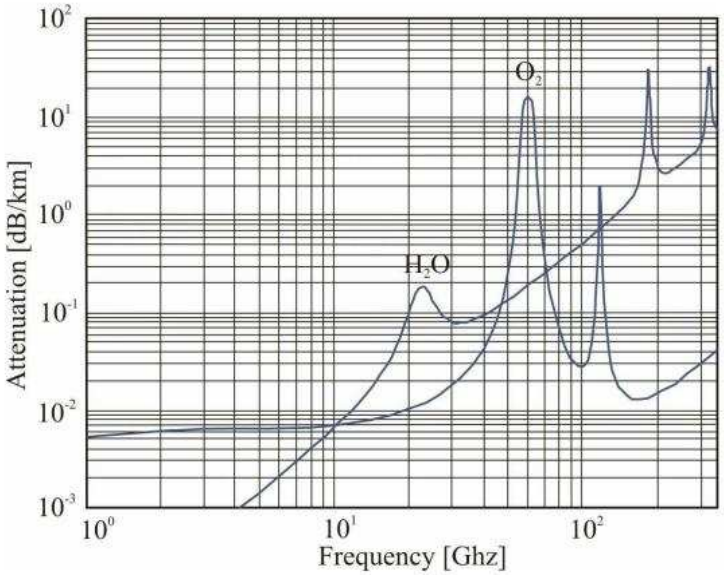

Figure 2.10 – Attenuation vs. Frequency.

As it is possible to verify, both two peaks are observed at the frequencies 22.3 GHz for water vapour (H_2O) and 60 GHz for oxygen (O_2). Once these values depend on atmosphere thickness, it becomes necessary to perform all calculations taking into account troposphere thickest layer (Ttrop), which has 20 km. New recommendations from International Telecommunication Union – Recommendation Sector (ITU-R) point out 6 km of oxygen as the

correct approximation. It is also mandatory to refer that this graph represents the absorption for a satellite in the zenith, in other words, for an elevation angle of 90º (θ = 90º). For lower angles, the atmospheric absorption (Labs) is given by:

$$L_{abs}(dB) = L_{abs|90^\circ}(dB/km)\ cosec\ \theta . T_{trop}(km) \tag{2.12}$$

Satellite communications use linear and circular polarization, but undesirable effects may transform it into an elliptical polarization. Circular polarization is less prone to depolarization issues. Depolarization may occur when an orthogonal component is created due to the passing of the signal through the ionosphere. There are two ways to measure its effect, cross-polarization discrimination (XPD) and polarization isolation (I).

When an electric field of magnitude E_1 is transmitted through a depolarizing medium, the received signal will have a copolar component (E_{11}) and a cross-polar component (E_{12}). XPD is defined according to the expression 2.13 [11].

$$XPD\ (dB) = 20 \log\left(\frac{E_{11}}{E_{12}}\right) \tag{2.13}$$

Isolation applies to two orthogonal signals that go by the same depolarizing medium. Both will have copolar and cross-polar components at the receiver. Polarization isolation is the ratio of the received copolar power to cross-polar power, and it is defined as [11]:

$$I\ (dB) = 20 \log\left(\frac{E_{11}}{E_{21}}\right) \tag{2.14}$$

Drops of rain also add depolarization. The ideal drop of rain has a spherical shape so that the necessary energy to keep it together is minimal. However, the real shape of a drop is flattened, where there is a major axis relatively to the others, forming a spheroid.

Since rainfall results in random directions of rain drops, which will vary even with the wind, they will be canted. This results in the rotation of polarization of the radio waves. This rotation may reach up to 10º, what may become a quite serious problem in linear polarization, but not that much in circular polarization because, such as in ionospheric depolarization, this value will only add to the rotation.

On the top of each rain area there is an ice layer which can cause depolarization. Ice crystals usually have the shape of a needle or a plate. When their disposition is random there is no depolarization, but when there's an alignment it may occur.

ITU-R recommends the use of a statistical value of 2dB added to the XPD determined for rain [11]. Furthermore, ice effects may be despised for time percentages inferior to 0.1%.

Table 2.6 [13] indicates polarization losses for several transmitting and receiving antenna combinations. So, for circular polarization transmissions, the worst case in reception implies a loss of 3 dB, half the signal power. Obviously, when the signal from a right hand circular polarization (RHCP) is transmitted for a left hand circular polarization (LHCP) antenna, or vice-versa, there is no any signal reception.

If there is a misalignment in transmitter and receiver antennas when both use circular polarization, in the receiver antenna the polarization will be more or less elliptical, depending on the severity of the misalignment. As the lack of accuracy in pointing increases, the more

elliptical will be the front end of the wave in the ground station, and therefore the greater will be losses for depolarization.

Table 2.6 – Polarization losses for different polarizations in antennas.

Transmit Antenna Polarization	**Receive Antenna Polarization**	**Ratio of Power Received to Maximum Power**		
		Theoretical	Practical Horn	Practical Spiral
		Ratio in dB	Ratio in dB	Ratio in dB
Vertical	Vertical	0	*	N/A
Vertical	Slant (45º or 135º)	-3	*	N/A
Vertical	Horizontal	-∞	-20	N/A
Vertical	Circ (RHCP/LHCP)	-3	*	*
Horizontal	Horizontal	0	*	N/A
Horizontal	Slant (45º or 135º)	-3	*	N/A
Horizontal	Circ (RHCP/LHCP)	-3	*	*
Circ (RHCP)	Circ (RHCP)	0	*	*
Circ (RHCP)	Circ (LHCP)	-∞	-20	-10
Circ (RHCP/LHCP)	Slant (45º or 135º)	-3	*	*

NOTE: The symbol * means the values are the same as theoretical. It is important to refer as well that switching the transmitting and the receiving antennas the same results will be obtained.

Sky noise is a combination of galactic and atmospheric effects, according as both these factors influence the quality of the signal in the reception. Galactic effects decrease with the increase of frequency (figure 2.11). They are due to the addition of the cosmic background radiation and the noise temperature of radio stars, galaxies and nebulae. This value is quite low and a good approximation is 3 K.

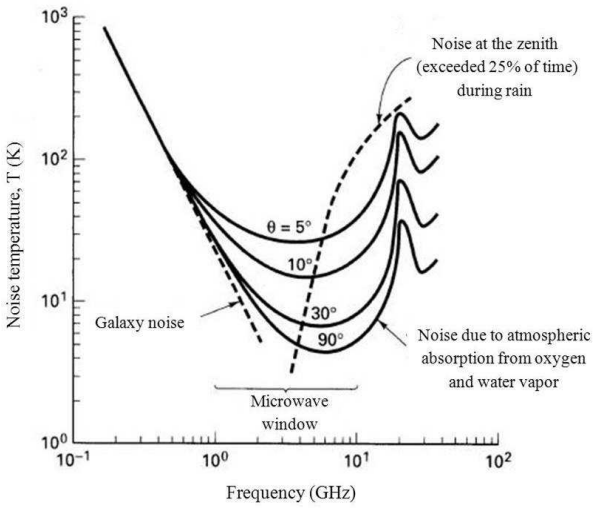

Figure 2.11 – Galaxy noise influence in noise temperature.

Figure 2.11 shows also an optimal window between 1 GHz and 10 GHz, rather useful for satellite transmissions due to its fairly low noise temperature.

Atmospheric effects in satellite transmissions increase with the increase of frequency (figure 2.12 [6]). As said previously, the effects of the atmosphere in signal attenuation become serious for frequencies above 10 GHz, and the same applies for noise temperature.

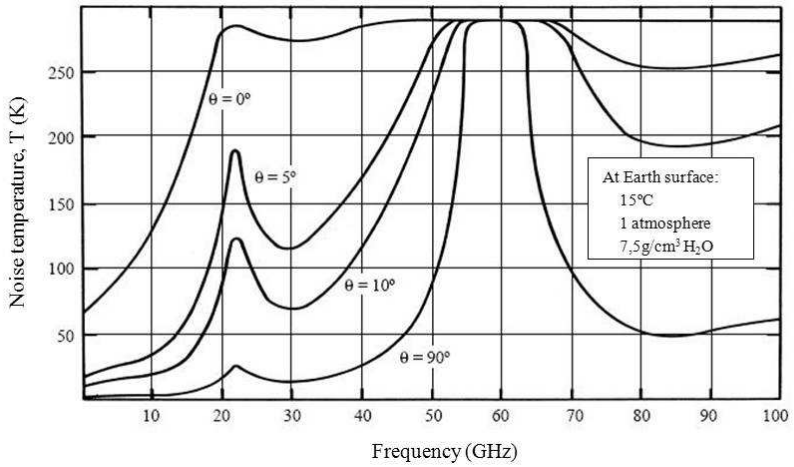

Figure 2.12 – Noise temperature variation with frequency.

Local effects refer to the proximity of the local ground stations, where may exist sources that interfere with the received signal and buildings that may block the signal. That's why the height of the ground station relatively to the surrounding buildings is an important factor. Nevertheless, this problem is more important in other communications systems, such as mobile services, and not so much for satellite communications.

Ideal reception implies that the value for misalignment losses would be 0 dB which means maximum gain at the ground station is achieved when both the transmitter and the receiver antennas are 100% aligned. Realistically it is virtually impossible to achieve a perfect alignment between the antennas of the ground station and the satellite, especially in the case of CubeSats, due to their fast movement of nearly 8 000 ms^{-1}.

There are two ways for misalignment:

- Off-axis loss at the satellite;
- Off-axis loss at the GS.

The first one is considered during the design of the satellite link. The second type of misalignment is the antenna pointing loss and it is usually small. However, it may harm the quality of the received signal causing nocive impairments. A fairly good approximation for this factor is 3 dB.

Antenna misalignment losses (Laml) are estimated using statistical data, so this value is an approximation based on real data observed in several GS.

Local losses refer to loss of signal quality in each ground station.

The receiving and emitting equipments also introduce some losses to the signal. Feeder losses occur in the several components between the receiving antenna and the receiver device, such as filters, couplers and waveguides. These losses are similar to the ones which occur also in the emission, between the emitting antenna and the output of the high power amplifier (HPA). Receiver feeder losses (RFL) are added to free space losses and are not necessary but to relate EIRP with the HPA output, which means that knowing the EIRP will allow the calculations without being aware of the RFL values. Although RFL will not be great, inevitably there will be losses in reception. A good approximation for that value is 0.46 dB.

It is also necessary to observe the specific region of the globe where the ground station is placed (equatorial, tropical, polar…). Depending on its latitude, each region has its own characteristics (e.g. temperature, moisture, thickness of atmospheric ice layer…), which may provoke variation in signal reception.

There are also other factors that may condition satellite communications. Even though they may have a minor importance in CubeSat transmissions, they may become relevant in other cases.

Sun outages are punctual losses of communication between satellites and the Earth due to satellite obscuration by the sun. It means that the ground station sees the sun behind the satellite, in what is called a "transit". It occurs in 5 or 6 days near the equinoxes and last for a maximum of 8 minutes each, in a total of 60 minutes per year. The noise temperature of the system becomes very high and communications suffer negative consequences at about 100 minutes per year (0.02%). Sun outage affects other kinds of satellite orbits, but not LEO's.

Satellite eclipses happen when the satellite crosses the cone of shadow of the Earth. They occur within 23 days before and after the equinoxes, at March 21st and September 23rd (figure 2.13 [6]). They last 70 minutes at their maximum and some strong thermal variations are produced. During the eclipse, the satellite operates only with batteries and some transponders are disconnected. However, this problem only affects geosynchronous satellites due to their fixed position relative to the Earth.

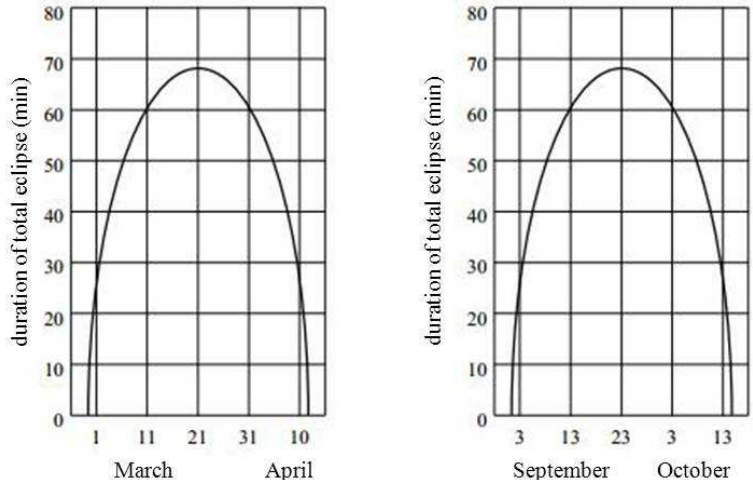

Figure 2.13 – Dates and duration of eclipses.

2.5 – Definition of Spread Spectrum

A digital communications system is considered a Spread Spectrum (SS) system if, cumulatively:

- The transmitted signal occupies a larger bandwidth than the minimal necessary bandwidth to transmit the information;
- The expansion of the bandwidth is achieved with a code which is independent of the information.

This code is a pseudonoise (PN) code and is employed as a modulation waveform to spread the signal energy. At the reception, the inverse operation will be performed, using the same PN code.

Spread Spectrum systems have several attractive characteristics:

- Better resistance to intentional or not intentional interferences or jamming;
- Ability to eliminate or attenuate the multipath propagation effect;
- Possibility of sharing of the same frequency bands with other users;
- Permission to be used in bands free of special license (e.g.: ISM band at 2.4 GHz);
- Privacy;
- Possibility of hiding a signal below noise floor.

There are two main kinds of SS systems:

- Frequency Hopping (FH);
- Direct Sequence (DS).

All the bandwidth is occupied at the same time in DS systems and in successive portions in FH systems, as it will be seen. In this dissertation, the used technique will be Direct Sequence. However, a brief explanation of FH will also be provided

2.5.1 – Frequency Hopping vs. Direct Sequence

Frequency Hopping Spread Spectrum (FHSS) systems are usually associated to Frequency Shift Keying (FSK) modulated signals.

As figure 2.14 illustrates, a PN sequence altogether with an FSK modulator enables the shift of the carrier frequency of the FSK signal pseudorandomly at a determined hopping rate. This signal will occupy a number of frequencies in time, each for a period known as dwell time. All the available bandwidth will be divided into N channels and hops are determined by the PN code that produces a Frequency Word containing information about the hop sequence. In each hop, the instantaneous occupied bandwidth is the same as FSK, much narrower than the bandwidth of the spread signal. The transmission power is concentrated in a single channel. On a long sequence of hops FH/FSK spectrum tends to occupy all the bandwidth of SS. FHSS systems can be hopped over a larger bandwidth than DSSS systems, once it only depends of the tuning range. At the reception, demodulation is noncoherent because it suffers of phase discontinuity [15]. The number of symbols per hop also allow for a different classification of this technique, Slow FH (SFH) and Fast FH (FFH).

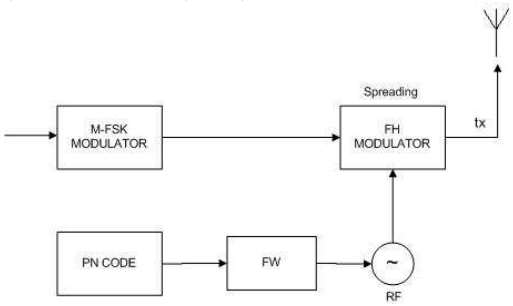

Figure 2.14 – Frequency Hopping modulator scheme.

Direct Sequence Spread Spectrum (DSSS) systems are usually linked with Phase Shift Keying (PSK) modulated signals.

A modulator scheme for DSSS is shown in figure 2.15. A PN sequence altogether with a PSK modulator allows for the phase shift of the PSK signal in a pseudorandom way, at a chipping rate Rc = 1/Tc. The symbol rate Rs = 1/Ts must be an integer multiple. Maximum chip rate and maximum spreading are limited. PSK modulation demands coherent demodulation.

There are 2 variations within this technique, short-code and long-code systems.

In the first case, PN code length is equal to the data symbol. In the second, PN code length is significantly longer than the data symbol, what makes that a different pattern will be associated with each symbol.

DSSS systems use all the available band at all times.

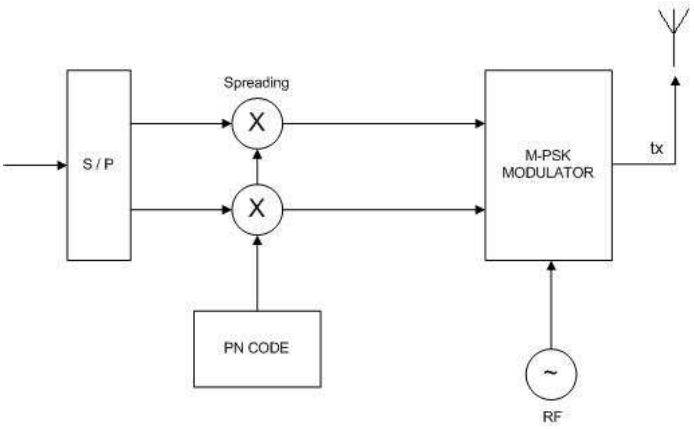

Figure 2.15 – Direct Sequence modulator scheme.

2.5.2 – Basic features of DSSS

This dissertation focuses on the coding techniques to use, and not in the electronics and system design that lies behind. However, a brief summary of the main points is considered necessary for a better comprehension of the work to be done.

There will be 2 inputs, binary data with symbol rate Rs and PN code with chip rate Rc.

The spreading is achieved through the direct multiplication of the binary data by the PN code, independent of the data. The baseband signal is achieved and the signal is now spread.

At the reception, only a receiver which already is prepared to decode this signal will be able to detect it. The received signal is again multiplied by the PN sequence to attain the original message sent in the transmitter, despreading the signal.

As said before, SS systems spread the information over a wider bandwidth: $B_{info} << Bss$.

The spread spectrum signal is quite similar to white noise. Amplitude and power in the SS signal are equal to binary data at the input, but once the bandwidth is so larger, the power spectral density (PSD) is much lower. SS techniques improve the performance of communication systems. This improvement is quantified by the processing gain (PG), which is the spreading factor (SF), and may be expressed as several ratios:

$$PG = SF = B_{ss}/B_{info} = Rc/Rs = Tb/Tc = Nc \tag{2.15}$$

This spreading brings benefits once it allows for multipath and narrowband interference rejection, and because signal is hidden below noise floor. However, it is not spectrally efficient for one single user, being strongly recommended for multiple access systems.

The importance of synchronism is great and totally understandable if one thinks in correlation values. When the PN sequence in the reception is the same as in the transmission and the synchronism is perfect, the autocorrelation is maximal and the signal is fully recovered. When the synchronism is not perfect or the PN sequence at the reception is different than the one that is used in transmission the crosscorrelation is close to zero.

But all transmissions suffer the influence of interferences and noise. Every time interference occurs in the channel between the transmitter and the receiver, it will add an undesirable component to the received signal, what adulterates the initial message. The reception scheme is shown on figure 2.16:

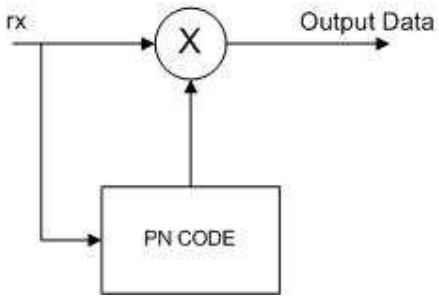

Figure 2.16 – Reception scheme for recovery of original data.

The reception signal is a sum of the transmitted signal and interference caused by other users, noise, jammers or others. In order to recover the original data, the incoming signal is multiplied by an exact replica of the spreading code. The original data is then multiplied twice for the same PN sequence, in transmission for spreading and in reception for despreading. The interference is multiplied once in the reception, what makes it become noise-like and spread, because it is uncorrelated with the PN sequence. So, after despreading, the original data is narrowband and interference is wideband. Applying a low pass filter (LPF) which allows for the recovery of the original data, the interference is almost entirely filtered out.

Multipath is treated almost like noise or interference. When a signal suffers its effect and reaches the reception with delay, it is treated like noise because the correlation of the spreading codes provokes its attenuation.

2.6 – Pseudo Noise Sequences

A PN sequence can be understood like a carrier that causes the spreading of the signal all over the available bandwidth. This code is noise-like but it is entirely deterministic. A proper selection of a code is determinant.

Sequences used in systems that operate in DSSS can be generated with the aid of codes like maximum length sequences (m-sequences), Walsh codes, Kasami codes, Barker codes or Gold codes.

Walsh codes are based on the matrices of Walsh-Hadamard and have the desirable property of being perfectly orthogonal in the absence of phase shift, while the others are not. That allows the absence of interference among synchronized transmitted signals from the same CDMA

station. However, for other phase shifts they have very low correlation. Besides, these codes do not spread uniformly all over the spectrum.

Barker codes have the lowest aperiodic autocorrelation values, but there are only 7 possible Barker sequences, what makes them impossible to be used in this case.

A PN sequence is generated by a shift register, XOR gates and a feedback loop. Considering n the number of stages of the shift register, the period N of a sequence is:

$$N = 2^n - 1 \tag{2.16}$$

The sequence must be maximum length sequence and n (consequently, N) must be as high as possible so that the sequence may be more noise-like. Maximum length sequences are usually named m-sequences. They have several distinguishing properties, but some assume major importance.

The property of balance says that in an m-sequence, the number of "1" is equal to the number of "0" plus one.

- Number of "1": 2^{n-1}
- Number of "0": $2^{n-1} - 1$

The series property states that the total number of series ("1" and "0") is (N+1)/2 = 2n-1. A series is a subsequence of equal bits. The number of equal bits is the subseries length. In each period, half of the series of "1" or "0" have length 1, a quarter have length 2, etc, according to table 2.7.

Table 2.7 – Number of subsequences of a given length in each m-sequence.

Lenght of the series	**Fraction**
1	1/2
2	1/4
3	1/8
…	…
i	$1/2^i$

The autocorrelation property is periodic of period N and it has only 2 values:

$$R(j)\begin{cases} N, j = 0 \\ -1, 1 \leq j \leq 2^n - 2 \end{cases} \tag{2.17}$$

Its autocorrelation function must be like figure 2.17, in this case of an m-sequence of N= 63.

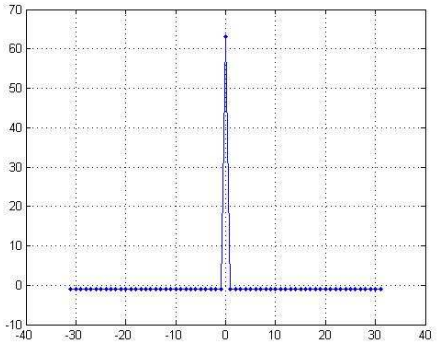

Figure 2.17 – Autocorrelation of an m-sequence.

The Euler function (2.18) helps in providing the number of m-sequences of a given length.

If p_i, 1, 2, …, I, are the prime factors of N, then:

$$\Phi(N) = N \prod_{i=1}^{I} p_i - 1/p_i \tag{2.18}$$

The number of m-sequences of length N is given by the expression 2.19:

$$Number\ of\ m - sequences = \Phi(\mathrm{N})/n \tag{2.19}$$

These sequences are the primitive polynomials that indicate the stages of the shift register that must be connected to feedback.

But there is another item to pay attention. When there is the need of more than one PN sequence the analysis of the crosscorrelation between those sequences becomes necessary. Usually, the lower it is the better.

The lower bound of Welch provides minimum cross correlation between 2 sequences of lengths M and N:

$$|Rc(j)|max \geq N\sqrt{(N-1)/(MN-1)} \tag{2.20}$$

If the crosscorrelation is three valued, then the sequences form a preferred pair.

Rc = {– t(n), -1, t(n) – 2}, with t(n) = $2^{\lfloor (n+2)/2 \rfloor} + 1$. There are no preferred pairs for sequences where n is a multiple of 4.

In order to perform the preferred pair generation, an m-sequence (u) is taken for a given length N = 2^n-1, where n is the size of the Linear Feedback Shift Register (LFSR). Then, the decimation of u is done by a decimation factor q, which will provide the second sequence (v), according to {v}' = u[q].

So that u and v can become a preferred pair, q has to be chosen such as conditions 2.21 may be satisfied:

$$1.\ n\ odd\ or\ mod(n,4) = 2$$

$$2.\ q\ odd\ and \begin{cases} q = 2^k + 1 \\ or \\ q = 2^{2k} - 2^k + 1 \end{cases} \tag{2.21}$$

$$3. \begin{cases} gcd(n,k) = 1 \rightarrow n\ odd \\ gcd(n,k) = 2 \rightarrow mod(n,4) = 2 \end{cases}$$

The combination of 2 PN sequences that form a preferred pair may result in Gold codes or Kasami codes.

A Gold sequence is a type of binary sequence used in telecommunications and satellite navigation (GPS), in situations of multiple access (CDMA). According to the definition of CDMA itself, Gold codes have low crosscorrelation within some limits, what is quite useful when several transmissions occur simultaneously.

Formally, a Gold sequence is an arbitrary phase of a sequence in the set G(u,v), defined as the expression 2.22 indicates:

$$G(u,v) = \{u, v, u \oplus v, u \oplus Tv, u \oplus T^2 v, \dots, u \oplus T^{N-1} v\} \tag{2.22}$$

where:

- $\oplus \rightarrow$ XOR operator
- $T^K \rightarrow$ operator which shifts vectors cyclically to the left by k places
- u, v → m-sequences of period generated by different primitive binary polynomials

Sequences associated to Gold codes are produced by binary addition (modulo 2) of cyclic shifted versions of 2 m-sequences of length $N = 2^n-1$.

A set of Gold code sequences consists in 2^n-1 sequences, each with a period of 2^n-1, and may be generated following the next steps.

First, it is mandatory to choose 2 maximum length sequences with the same length 2^n-1, such as its absolute crosscorrelation is not superior to $2^{(n+2)/2}$, where n is the size of the LFSR used to generate the m-sequence.

The set of the 2^n-1 exclusive-or of both sequences in its several phases is a set of Gold codes.

Absolute crosscorrelation in this set of codes obeys to

$$\begin{cases} 2^{(n+1)/2} + 1 \rightarrow n\ odd \\ 2^{(n+2)/2} + 1 \rightarrow n\ even \end{cases} \tag{2.23}$$

Exclusive-or of 2 Gold codes of the same set is another Gold code in the same phase.

Within a set of Gold codes, nearly half is balanced (number of “1” and “0” differ of only one).

If 2 m-sequences of cyclic shift T^1 and T^2 are used in the generation of Gold codes, then the generated Gold code will be unique for each combination of T^1 and T^2. This means that several Gold codes will be created with a great number of users using the same spectrum band, what encounters what has been previously said about access in these systems. A set of Gold sequences contain $N = 2^n + 1$ sequences.

When both sequences are randomly chosen for code generation, crosscorrelation properties may not be as good as necessary. That’s why there are preferred pairs of sequences that assure good crosscorrelation as well as good autocorrelation of the generated Gold code. Crosscorrelation is three valued such as the original sequences.

The advantage of Gold sequences relatively to m-sequences is the increased number of sequences with crosscorrelation with only three values, what is desirable in CDMA.

Kasami sequence generation is performed in similar steps to the ones gave to achieve Gold sequences. There is the small set and the large set of Kasami sequences. In both cases, *n* must be even.

The small set has only $2^{n/2}$ possible sequences, what is inconvenient, although the three valued crosscorrelation is significantly reduced, being quite close to the lower bound of Welch.

The large set contains both Gold sequences and the small set of Kasami, what results in an increased number of possible sequences. However, the crosscorrelation reaches higher values, what makes these sequences less attractive to this specific application.

2.7 – Two-Line Elements

Orbital elements of satellites describe their orbits around Earth. The Two-Line Elements set is a specific data format used to carry information. The position of a satellite can be computed knowing the TLE and the orbital model in use for that satellite. It is quite essential to keep records of the orbital elements of all space objects. For LEO satellites, TLE have the additional advantage of providing information about decay prediction. In the case of VORSat, it is an even more useful feature because one of the milestones, as it has been already referred, is the prediction of de-orbiting and consequent recovery of a capsule that the satellite is going to carry inside it.

They are publicly disclosed and disseminated over the Internet in the form of TLE.

TLE are composed by 3 lines of information. Line 0 has 24 columns maximum and the remaining lines have 69 columns maximum.

The composition of complete TLE information respects table 2.8.

Table 2.8 – TLE Format.

LINE 0	
COLUMNS	CONTENT
1 - 24	Satellite Name
LINE 1	
COLUMNS	CONTENT
1	Line Number
3 - 7	Satellite Catalog Number
8	Elset Classification
10 - 17	International Designator
19 - 32	Element Set Epoch (UTC)
34 - 43	1st Derivative of Mean Motion With Respect to Time
45 - 52	2nd Derivative of Mean Motion With Respect to Time (decimal point assumed)
54 - 61	B* Drag Term
63	The Number 0
65 - 68	Element Number
69	Checksum
LINE 2	
COLUMNS	CONTENT
1	Line Number
3 - 7	Satellite Catalog Number
9 - 16	Orbit Inclination (degrees)
18 - 25	Right Ascension of Ascending Node (degrees)
27 - 33	Eccentricity (decimal point assumed)
35 - 42	Argument of Perigee (degrees)
44 - 51	Mean Anomaly (degrees)
53 - 63	Mean Motion (revolutions / day)
64 - 68	Revolution Number at Epoch
69	Checksum

Some of these fields require an explanation for a better understanding.

Satellite Catalog Number is assigned sequentially to each object. This number is always aligned to the right. When it is inferior to 10 000 the left spaces must be padded with zeros or spaces.

Elset Classification shows the security classification of an object. It may be “U” for Unclassified or “S” for Secret.

The International Designator is another way for object identification. The first 2 characters designate the launch year. The following 3 characters point out the launch number of that year. The last 3 characters indicate the piece of the launch.

Columns 19 and 20 in the Element Set Epoch field indicate the last 2 digits of the launch year. It is necessary to add 1 900 for years which have last 2 digits ≥ 57 and 2 000 for all the others. The following characters designate the year of the day and the fractional portion of the day.

1st Derivative of Mean Motion must be divided by 2 and 2nd Derivative of Mean Motion must be divided by 6.

Column 63 of line 1 contains number “0” but originally it should have been the “Ephemeris Type”.

Checksum is the sum of all characters in each line in modulo 10. Blank spaces, periods, letters and the plus sign are assigned a “0” and the minus sign is assigned a “1”.

2.8 – Time Difference of Arrival Antennas

Notwithstanding the construction of the antenna is of paramount importance, a Time Difference of Arrival antenna is easy to build and has no great requirements to operate. Its basic design consists of a small dual-antenna array and an electronic antenna switching unit. The array is commonly composed of 2 vertical dipole antennas with separations of 30 to 90 cm, assembled on a support with the shape of a T, in order to allow the rotation of the array (figure 2.18 [16]).

The antenna switching unit will allow the switch of the receiver between the dipoles at a rate of 1 000 times per second. There are additional features that can be implemented, but with only the mentioned specifications the antenna will work.

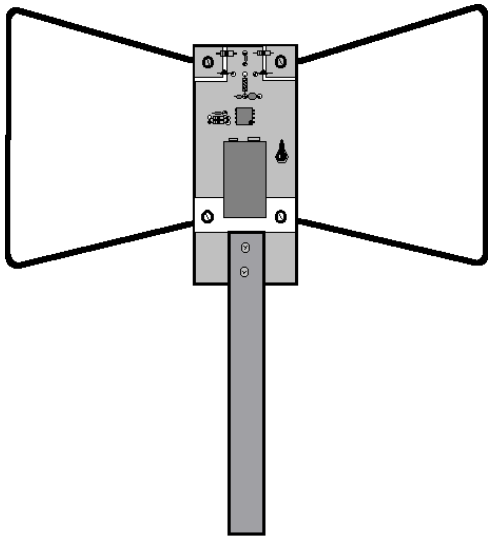

Figure 2.18 – A TDOA antenna.

TDOA antennas are reception only equipments and are used when the goal is to increase precision in the search and determination of the direction of fields. It detects the phase difference of an RF signal in reception by each dipole. The phase of the RF signal will be the same if the dipoles are at the same distance of the source but by rotating the array or if the source moves, one of the dipoles will be closer to the source and that will cause a phase difference between the received signals. The receiver will emit an audio tone that will become higher with the increase of the phase difference. This tone will disappear when dipoles are at the same distance of the source of the RF signal [16].

In the case of these antennas it is not easy to determine whether the source is in front or behind the antenna when the phase difference does not exist, but there are techniques to find it out. In the case of reception of signals from VORSat, the reception will only be accomplished during the maximum of 15 minutes of each passage over each ground station.

2.9 – Ongoing Studies on Attitude Measurement

Attitude determination in VORSat uses a pioneer technique, already described.

However, other techniques of attitude estimation had already been applied and studied, with acceptable results.

Norwegian satellites UWE-2 and UWE-3 had as primary objective to study the attitude in orbit using onboard sun sensors, magnetometers and 3-axis gyros. Three different methods were used: Enhanced Triad Algorithm (ETA), Enhanced q-Method Algorithm (EQA) and Isotropic Kalman Filter (IKF). Tests that were done showed that IKF is the best option within these three hypotheses [17].

In Harbin Institute of Technology, in China, other technique for attitude determination is currently under study. It is based on the fact that a traditional single axis attitude measurement sensor can determine only the angle between the sensor perpendicular and a single incident vector like a star or sun light. So, at least three sensors are required to determine the incident vector and six more sensors are needed for the attitude of the satellite body. Because this method is hard to apply on microsatellites, the substitution method is to obtain the vectors through observation of x-rays emitted by pulsars [18].

These are only two examples of what has been done so far. Other techniques for attitude determination of micro, nano and picosatellites are on study at the moment, but most of them use onboard equipment such as sensors. What is intended in VORSat is to compute satellite attitude from the ground, using the angle of sight as one of the axis.

The overall of the projects pursues attitude control as well. As already referred, that is only a partial concern for VORSat project.

2.10 – Summary

This chapter provided an overview of the several different topics this dissertation is going to be based on.

First of all, it has been presented a brief history of satellites and its operation. Then, a comparison of all kinds of orbits and its specific features has been made, in order to provide a full comprehension of CubeSats own characteristics. A brief summary of the launches made so far has also been presented.

Losses in satellite communications have been studied and the major characteristics of operations with PN sequences have been detailed.

Also, an introduction of the TLE to be sent and some basic notions about TDOA antennas were also made.

Chapter 3

Attitude Determination

Attitude determination is the major milestone of this dissertation and probably of this project. This chapter will be focused in the downlink transmission, in attitude determination and in the losses suffered on its path to Earth. It includes the scheme of transmission of antennas, the choice of sequences to use and the way they have been obtained, as well as how it allows determination of the attitude of VORSat.

3.1 – Transmission Scheme

Project VORSat has suffered some changes since its conception. Initially, it was being designed to operate with 18 antennas, 3 per each one of the 6 faces of the cube.

Meanwhile, developments dictated that there will be only 4 faces of the cube destined for attitude determination, what results in 12 antennas, with the same 3 antennas per face. The other 2 faces, the tops of the prism formed by a 3U satellite, have other purposes, like communication with other satellites.

Both satellites involved in this specific project are meant to have the same transmission scheme. This study will be made for VORSat and an analogy is made to the other space craft.

Transmission will be performed by one antenna at a time. A switch will allow the commutation of antennas so that one burst is a result of the transmission of 3 antennas. A full cycle is completed when all the 12 antennas transmit. All 4 faces must repeat the same information, because it is predictable that only one face may be in the direction of the Earth in each cycle. This ensures the correct transmission of information to the ground.

The number of bit sequences available for use in each satellite influences the transmission scheme.

The chosen polynomials of length N = 63 only allow 6 m-sequences, as it will be explained in chapter 3.2. This means that the number of available sequences for each satellite is 3. It is mandatory to refer that the sequences cannot be shared by the satellites. Otherwise, the probability of interference, and consequently the bit error ratio would be significantly higher.

With only 3 sequences per satellite, 1 sequence was reserved for synchronism and attitude determination and 2 for data transmission:

- PRBS1: synchronism / attitude determination
- PRBS2, PRBS3: data
- PRBS4, PRBS5, PRBS6: 14BISat

These sequences have specific autocorrelation and crosscorrelation properties.

- PRBS1 to PRBS3 must have excellent autocorrelation properties;
- Crosscorrelation between PRBS1 and PRBS2 has to be good;
- Crosscorrelation between PRBS1 and PRBS3 has to be good;
- Crosscorrelation between PRBS1 to PRBS3 (VORSat) and PRBS4 to PRBS6 must be high but there is no need to be excellent.

Attitude of VORSat will be determined using the autocorrelation of the synchronism sequence.

Sequences for data transmission will be transmitted shifted in time and in carrier phase to transmit information, to transmit telemetry data or to send the TLE. Information about the face that is transmitting will be carried in a specific field of all words that will be sent.

3.2 – Sequences and Basic Features

During the research for the best option to send information, several possible solutions have been considered. The main aspects to focus in are robustness, immunity to transmissions errors caused by noise, jamming or interference and the number of information bits allowed, taking into account the needs for this particular case.

In order to find out the length of the sequences to use and, consequently, the degree of the polynomial, some calculations had to be made. The intention is to have approximately 10 bursts per second. This means that with 12 antennas and 10 bursts per second, 1 PN sequence is transmitted in each 1/120 seconds. In order to provide a margin for Doppler effect in the audio band, the signal in reception must occupy nearly 16 kHz. So, the length of the two sequences to use may be provided by the following expression

$$N \times 2 \times 120 \approx 16\,kHz$$

The conclusion to take is that the best option is to use sequences of length close to 66.

Polynomials of degree 6 have length 63 and polynomials of degree 7 have length 127. So, the closest one can get is to use length 63. Polynomials of degree 6 also present the advantage of having a great amount of bits with crosscorrelation with the value “-1”, as it will be explained later.

The number of m-sequences with n = 6 is given by the expression 2.19.

$$\Phi\,(N)/n = \Phi\,(2^n - 1)/n = 6$$

The 6 polynomials with n= 6 are:

- $x^6 + x + 1$
- $x^6 + x^4 + x^3 + x + 1$
- $x^6 + x^5 + 1$
- $x^6 + x^5 + x^2 + x + 1$
- $x^6 + x^5 + x^3 + x^2 + 1$
- $x^6 + x^5 + x^4 + x + 1$

For a mere question of number of connections, the sequences $x^6 + x + 1$ and $x^6 + x^5 + 1$ may be the best option because the circuit to implement has only 2 connections, but that is not a decisive criterion. The most important aspect is correlation.

According to the requirements mentioned above for autocorrelation and crosscorrelation between PRBS1, PRBS2 and PRBS3, it was defined that:

- Synchronism: $x^6 + x^5 + x^2 + x + 1$
- Data1: $x^6 + x + 1$
- Data2: $x^6 + x^5 + x^3 + x^2 + 1$

From this polynomial, sequences *u* and *v* have been generated (figure 3.1), with the condition that they form a preferred pair. The sequence *v* was generated by decimation of the frequency *u* by a decimation factor q = 5. N and q are prime numbers (gcd (N, q) = 1). Therefore, this decimation originates a sequence with the same length.

$$Period\ of\ u[q]: \frac{N}{\gcd(N,q)} = 63 \tag{3.1}$$

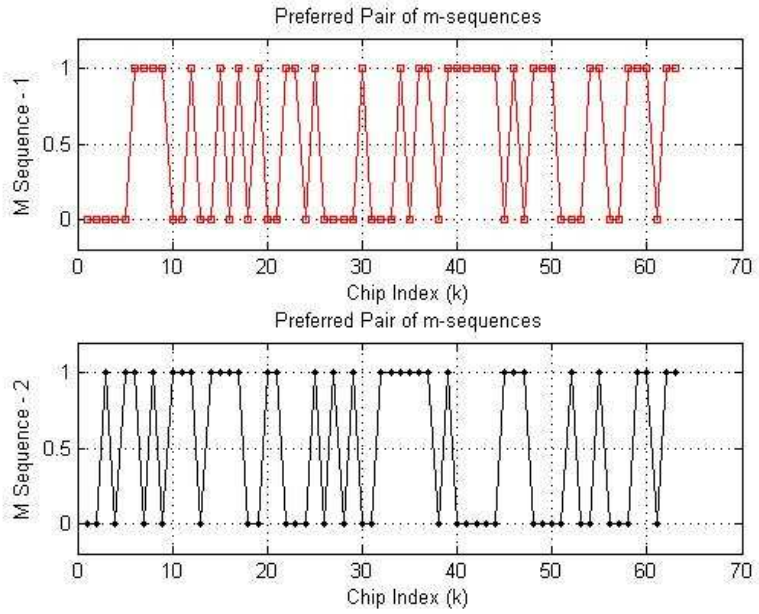

Figure 3.1 – M-sequence-1 (u) and m-sequence-2 (v).

The autocorrelation of an m-sequence has only two values (-1 and N), as already explained. So, the autocorrelation of a sequence of 63 bits must be -1 in all points except in the centre. Both sequences u and v have autocorrelation values R = {– 1, 63}.

Crosscorrelation between 2 sequences of N= 63 must have $|Rc(j)|_{max} \geq 7.88$, according to the expression 2.20.

Knowing that n = 6 is even, $t(n) = 2^{(n+2)/2} + 1 = 17$.

The absolute crosscorrelation of this pair is Rc = {– t(n), -1, t(n) – 2} = {-17, -1, 15}, what respects Welch lower bound, and the simulation confirms it in figure 3.2. Relative crosscorrelation has minor importance in this case, even though it is smaller for longer sequences.

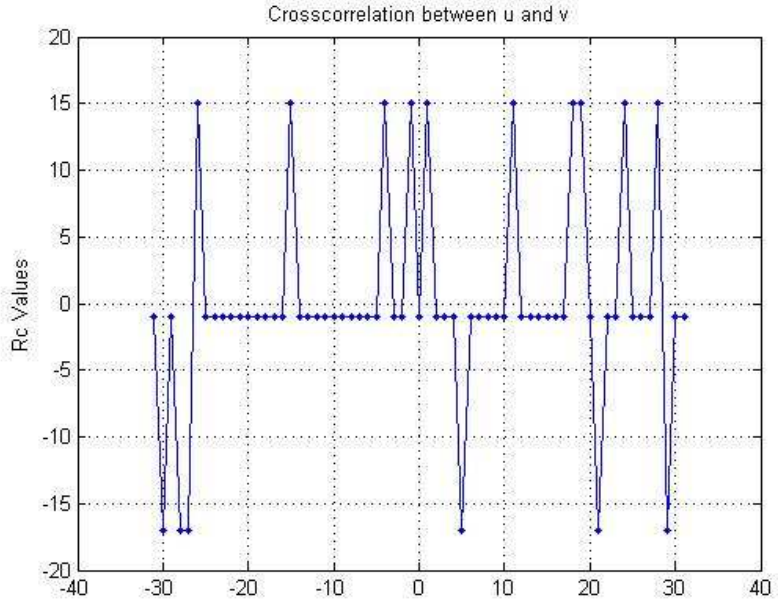

Figure 3.2 – Crosscorrelation of sequences *u* and *v*.

As expected, the cross correlation between a preferred pair is three valued. There are 10 chip delays with the value 15 and 6 with the value -17. Once the sequence has 63 bits, the remaining 47 have the value -1. Theory states that for n even and not multiple of 4, the frequency of occurrence of the values of crosscorrelation of a sequence are:

$$Rc(j) = \begin{cases} -1 \rightarrow \approx 75\% \\ -t(n) \rightarrow \approx 12.5\% \\ t(n) - 2 \rightarrow \approx 12.5\% \end{cases} \tag{3.2}$$

In this case, n = 6. The frequency of occurrence is provided by expression 3.2.

$$Rc(j) = \begin{cases} -1 \rightarrow 47/63 \approx 74.60\% \\ -17 \rightarrow 6/63 \approx 9.52\% \\ 15 \rightarrow 10/63 \approx 15.87\% \end{cases}$$

Values are close to the expected. It is important that nearly 75% of the frequency of occurrence of Rc(j) = -1 is as high as possible. For n odd, it would only be close to 50%. For n even and multiple of 4, there are no Gold sequences.

For all calculations it is considered a sampling rate (fs) of 48 000 sps, resulting from 6 samples per chip at a chip rate (Rc) of 8 000 cps.

First calculations for 63 chip delays provided quite reasonable results, but failed in another leading aspect, the definition of peaks, that was significantly worsened due to the chips which are not crosscorrelated as -1.

The option fell on availing the remaining 47 chip delays. Sent in QPSK modulation by 3 antennas, they allow for the codification of $\log_2(4x47)^3$ = 22 bits of information. With a full cycle of 0.0945 sec, a bit rate of 232.8 bps is achieved. It is possible, however, to use only 41 of the 47 possible chip delays, because 22 bits of information per face can still be encoded. This is a satisfactory result in terms of bit rate, but the peak definition could still be improved.

Thus, among the 47 chip delays of crosscorrelation -1, the 26 that have vicinity also with level -1 can be used. All the other polynomials that originate sequences with n = 6 have been tested and all present the same number of possible delays. 26 chip delays sent in QPSK modulation by 3 antennas allow for the codification of $\log_2(4x26)^3$ = 20 bits of information. With the same full cycle of 94.5 msec, a bit rate of 211.6 bps is achieved. The great advantage of using delays with these characteristics lies on, at expenses of 2 bits and a lower throughput, allowing a much better peak definition. As it will be seen in this chapter, an improvement in peak definition means lower interferences between sequences in order to accomplish the desirable result. This solution allows for face decoding.

The final solution considers then 2 sequences using the same 26 phase shifts, modulated in QPSK. This will allow for 2 x 26 x 4 = 208 combinations. Each antenna will allow the transmission of $\log_2(208)$ = 7 bits of information, which would totalize 21 bits per face. But if the transmission is made in a block “per face” and not “per antenna”, $\log_2(208)^3$= 23 bits of information can be sent. It compensates to perform transmission per face. That gain reflects significantly in the bit rate. If one should consider the transmission of each antenna separately, a bit rate of 222.2 bps would be achieved, but with the transmission of a block per face it is possible to get a throughput of 243.4 bps, a difference of more than 20 bits per second.

Table 3.1 resumes the main characteristics of the final solution.

Table 3.1 – Characteristics of the solution to implement.

FEATURE	VALUE	UNITS	MEANING	EXPRESSION
Sampling Rate	48000	sps		
Chips	63			
Samples	6	spc		
Chip Rate	8000	cps		
Tseq	7,9	msec	Time each sequence takes to be sent	Chips / Chip Rate
Tface	94,5	msec	Time between visits of each face	Tseq x 12
Fface	10,582	Hz	Face visitation frequency	1 / Tseq
Sequences	2			
Phase Shifts	26			
Modulation	4		Possible phase shifts in QPSK	
Combinations	208		Number of possible combinations	Seq. x Ph. Shifts x Mod.
Bits per Antenna	7	Bits	Number of bits/antenna sent	$\log_2(208)$
Tx Antenna	21	Bits	Number of bits w/ separate antenna tx	Bits/Ant x Nr Antennas
Tx Face	23	Bits	Number of bits/face sent	$\log_2(208^3)$
Bit Rate (Tx Ant)	~ 222.2	bps		Tx Ant / Tface
Bit Rate (Tx Face)	~ 243.4	bps		Tx Face / Tface

3.3 – Modulation

It is mandatory to refer that a search for the best modulation has been made during the whole process of finding the best solution to implement. The goal was to maximize the number of bits to send with the lowest BER. Only QPSK, 5-PSK and 6-PSK modulations were considered.

As an example, in an early stage 3 sequences for information transmission per satellite were to be used, allowing face decoding. Table 3.2 illustrates the number of information bits allowed for each modulation.

Table 3.2 – Number of Information Bits available depending on each modulation and the number of chip delays used, with face decoding.

Nr. Chip Delays	**QPSK** Info Bits	**5-PSK** Info Bits	**6-PSK** Info Bits
47	22	23	24
…			
43	22	23	24
42	22	23	23
41	22	23	23
40	21	22	23
…			
34	21	22	23
33	21	22	22
32	21	21	22
31	20	21	22
…			
27	20	21	22
26	20	21	21
25	19	20	21
24	19	20	21

Table 3.3 shows clearly that without face decoding the increase of the number of information bits available is significant. As an example, for 26 chip delays using QPSK modulation, face decoding allows 20 information bits while without face decoding the number is incremented to 24. However, as explained before, only 2 sequences for information are available for each satellite. In this case, there is a loss of 1 information bit. 5-PSK and 6-PSK modulations allow 24 bits but the gain of just 1 bit is not enough to justify the increased risk of symbol error in transmission. A symbol could cross the decision region much easier because the separation between symbols in these modulations is:

- QPSK: 90º
- 5-PSK: 72º
- 6-PSK: 60º

Table 3.3 – Number of Information Bits available depending on each modulation and the number of chip delays used, without face decoding, with 3 PRBS and 2 PRBS for information transmission in the left and in the right respectively. Marked in grey it is the final solution.

USING 3 SEQUENCES FOR Tx INFO			
Nr. Chip Delays	**QPSK** Info Bits	**5-PSK** Info Bits	**6-PSK** Info Bits
28	25	26	26
27	25	25	26
26	24	25	26
25	24	25	26
24	24	25	26
23	24	25	26
22	24	25	25
21	23	24	25
20	23	24	25
19	23	24	25

USING 2 SEQUENCES FOR Tx INFO			
Nr. Chip Delays	**QPSK** Info Bits	**5-PSK** Info Bits	**6-PSK** Info Bits
28	23	24	25
27	23	24	25
26	23	24	24
25	22	23	24
24	22	23	24
23	22	23	24
22	22	23	24
21	22	23	23
20	21	22	23
19	21	22	23

With QPSK defined as the signal modulation to use, it is possible to present the respective modulation scheme (figure 3.3).

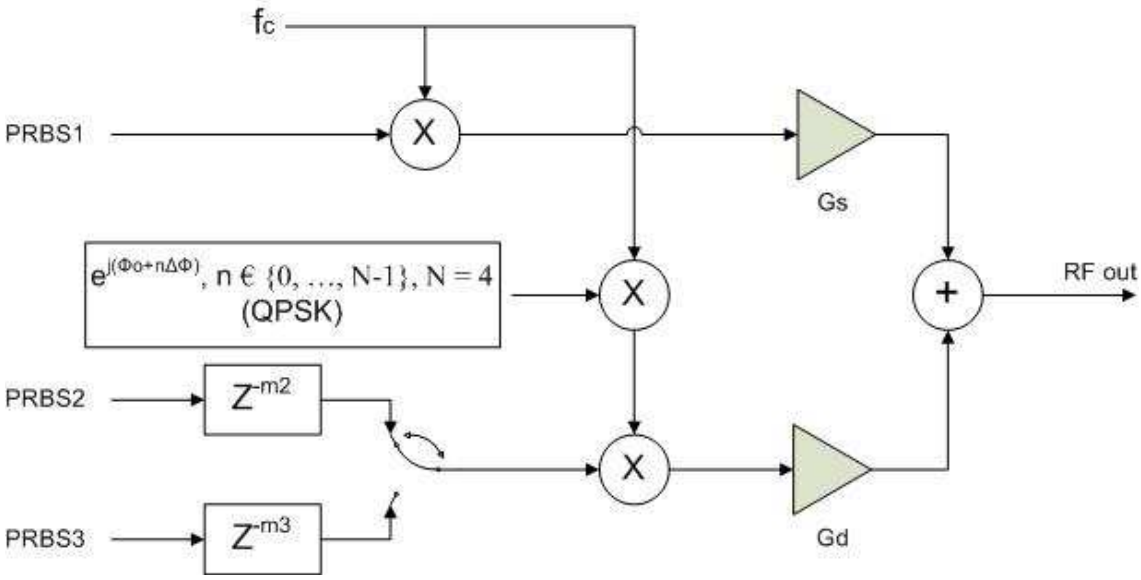

Figure 3.3 – Modulation Scheme.

As figure 3.3 illustrates, PRBS1 will be multiplied by the carrier. PRBS2 and PRBS3 will be transmitted alternately, and modulated in QPSK.

3.4 – Peak Definition

In order to prove the feasibility of determining attitude with these techniques, several other steps must be taken.

Peak definition was sought using Matlab. After generating sequences *u* and *v*, vector *I* containing the chip delays where the crosscorrelation between *u* and *v* takes the value -1 is created, where “1” means Rc = -1 and “0” means Rc = -17 plus Rc = 15. There are 47 “1” and

16 “0”. *I* must be resized because there are only 26 required chip delays, the ones which have vicinity also with value -1. *I* signalizes now 26 “1”.

Vector *Ica* contains the indexes of the chips with Rc = -1. *Ica* has, obviously, the same number of “1” of *I*.

In order to fulfill the goal of having 6 samples per bit, sequences *uu* (*u* sampled 6 times) and *vv* (*v* sampled 6 times) have been created. The crosscorrelation between *uu* and *vv* is, as expected, similar to the one between u and v, excepting the number of samples (figure 3.4).

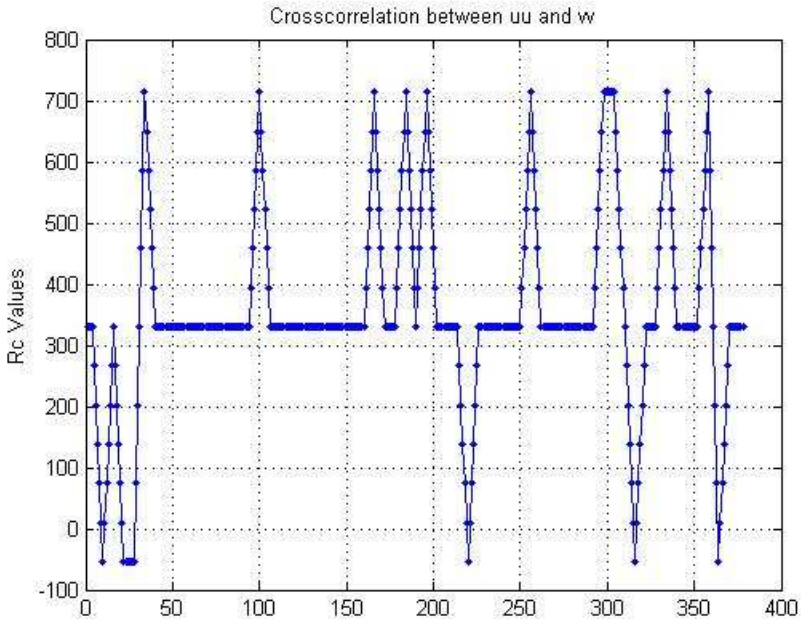

Figure 3.4 – Crosscorrelation between *uu* and *vv*.

To achieve modulation of a message in QPSK, it is necessary to perform a base change. In this particular case, the new base is 208.

The base change can be accomplished following the next steps:

Original message: a
New base: b
>> int1 = a/b^2
>> int2 = $(a - int1(b)^2)/b$
>> int3 = $a - int1(b)^2 - int2(b)$
>> int1 = shift1 x 4 + QPSK1
>> int2 = shift2 x 4 + QPSK2
>> int3 = shift3 x 4 + QPSK3

With these values, it is possible to complete a table with information about the transmission of the 3 antennas of 1 face. Table 3.4 is prepared for the 26 possible phase shifts of this particular case.

Table 3.4 – Phase shifts of the signal to be transmitted in the new base for each antenna.

	Phase Shift (0-25)	**QPSK** (0-3)
Antenna 1	shift1	QPSK1
Antenna 2	shift2	QPSK2
Antenna 3	shift3	QPSK3

According to steps presented above, the base change of the generic message "1231231" results in:

>> int1 = 4 x 7 + 0
>> int2 = 4 x 23 + 3
>> int3 = 4 x 19 + 3

The previous table may be filled with these values (table 3.5).

Table 3.5 – Phase shifts of the signal to be transmitted with the generic message "1231231".

	Phase Shift (0-25)	**QPSK** (0-3)
Antenna 1	7	0
Antenna 2	23	3
Antenna 3	19	3

Matrix *s* contains the phase shifts that allow the QPSK modulation.
The phase shifts that are going to be transmitted by the antennas are:

- Ica (7+1) = 16
- Ica (23+1) = 55
- Ica (19+1) = 51

I is replicated 3 times and sampled 6 times, originating *II*.

The goal is to isolate as much as possible the peaks of transmission, so that a better definition can be achieved. Figures 3.5, 3.6 and 3.7 show clearly the values of *Ica* above (16, 55 and 51) multiplied by 6 samples (96, 330 and 306).

It is important to refer that *II*, in green, takes value "1" multiplied by 100 where the crosscorrelation is low, so that it may be clear that the signal that can be seen is *vv*. By this way, the peak is clearly defined. The search for the crosscorrelation chip delays that have value -1 and vicinity also -1 is now explained by the simulation performed in Matlab. The intention was to isolate the peaks as much as possible so that less interference caused by other sequences exists.

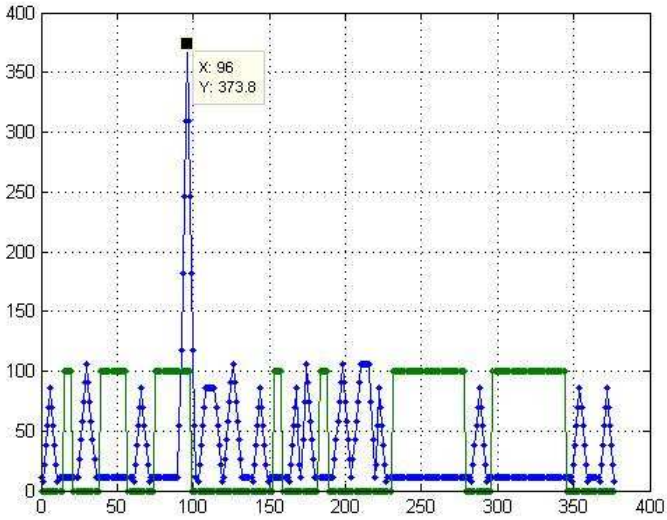

Figure 3.5 – Peak 1.

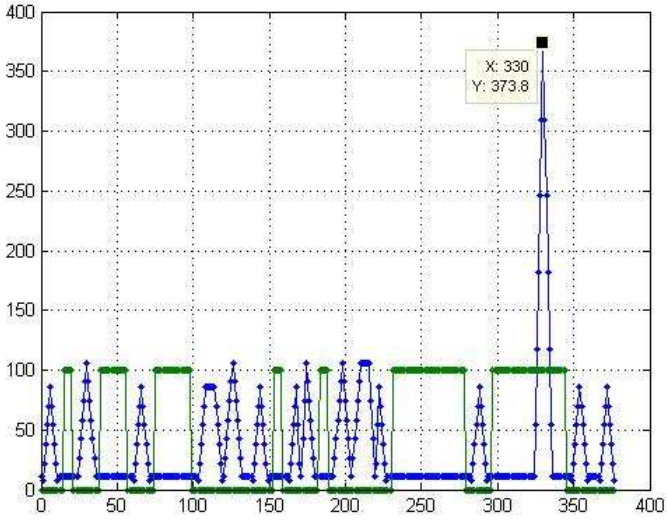

Figure 3.6 – Peak 2.

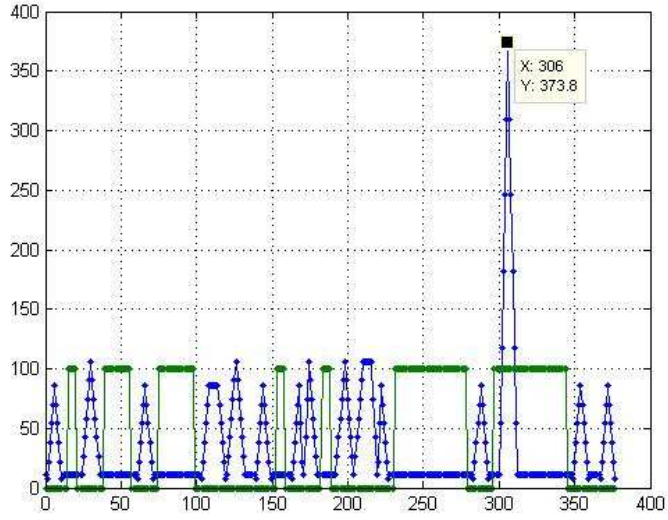

Figure 3.7 – Peak 3.

This signal will be windowed by a Tukey window, so that errors can be minimized.

When computing a non-periodic signal, it will suffer leakage, which is basically the dispersion of the signal, reducing its amplitude, causing losses.

Windowing reduces leakage, so it is mandatory to choose a proper window. Tukey window is the best option, because though there are better options for leakage avoidance and amplitude accuracy, it is good for frequency accuracy [19]. It is indicated for random signals. Although, it has the great advantage of being the best option by far in the reduction of the side lobes, which is of great importance since what is being looked for is peak definition.

After windowing, figures 3.8, 3.9 and 3.10 are attained.

All peaks suffer a shift of 4, due to the effect of the Tukey Window. This is the effect of the filter that has a degree 9.

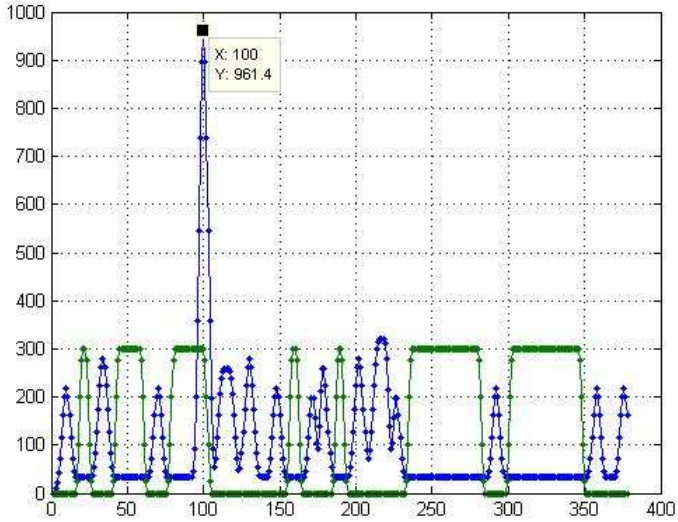

Figure 3.8 – Peak 1 with Tukey Window.

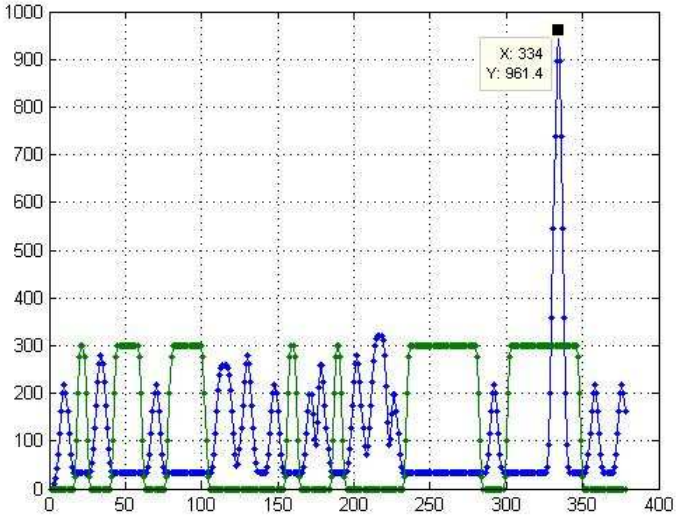

Figure 3.9 – Peak 2 with Tukey Window.

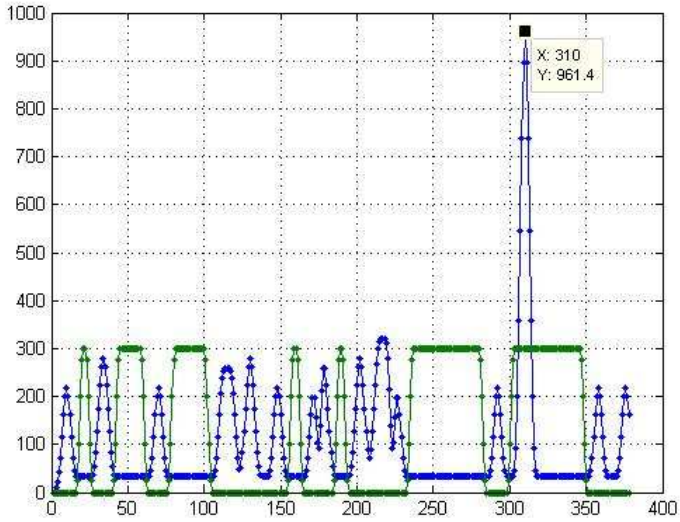

Figure 3.10 – Peak 3 with Tukey Window.

3.5 – Synchronism

All Spread Spectrum communications systems require synchronization.

In order to do so, the same sequence used to despread the signal in the reception must be fully synchronized with the sequence used in the transmitter. Once autocorrelation peak is sharp, any mismatch will be punished with losses in processing gain.

Propagation delay, relative clock shifts and different phases between transmission and reception are sources of uncertainty. Also, Doppler effect may cause loss of synchronization.

With f_c = 2.45 GHz, c = 3 x 10^8 and $v_r \approx 7\,800$ ms^{-1}, the Doppler effect in this case causes a frequency uncertainty of:

$$\Delta f = -\frac{v_r}{c}.f_c = 63.7\ kHz \tag{3.3}$$

Two steps have to be taken, acquisition and tracking, for alignment and maintenance of the best possible waveform, so that the correlation must be the best possible and therefore the best SNR can be maintained.

Acquisition may be serial or serial/parallel.

Serial has an acquisition time of

$$T_{acq} = 2N_c^2 T_c \tag{3.4}$$

Serial/parallel has an acquisition time of

$$T_{acq} = \frac{2}{3}N_c^2 T_c \tag{3.5}$$

The second option reduces greatly acquisition time, but it brings more costs and complexity. For long codes, serial acquisition is unacceptable.

Acquisition will be accomplished by selecting excerpts of the received signal and multiplying it by the synchronism sequence, so that the peak of its autocorrelation can be found. When that happens, it is necessary to maintain the synchronization in order to achieve a correct reception of the signal.

The peak in the autocorrelation helps in the retrieval of the carrier phase. In each antenna, the multiplication by $e^{-j2\pi(fc+\Delta f)t}$ is performed. The signal then passes by a LPF so that it is assured the signal is in the audio band, followed by the correlation with PRBS1 in baseband. The carrier phase is obtained in the peak. The comparison between the phases of the 3 antennas allows the determination of $\Delta\Phi_V$ and $\Delta\Phi_H$ (figure 3.11).

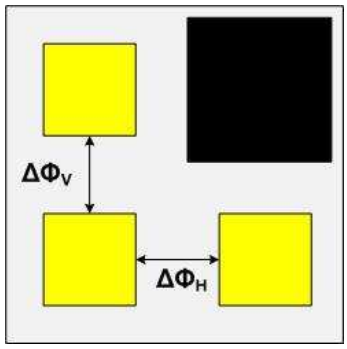

Figure 3.11 – One face of VORSat, with the determination process of $\Delta\Phi_V$ and $\Delta\Phi_H$.

The process of synchronization has not been deeply approached in this dissertation, but is one of the next steps.

3.6 – System Noise

To calculate the link budget, the noise that contaminates the system is an essential component one must not forget.

The system noise temperature (T_{sys}) is the sum of the antenna noise temperature (T_{ant}) and the composite temperature of other components (T_{comp}), according to:

$$T_{sys} = T_{ant} + T_{comp} \tag{3.6}$$

T_{ant} may be known if the total attenuation due to rain and gas absorption (L_{abs}), the temperature of the rain medium (T_m) and the temperature of the cold sky (T_C) are also known. Then, the following expression may be applied:

$$T_{ant} = T_m\left(1 - 10^{-Labs/10}\right) + T_C.10^{-Labs/10} \tag{3.7}$$

Usually, for clouds it is considered T_m = 280 K and for rain T_m = 260 K.

Other components also provoke attenuation of the signal. In order to calculate T_{comp} it is necessary to determine the effective noise temperature and the gain of each stage of the ground station receiver path, according to the expression 3.8:

(3.8)

$$T_{comp} = T_1 + \frac{T_2}{G_1} + \frac{T_3}{G_1 G_2} + \frac{T_4}{G_1 G_2 G_3}$$

The effective noise temperature of each component is provided by:

$$T_N = (F - 1)T_0 \tag{3.9}$$

where:

T_N →Effective noise temperature of stage N (K)
F →Noise figure (dB)
T_0 →Reference temperature (290 K)

Temperature of cold sky (T_C) is the sum of galactic effects and atmospheric effects. A good approximation for this value, combining figures 2.11 and 2.12, is 10 K. Then, it is possible to perform the following calculations. Considering:

T_m = 280 K
T_C = 10 K
L_{abs} = 2 dB (as calculated in section 3.7)

the antenna temperature is:

$$T_{ant} = 280\left(1 - 10^{-2/10}\right) + 10.10^{-2/10} = 109.64\ K \tag{3.10}$$

The reception scheme of the ground station placed in FEUP may be illustrated by figure 3.12.

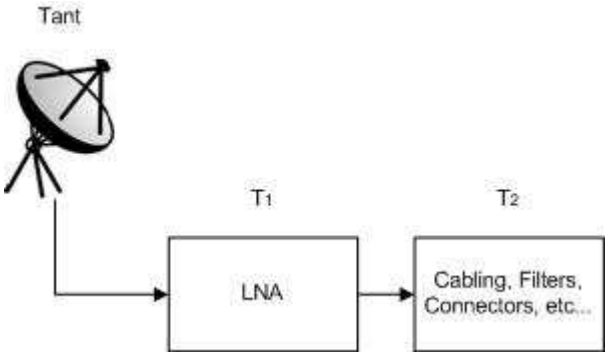

Figure 3.12 – Reception scheme of GS at FEUP.

The first stage of downlink reception is the Low Noise Amplifier (LNA), which is connected to the receiver by short cables and connectors.

The value for the noise figure F in dB will be converted for decimals by:

$$F = 10^{F(dB)/10} \tag{3.11}$$

In the case of the cables, the noise figure is obtained through the attenuation, by the following expression:

$$F = 1 + \frac{(L-1)\,T}{T_0} \tag{3.12}$$

Considering T the physical temperature of the component when $T = T_0$, then F = L.

With the noise figures of the components:

F_{LNA} = 0.5 dB
F_{cabl} = 5 dB

The effective noise temperatures are:

$$T_{LNA} = (F_{LNA} - 1)290 = 35.38\ K$$
$$T_{cabl} = (F_{cabl} - 1)290 = 627\ K \tag{3.13}$$

Knowing that G_{LNA} = 28 dB:

$$T_{comp} = 35.38 + \frac{627}{10^{2.8}} = 36.37K \tag{3.14}$$

The system noise temperature is:

$$T_{sys} = T_{ant} + T_{comp} = 146\ K \tag{3.15}$$

3.7 – Link Budget

The necessary knowledge has been provided in previous sections, as well as some indicators about the values these calculations are going to use.

VORSat will have no uplink for attitude determination. Ergo, what is shown next represent only downlink communication.

Considering:

C →Transmission power (W)
L_e →Transmission losses (dB)
G_e →Transmission antenna gain (dB)
L_{aml} →Misalignment losses (dB)

VORSat will have a power of 0.5 W, of which α is intended for synchronism / attitude signals and 0.5-α for data transmission.

It is also considered that the transmitter will have 80 % efficiency.

The transmission antennas are in a design stage and are being projected to have a transmission gain in an order of magnitude of 5 dB or 6 dB. However, for this link budget calculation, a conservative value of 4.5 dB will be used in order to attain a better margin.

As previously mentioned, it is estimated that 3 dB may be lost due to misalignment.

EIRP will be provided by:

$$EIRP = C.L_e.G_e.L_{aml} \tag{3.16}$$

It becomes possible to elaborate table 3.6.

Table 3.6 – Calculation of EIRP.

Transmission Power	C	0,5	W	-3,01	dB
Transmission Losses	Le	0,80	%	-1	dB
Transmission Antenna Gain	Ge			4,5	dB
Misalignment Losses	Laml	0,5		-3,01	dB
EIRP	**EIRP**	**0,56**	**W**	**-2,52**	**dB**

The following proceeding is the calculation of propagation losses.

The first step is to determine free space loss. This is the feature that most influences satellite communications. In order to achieve an approximate value for free space losses in the worst case scenario, it is obligatory to determine the maximum distance between VORSat and the ground station.

Considering:

r_E →Mean radius of the Earth (m)
θ →Elevation angle (º)
d →Distance GS – Satellite (m)
r_S →Distance centre of the Earth – Satellite (m)

it is possible to represent schematically in figure 3.11 how to calculate that distance and how it varies with the elevation angle:

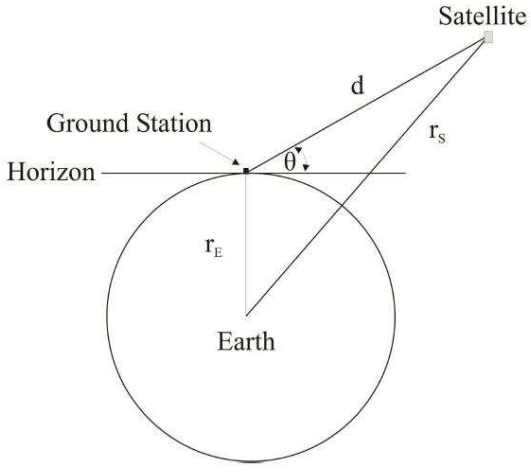

Figure 3.13 – Variation of the distance VORSat – GS with the elevation angle.

From the cosine law:

$$r_S^2 = d^2 + r_E^2 - 2.d.r_E.\cos\left(\theta + \frac{\pi}{2}\right) \tag{3.17}$$

and isolating d in one side of the equation, a dependence of θ is obtained:

$$d = -r_E.\sin(\theta) + \sqrt{r_E^2.(\sin(\theta))^2 + r_S^2 - r_E^2} \tag{3.18}$$

Assuming the worst case for θ and r_S:

r_E = 6 371 km
θ = 5º
r_S = 6 671 km

d is approximately 1 500 km.

According to the expression 2.10, knowing that VORSat will operate at a frequency of 2.45GHz and its signals will be received from very different distances as a result of its LEO, figure 3.12 can be made.

For VORSat link budget calculations, a value of 163.75 dB will be used due to the maximum distance of 1 500 km, what is confirmed by empirical calculations for f = 2.45 GHz and c = $3x10^8$ ms^{-1}.

$$L_{fs} = 10\log\left(\frac{4\pi df}{c}\right)^2 = 163.75\ dB$$

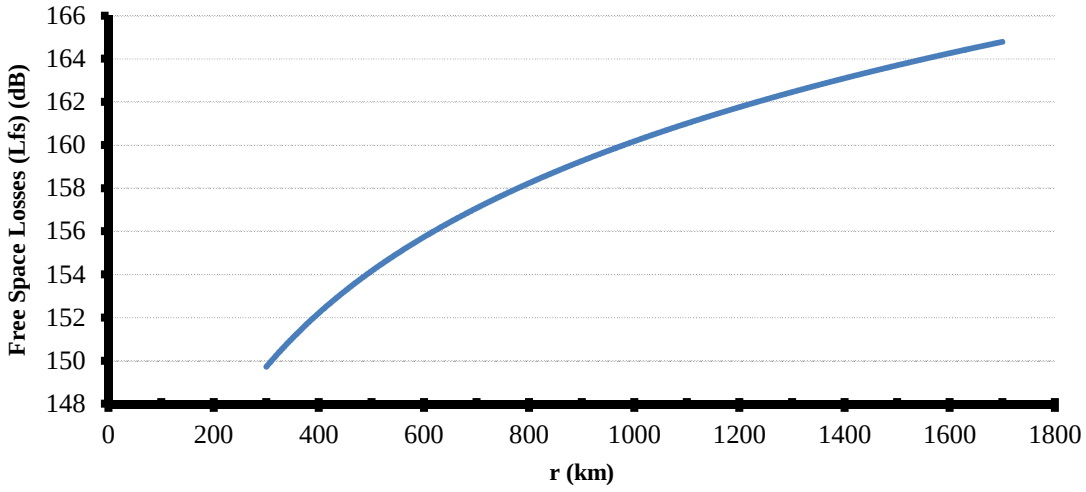

Figure 3.14 – Variation of the Lfs with the distance, considering f = 2.45 GHz.

Atmospheric losses have also to be determined. As said previously, this kind of losses is caused by ionospheric, tropospheric and local effects. Major problems in ionospheric effects are polarization rotation and scintillation effects.

Polarization rotation won't be a problem once the 2.45 GHz of VORSat are significantly below the threshold of 10 GHz when satellite communications start to suffer relevant problems. Also, circularly polarized VORSat will be less prone to polarization rotation issues. Likewise, scintillation effects are barely felt in Portugal as already mentioned. Therefore, ionospheric effects may be neglected.

From other layer in atmosphere come different impairments for satellite communication. Tropospheric effects can be due to attenuation, rain attenuation, gas absorption, depolarization and sky noise.

Attenuation is not relevant for frequencies below 10 GHz.

Rain attenuation won't be calculated because these events will be quite punctual and will affect few passages of VORSat. Also, a margin to compensate impairments caused by rain will be included in gas absorption losses, because these two features are the ones necessary to perform the calculations of the antenna noise temperature.

Gas absorption will cause loss of signal. The 2 peaks observed in figure 2.10 are significantly far from 2.45 GHz. At this frequency, the specific attenuation of oxygen is extremely low, around 0.006 $dBkm^{-1}$. Water vapour contribution is significantly smaller. The same figure represents the absorption in the zenith, in other words, for an elevation angle of 90º ($\theta = 90º$). For lower angles, the atmospheric absorption (L_{abs}) is higher. When VORSat is near the zenith, L_{abs} is 0.036 dB, but since it will pass through its sub-satellite point in several elevation angles, one ought to determine L_{abs} also for the worst case, the threshold of visibility, $\theta = 5º$ (figure 3.13).

Taking into account that the ITU-R recommend calculations with oxygen thickness of 6 km, the atmospheric absorption (L_{abs}) at $\theta = 5º$ will be provided by expression 2.12:

$$L_{abs|5°}(dB) = 0.41\ dB$$

This value is superior to the $L_{abs|90º}$ and it makes sense, once the atmospheric layer the signal has to overcome is thicker. The values for attenuation decrease rapidly with the increase of the elevation angle, according to the graphic shown below.

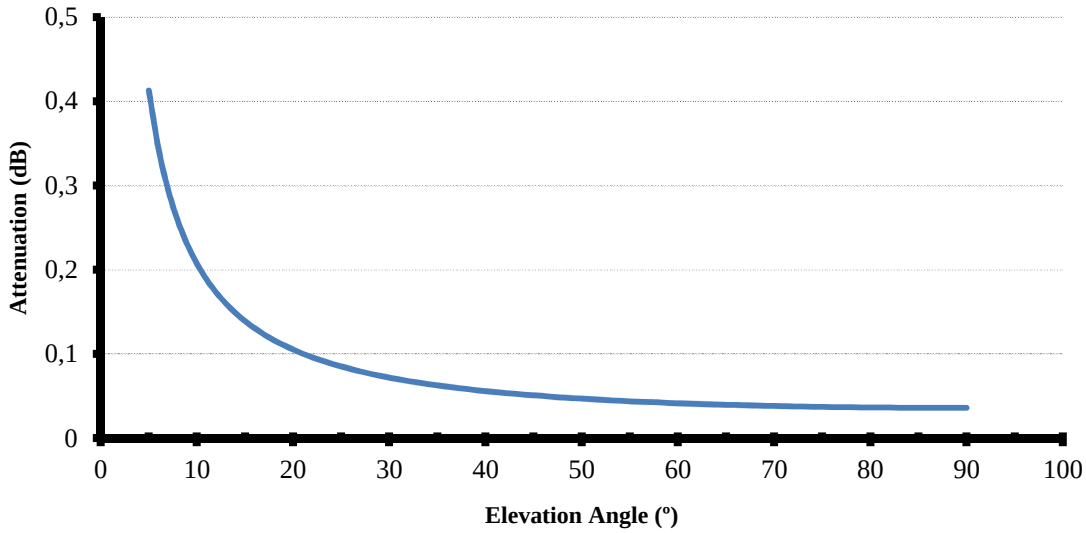

Figure 3.15 – Variation of the attenuation with the variation of the elevation angle of the satellite.

The losses for gas absorption are L_{abs} = 0.41 dB. However, a value of 2 dB will be used in calculations in order to include other losses such as rain attenuation, thereby providing a margin of approximately 1.59 dB.

It is hard to predict the exact amount of losses caused by depolarization. VORSat will transmit the same circularly polarized signals in both transmission and reception, what means

that losses will not be severe. It may be considered that the receiver has 90% efficiency, and that results in losses of 0.46 dB.

Local effects won't be considered in these calculations once the surroundings of the GS placed at FEUP have almost no interference in signal reception.

Propagation losses calculations end with the pointing losses. This is a statistical estimation, and 3 dB is considered a good approximation.

Propagation losses are the combination of all the items mentioned so far (table 3.7).

$$L_{prop} = L_{fs} + L_{abs} + L_{pol} + L_{aml}$$
$$L_{prop} = 169.22\ dB \tag{3.19}$$

Table 3.7 – Calculation of the propagation loss.

Free Space Loss	Lfs			-163,75	dB
Rain Attenuation + Gas Absorption	Labs			-2	dB
Polarization Loss	Lpol	0,9	%	-0,46	dB
Antenna Misalignment Loss	Laml	0,5		-3,01	dB
Propagation Loss	**Lprop**			**-169,22**	**dB**

Considering an isotropic antenna in the reception, the received power will be given by:

$$P_r = EIRP + G_r - L_{fs} \tag{3.20}$$

The parabolic dish antenna parameters allow the calculation of the reception antenna gain (table 3.8).

Table 3.8 – Calculation of reception antenna gain.

Diameter	D	3	m		
Total Efficiency	η	0,5		-3,01	dB
Gain	**Gr**	**2962,11**		**34,72**	**dB**

The determination of P_r becomes possible and:

$$P_r = -131.55\ dB$$

Next step for calculations is the determination of the figure of merit of the receiver, G/T_{sys}, where:

G_r →Antenna gain of the receiver (dB)
T_{sys} →System noise temperature (K)

The figure of merit provides information on the performance of the receiver, as it increases with the figure of merit.

Calculations for the system noise temperature have already been made and the results are presented in table 3.9.

Table 3.9 – Calculation of the system noise temperature.

Reference Temperature	To	290	K		
Rain Medium Noise Temperature	Tm	280	K		
Temperature of the Cold Sky	Tc	10	K		
Rain Atten. + Gas Absorption	Labs			2	dB
Antenna Noise Temperature	Tant	109,64	K		
Noise Temperature of Components	Tcomp	36,37	K		
System Noise Temperature	**Tsys**	**146,02**	**K**		

$$\frac{G_r}{T_{sys}} = \frac{34.72\ dB}{146.02\ K} = 13.07\ dBK^{-1} \tag{3.21}$$

This link budget will be completed in chapter 4 after the data relative to code is treated.

3.8 – Summary

In this chapter, it has been explained the whole process of finding the best PN sequences to be used and how the transmission is going to be made.

Also, it has been shown how a good peak definition is achieved and how important that is for this project's purpose. The choice for QPSK became justified and calculations for the link budget have been made, including the detailed determination of all potential factors of noise and losses.

Chapter 4

Message Definition

Message encoding obeys to strict criteria in building frame data. Frame structure is a key part on the evaluation of the efficiency of a transmission and on the correct encoding of a message. In this chapter, the conclusion of the link budget is also presented.

4.1 – TLE

Not all the Two-Line Elements must be sent by the satellite. Transmitting the TLE in their full format would compromise the coding efficiency and the transmission, because it would require an unaffordable amount of bits. There are some information fields that can be avoided, not only due to their redundancy, but also because they possess information already known by who is going to decode the message.

TLE include capital letters, digits, space, period and the minus and plus symbols. Considering 26 letters, 10 digits and 4 symbols, it would be necessary 6 bits to encode all the characters. However, the fields that contain letters are:

- Line 0: Name;
- Line 1: Elset Classification, International Designator.

The name is supressable. The decoder will know which satellite is transmitting.

The Elset Classification needs a “U” for Unclassified and an “S” for Secret. One can consider there is no need to transmit this field because VORSat will be in the category “Unclassified”. The International Designator indicates the year, the number of the launch in that specific year and the piece of the launch. These fields are not mandatory to be transmitted if any of them is transmitted. However, if one of them is, all must be. This means that the needed characters are reduced to 14. In the case of VORSat, they will respect table 4.1:

Table 4.1 – Coding of characters to be sent.

DECIMAL	HEXADEC	OCTAL	BINARY	CHAR
0	0	00	0000	**0**
1	1	01	0001	**1**
2	2	02	0010	**2**
3	3	03	0011	**3**
4	4	04	0100	**4**
5	5	05	0101	**5**
6	6	06	0110	**6**
7	7	07	0111	**7**
8	8	10	1000	**8**
9	9	11	1001	**9**
10	A	12	1010	+
11	B	13	1011	-
12	C	14	1100	**.**
13	D	15	1101	**SP**
14	E	16	1110	
15	F	17	1111	

All codification can be made in 4 bits, which represents a great gain in transmission. From all of the TLE, it is mandatory to transmit the ones represented in table 4.2.

Table 4.2 – Orbital Elements and Number of Bits necessary to their transmission.

ORBITAL ELEMENT	DESIGNATION	NUMBER OF BITS
Satellite Catalog Number	SCN	20
Element Set Epoch	ESE	56
1st Derivative of Mean Motion	1S	40
2nd Derivative of Mean Motion	2S	32
B* Drag Term	BDT	32
Element Number	EN	16
Checksum (line 1)	Ch	6
Orbit Inclination	OI	32
Right Ascension of Ascending Node	RA	32
Eccentricity	Ecc	28
Argument of Perigee	AP	32
Mean Anomaly	MA	32
Mean Motion	MM	44
Revolution Number at Epoch	RN	20
Checksum (line 2)	Ch	6

4.2 – Frame Structure

The structure of the frame to be sent will be composed by 4 frames, each of them with 2 sub-frames. Frames 1 to 3 will be always sent and frame 4 will be composed by 3 pages that will be transmitted alternately, as figure 4.1 indicates.

Each sub-frame starts with a telemetry word (TLM). The second word of frames 1 and 3 is a handover word (HOW). Each sub-frame will have 8 words, what makes a total of 16 words per frame, where 2 words are always dedicated to telemetry. Each word is composed by 23 bits. From these 23 bits, 3 are for face/frame ID, 4 for checksum and the 16 bits left for information. 16 words with 16 bits of information allow for 256 bits of information in each frame.

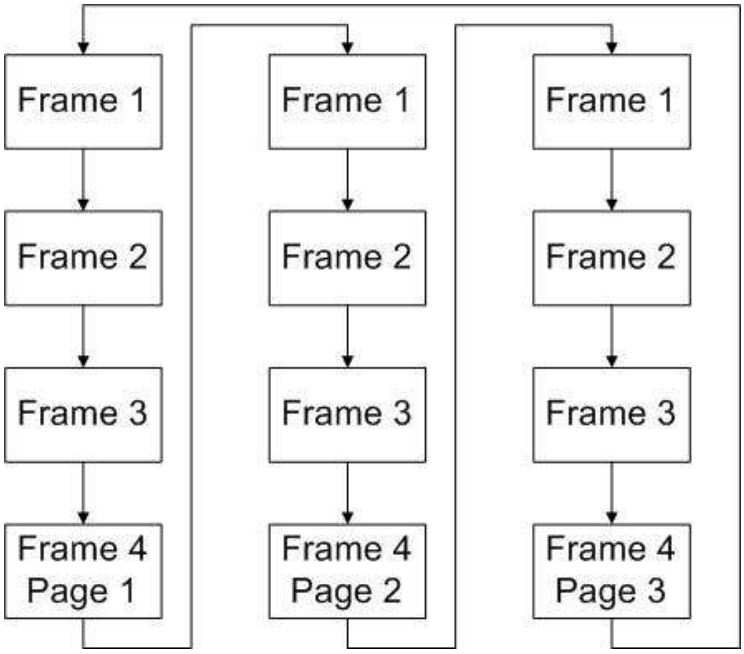

Figure 4.1 – Frame Sequence.

One word is transmitted in 94.5 msec, ergo a sub-frame is transmitted in 0.756 sec. One full frame takes 1.512 sec to be sent. All 4 frames, considering 1 page of frame 4 are transmitted in 6.048 sec. All the information would take 18.144 sec to be transmitted, but as it is going to be shown next, the information contained on the 3 pages of frame 4 may be sent more sparsely.

Message structure of frames 1 to 3 obeys to figure 4.2.

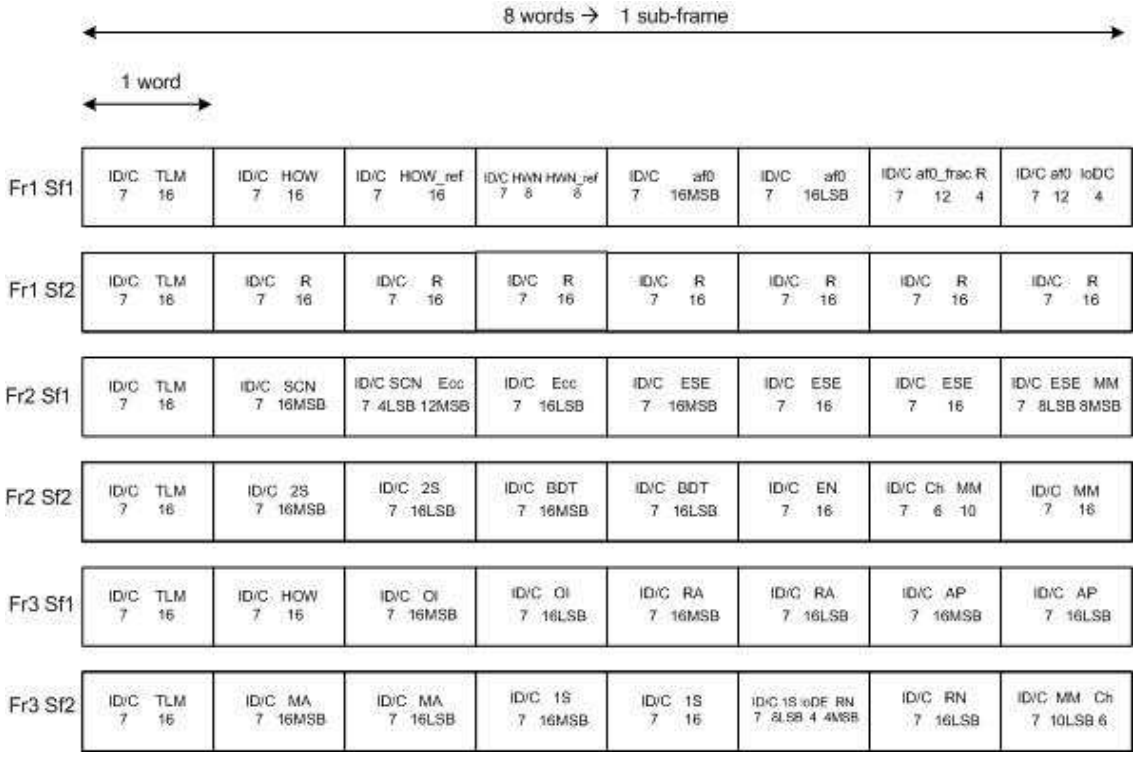

Figure 4.2 – Structure of Frames 1 to 3.

Frame 4 with its 3 pages is represented in figure 4.3.

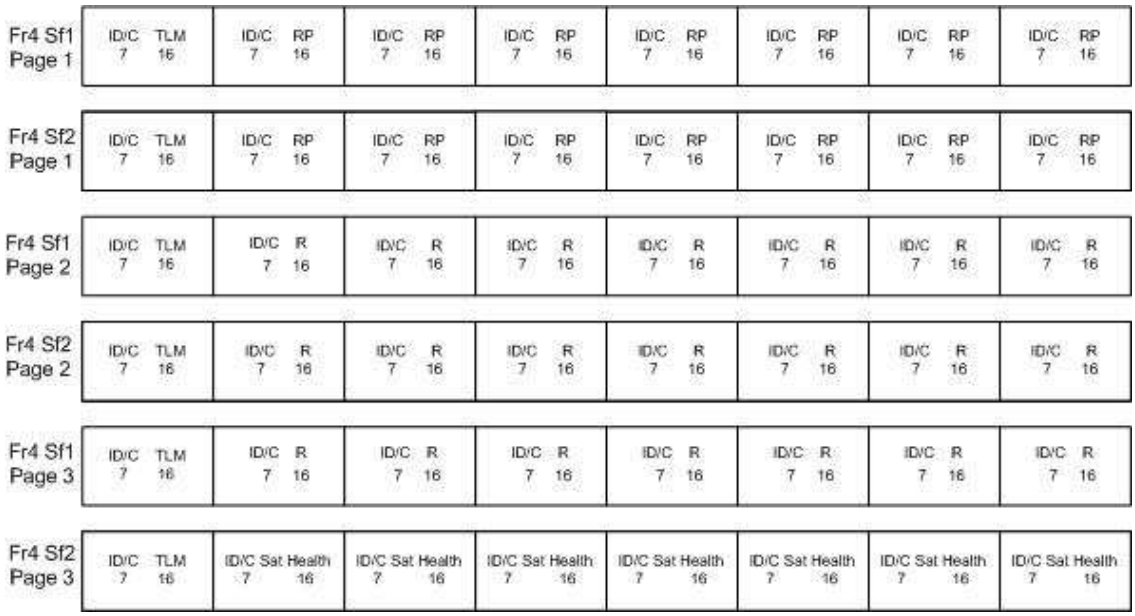

Figure 4.3 – Structure of Frame 4.

Sub-frame 1 of frame 1 is almost fully dedicated to clock correction, where parameters af_1, af_0 and af_{0frac} have great importance in contributing for an increased accuracy in clock correction, because they allow the computation of the GPS time, according to the expression 4.1, where the rate is the 6.048 sec already mentioned.

$$UTC_1 = af_0 + (clock_0 - clock_1).rate(1 + af_1) + af_{0frac} \tag{4.1}$$

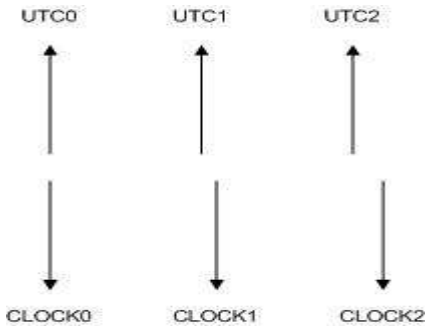

Figure 4.4 – Clock drift.

As figure 4.4 illustrates, there is a normal clock drift with time. Considering a typical crystal, the frequency clock drift is usually less than 10 parts per million. It is desirable that the precision of this drift leads to an error of 1 msec at the end of one day. The number of parts per million of 1 msec in one day is given by 0.001/(24 x 3 600) = 0.01157 ppm.

If the precision of the drift is 0.01 ppm, the error at the end of one day due to the precision is 0.01 x 24 x 3 600 = 0.864 msec, lower than 1 msec. With 12 bits, and in units of 0.01 ppm, there can be represented drifts in the interval [-20.48; +20.47].

From expression 4.1, some important deductions ought to be made.

If $clock_0$ and $clock_1$ match, then $UTC_1 = af_0$. Knowing that af_0 is the offset difference between both clocks, if the offset is equal to UTC_1, then there will be no drift (af_1).

Drift af_1 may be calculated starting from the expression 4.1, as:

$$af_1 = \frac{(UTC_1 - UTC_0)}{(clock_1 - clock_0)} . \frac{1}{rate} - 1 \tag{4.2}$$

The required precision for af_0 is 1 sec.

$Clock_0$ e $clock_1$ require precision of 1 msec.

Both clocks are based on 3 fields, HOW, HWN and HOW_ref, all of them explained forward.

Expression 4.1 can still be rewritten in another way, resulting in the expression 4.3.

$$UTC_1 = af_0 - af_{0frac} + (clock_0 - \lfloor clock_1 \rfloor).rate(1 + af_1) \tag{4.3}$$

In 4.3, af_{0frac} = HOW_ref . rate, it has an accuracy of 1 msec.

Parameter af_1 has a precision of 0.01 ppm.

In terms of required bits, af_1 needs 12 bits, af_0 needs 32 bits and af_{0frac} 12 bits.

Half Week Number (HWN) has the resolution of exactly three and a half days. It is incremented every half week. It is designed to have a capacity much higher than the real needs. CubeSats have an expected lifetime of few months but the field HWN is designed to take 2 years. With an average of 52 weeks per year, this field requires 208 possibilities, what means that 8 bits are needed. HWN_ref will allow the computation of the HWN and also requires 8 bits.

The Issue of Data, Clock (IoDC) and the Issue of Data, Ephemeris (IoDE) fields indicate which version of clock or data, respectively, is being sent. Only 4 bits are enough to avoid any mistakes in decoding the message. These fields have a major importance once it allows the completion of the reception full transmission if it has not been fully received. By this way, the problem of partial reception of data is minimized. Both fields are reset after 1111.

Sub-frame 2 of frame 1 contains 7 words reserved for engineering purposes.

Frames 2 and 3 are entirely destined for the transmission of the TLE. From the 27 words of these 2 frames, there are 432 bits available. The TLE require 428 bits, which means that all the TLE to be transmitted fit almost perfectly in these 2 frames, wherein 4 bits are free to be occupied with IoDE.

Frame 4 contains special data that doesn't need to be sent with the same periodicity. Page 1 is one full frame reserved for the re-entry predictions. This information will provide better accuracy on the splashdown area when de-orbiting phase comes close. Page 2 is reserved for engineering data, like sub-frame 1 of page 3. This page can also be used for a more permanent update of the re-entry predictions when VORSat enters its de-orbiting phase. Sub-frame 2 of page 3 is reserved for the transmission of data concerning satellite's health, which may include the health for signal components or the integrity of the data sent.

4.3 – Word Structure

As said before, all frames are composed by 16 words. Each word is composed by 3 minor fields (figure 4.5).

The ID identifies which face and frame is transmitting the message. If ID0 is “1”, it marks the beginning of a frame. Bits ID1 and ID2 will then indicate which of the 4 frames is being transmitted. If ID0 is “0”, it states that it is not the beginning of a frame. Bits ID1 and ID2 will then provide information on each of the 4 faces dedicated to attitude determination is transmitting.

The checksum performs error detection within each word, as detailed in section 4.4.

Bits 8 to 23 are for information.

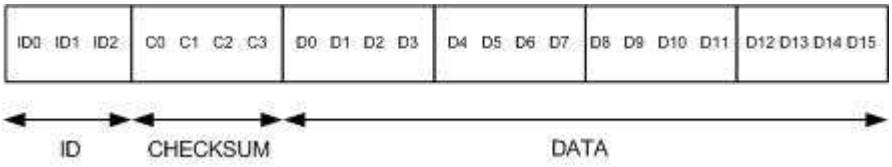

Figure 4.5 – Structure of the Data Word.

However, there are 2 kinds of word that have its own composition.

Like all the other words, TLM word has ID and checksum bits in the first 7 bits (figure 4.6).

Bits 8 to 11 are destined to identify the subject of the telemetry data that follows. Each specific type of data (power, temperature, ISL status, batteries, etc.) will have its own code in the field “Type”.

Bits 12 to 23 are destined to send the telemetry data. It is considered that 12 bits should provide enough precision in data, because they provide 2^{12} = 4 096 levels in quantization, which means that 12 bits allow an accuracy of nearly 0.025 % in that specific item status.

TLM word is updated every 50 cycles (302.4 sec).

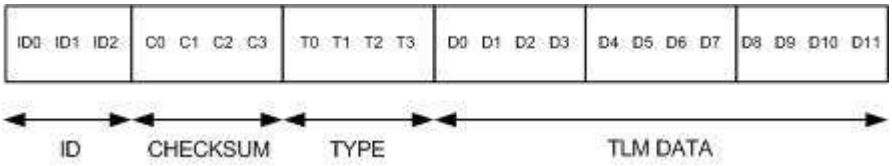

Figure 4.6 – Structure of Telemetry Word.

All handover words obey to the rule that forces all the words to have the first 7 bits dedicated to ID and checksum fields (figure 4.7). The following 16 bits (bits 8 to 23) contain the time-of-week (TOW) count. These 16 bits are the same in frames 1 and 3 of each cycle, where the HOW is sent. This TOW is incremented by 1 each cycle (6.048 sec) and its resolution is precisely 6.048 sec. This counter is reset twice a week. During each half week, TOW count commutates 50 000 times, therefore the need of 16 bits. HOW_ref requires 16 bits and, together with the HOW, will allow in the computation of the time of satellite.

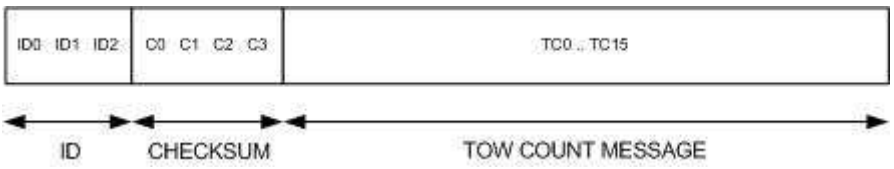

Figure 4.7 – Structure of Handover Word.

4.4 – Code Correction Techniques

The transmissions from VORSat do not include Forward Error Correction (FEC) techniques. Certainly they would potentiate the transmission quality reducing the probability of wrong bit and increasing the number of error detections, but they also would require a greater capacity of the satellite. The implementation of FEC techniques could be one possible use for the bits marked with an "R" for "Reserved" on the frame structure, which are reserved for engineering purposes.

Instead, the option fell on placing checksum in all words, so that errors can be detected immediately. Even that they cannot be corrected, checksum will detect the wrong word and on the ground it will be possible to know which fragment of code is corrupted.

The checksum nibble of an information word is filled according to the following exclusive or operation:

- $C0 = D0 \oplus D4 \oplus D8 \oplus D12$
- $C1 = D1 \oplus D5 \oplus D9 \oplus D13 \oplus ID0$
- $C2 = D2 \oplus D6 \oplus D10 \oplus D14 \oplus ID1$
- $C3 = D3 \oplus D7 \oplus D11 \oplus D15 \oplus ID2$

For a TLM word, the checksum bits obey to:

- $C0 = T0 \oplus D0 \oplus D4 \oplus D8$
- $C1 = T1 \oplus D1 \oplus D5 \oplus D9 \oplus ID0$
- $C2 = T2 \oplus D2 \oplus D6 \oplus D10 \oplus ID1$
- $C3 = T3 \oplus D3 \oplus D7 \oplus D11 \oplus ID2$

The checksum of the HOW is obtained according to:

- $C0 = TC0 \oplus TC4 \oplus TC8 \oplus TC12$
- $C1 = TC1 \oplus TC5 \oplus TC9 \oplus TC13 \oplus ID0$
- $C2 = TC2 \oplus TC6 \oplus TC10 \oplus TC14 \oplus ID1$
- $C3 = TC3 \oplus TC7 \oplus TC11 \oplus TC15 \oplus ID2$

4.5 – Link Budget for Encoding

From the knowledge of:

k →Boltzmann constant ($k = 1.38 \times 10^{-23}$ JK^{-1} = -228.6 dBW/K/Hz),

it becomes possible to determine the ratio of received power (P_r) to noise spectral density (N_0), where:

$$\frac{P_r}{N_0} = \frac{G_r Pri}{kTs} = 69.71\ dBHz \tag{4.4}$$

In a tabular form, this calculation may be presented in table 4.3.

Table 4.3 – Calculation of P_r/N_0.

Free Space Loss	Lfs			-163,75	dB
Rain Attenuation + Gas Absorption	Labs			-2	dB
Polarization Loss	Lpol	0,9	%	-0,46	dB
Antenna Misalignment Loss	Laml	0,5		-3,01	dB
Reception Antenna Gain	Gr			34,72	dB
System Noise Temperature	Tsys	146,02	K		
Figure of Merit	Gr/Tsys			13,07	dB/K
Received Power	Pri	6,04E-18	W	-131,55	dB
Boltzmann Constant	k	1.38E-23	J/K	228,6	dB/K/Hz
Ratio Received Power / Noise Spectral Density	**P_r/N_0**			**69,71**	**dBHz**

This calculation has been performed for the case of the maximum distance.

Next step is the determination of the bit error ratio. It depends on 3 possible sources of noise:

1. QPSK modulation;
2. Chip Delay;
3. PN codes.

Also, this determination must be made for the 2 distances considered more relevant in this case:

1. 1 500 km (maximum distance);
2. 500 km (distance at which the transmission must occur in perfect conditions).

For the determination of the probability of error in QPSK it is necessary to perform the following steps.

The determination of the signal to noise ratio (SNR) obeys to the expression 4.5.

$$SNR = B \times EIRP \times L_{fs} \times L_{pol} \times L_{aml} \times L_{abs} \times \left(G_r/T_{sys}\right)/k \tag{4.5}$$

Code to Noise Ratio (CNR) is provided by:

$$CNR = SNR \times Chip\ Gain \tag{4.6}$$

Chip Gain will take always the value $\sqrt{63}$, due to the length of each PN code.

So that the Bit Error Ratio can be calculated, it is necessary to perform the determination of the probability of symbol error in QPSK, according to the expression 4.7.

$$P_{QPSK} = erfc\left(\sqrt{\frac{E_S}{2N_0}}\right) - \frac{1}{4}erfc^2\left(\sqrt{\frac{E_S}{2N_0}}\right) \tag{4.7}$$

E_s/N_0 depends on the modulation. In this case, M = 4.

$$\frac{E_S}{N_0} = \frac{E_b}{N_0}.\log_2 M \tag{4.8}$$

The second factor of the expression 4.7 may be negligible. Also, $E_s/N_0 = 2\ E_b/N_0$. A simple substitution will allow the calculation of P_{QPSK} according to:

$$P_{QPSK} = erfc\left(\sqrt{\frac{E_b}{N_0}}\right) \tag{4.9}$$

According to what has been said, the following conclusions can be taken, also presenting the value for Lfs.

For d = 1 500 km:

- Lfs = 163.75 dB
- SNR_{dB} = -6.09 dB
- Chip $Gain_{dB}$ = 17.99 dB
- CNR_{dB} = 11.90 dB
- $P_{QPSK} = 1.07 \times 10^{-6}$

For d = 500 km:

- Lfs = 154.2 dB
- SNR_{dB} = 3.46 dB
- Chip $Gain_{dB}$ = 17.99 dB
- CNR_{dB} = 21.45 dB
- $P_{QPSK} = 5.76 \times 10^{-11}$

As expected, the free space losses decrease with the approximation between antennas. Also, both SNR and CNR take higher values with that approximation, allowing that the probability of error due to the QPSK modulation is very small for 500 km although it still exists. It is also clear that the worst probability for 1 500 km is still acceptable in terms of the integrity of the data received.

The next step is to calculate the error when deciphering the chip delay.

In order to do so, one must understand that the transmission (y_k) is the sum of the real signal (S_k) and the added noise (η_k):

$$y_k = S_k + \eta_k \tag{4.10}$$

The error is sought by multiplying by the PRBS and adding two parcels:

- The signal with a peak of 63 and -1 off-peak;
- Noise as a Gaussian variable with standard deviation $\sqrt{63}\sigma_\eta$, where $\sigma_\eta = 1/\sqrt{SNR}$.

For the normal distribution it is used the approximation provided in [20].
In this particular case,

$$1 - \Phi\left(\frac{62}{(\sqrt{63})\sigma_\eta}\right) \approx 1 - \Phi\left(\sqrt{63}\, SNR\right) \tag{4.11}$$

By adjusting the respective parameters that correspond to each distance, the following results for the probability of error due to the chip delay (P_{CD}). For:

- d = 1 500 km: $P_{CD} = 1.31 \times 10^{-5}$
- d = 500 km: $P_{CD} \approx 0$

At the distance of 1 500 km there still is a probability of error in reception due to faults when decoding chip delay, what virtually doesn't exist for the case of transmission at 500 km.

The last item is the contribution of 2 PN codes in the transmission.

Considering the 26 chip delays of the 2 PN sequences, the probability of error due to the PN codes (P_{PN}), for each distance is the result of the operation 26 x P_{CD}:

- d = 1 500 km: $P_{PN} = 3.39 \times 10^{-4}$
- d = 500 km: $P_{PN} = 0$

Obviously for 500 km it is virtually nil. For 1 500 km, a slight increase is detected.

All of these 3 items (QPSK, chip delay and PN codes) have its contribution for the total BER. Once they represent probabilities that low and independent, they may be added.

$$BER = P_{QPSK} + P_{CD} + P_{PN} \tag{4.12}$$

Once all these probabilities are independent, total BER results from their addition. Total BER for each distance is:

- d = 1 500 km: $BER = 3.53 \times 10^{-4}$
- d = 500 km: $BER = 5.76 \times 10^{-11}$

Some conclusions may be taken from here.

At 1 500 km arises the worst case for the integrity of transmission. The bit sequences and the chip delay become the dominant origin for errors, even if the errors from modulation are not negligible.

At 500 km, there is a very low probability of error due to the QPSK modulation. Both probability of errors due to PN codes and chip delay are virtually nil, what makes that P_{QPSK} is the dominant possible error source at this distance.

Since the calculations are being performed for the worst case, one can conclude that the BER for this satellite link is 3.53×10^{-4}.

4.6 – Summary

This chapter provides a detailed analysis of the frame structure and the transmission of data of VORSat.

It has been defined the length and duration of each frame, and therefore of the full transmission. All data have been encapsulated in the available space in frames in order to maximize the efficiency of transmission.

It has also been calculated the BER of the transmission.

Chapter 5

Tests and Results

In order to prove the feasibility of attitude determination of VORSat and to verify all the calculated data of this document, several tests have been made in the anechoic chamber of FEUP.

5.1 – Equipment and Setup

The necessary equipment has been:

- 2 I/Q Modulators;
- Radio Receiver AOR5000;
- Sound Card Creative;
- 1 rotator;
- 3 computers;
- 3 antennas.

All tests have been performed in the anechoic chamber of FEUP, so that external influence could not interfere with the results. The setup obeys to figure 5.1.

One computer had a running code to generate a random wave. A sound card generates the sequences and splits, in stereo, the signal for 2 modulators. I/Q Modulator 2 is enslaved to I/Q Modulator 1 so that both can receive the signal at the same time. Each modulator sends the QPSK signal for its respective antenna. There is a rotor controlled by a computer, so that rotation of transmitting antennas can be accomplished. In the reception, an antenna is connected to a radio receiver. A computer will then process the received signal.

So that the simulation can contain 3 transmissions, corresponding to 3 antennas, I/Q Modulator 1 and Tx Antenna 1 transmit twice in each burst. Antennas were calibrated to a frequency of 2.398 GHz and were distanced 9 cm from each other (figures 5.2 and 5.3), which is quite similar to what they should be in VORSat final assembly.

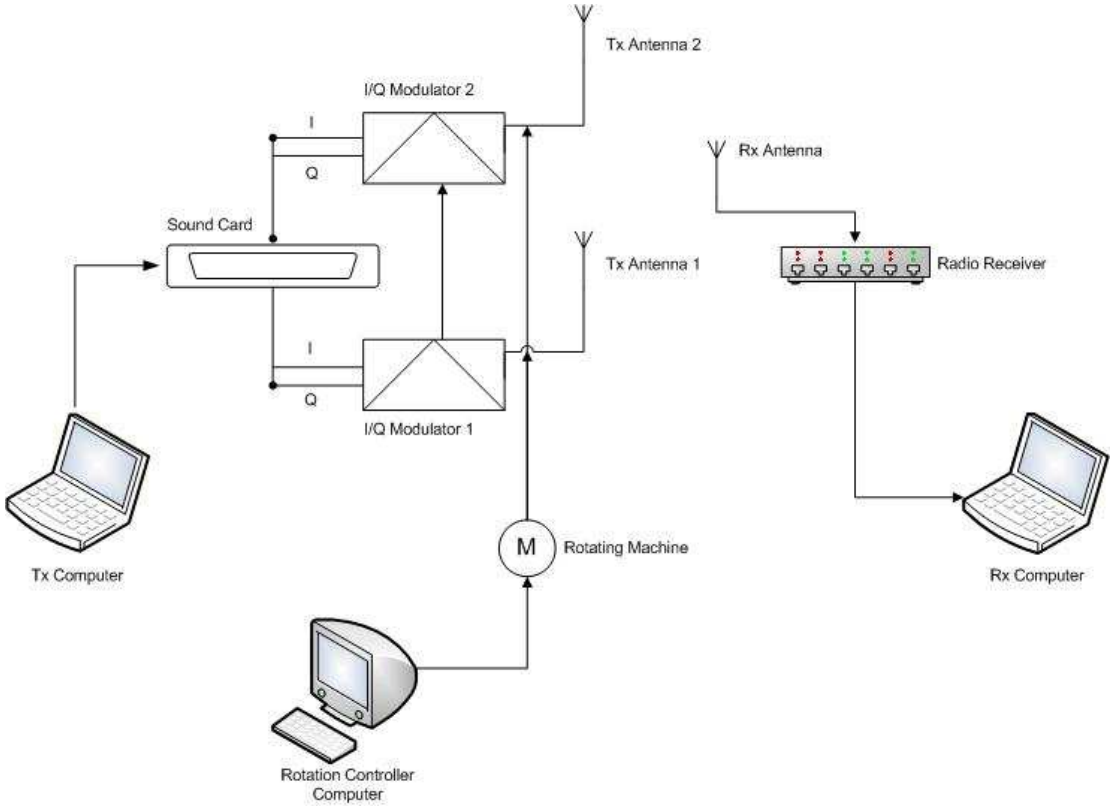

Figure 5.1 – Experiment Setup.

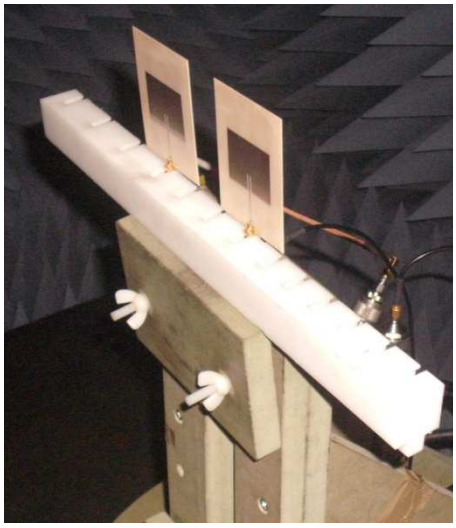

Figure 5.2 – Tx Antennas Setup.

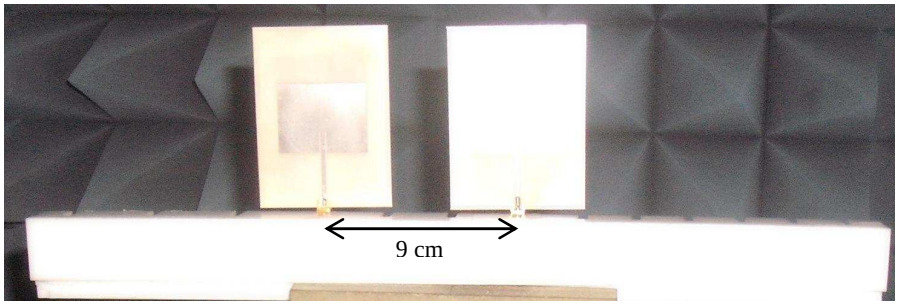

Figure 5.3 – Antennas are distanced 9 cm from each other.

5.2 – Procedures

The experiment had 4 different milestones:

1. To prove the concept of the usage of PN sequences is possible;
2. To demonstrate the feasibility of measuring a satellite's attitude from the ground;
3. To observe signal's behaviour for different distances;
4. To demonstrate that for the worst case scenario it is still possible to detect signal with the available power of 0.5 W.

In order to do so, many steps had to be taken.

First of all, it has been necessary to verify that I and Q of modulators have the correct phases. This is very important, because it can cause errors in detection.

Figures 5.4 and 5.5 show tests performed for I/Q Modulator 1 and for I/Q Modulator 2, respectively. Table 5.1 illustrates the correction of the performed tests. Even though the precision of the measurement is not great, the phase difference is approximately 0.25 cycles between all phases, as it is supposed to be.

Table 5.1 – Phase Differences in I/Q Modulators 1 and 2.

I/Q MODULATOR 1		
Signal Phase		**Cycles**
-0,1438	-0,4014	**0,26**
0,0885	-0,1438	**0,23**
0,3511	0,0885	**0,26**
-0,4014	0,3511	**0,25**

I/Q MODULATOR 2		
Signal Phase		**Cycles**
-0,2120	-0,4479	**0,24**
0,0359	-0,2120	**0,25**
0,2991	0,0359	**0,26**
-0,4479	0,2991	**0,25**

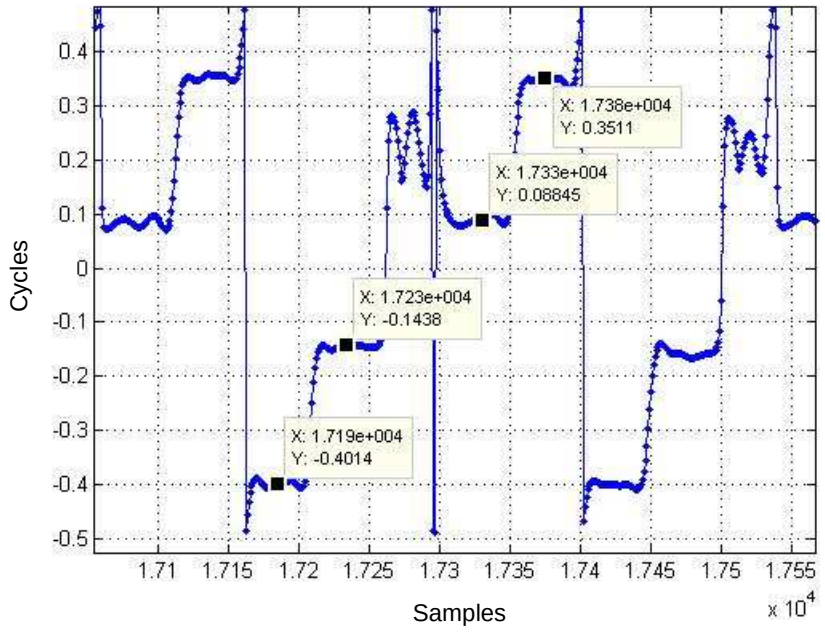

Figure 5.4 – Test for I/Q phases in I/Q Modulator 1.

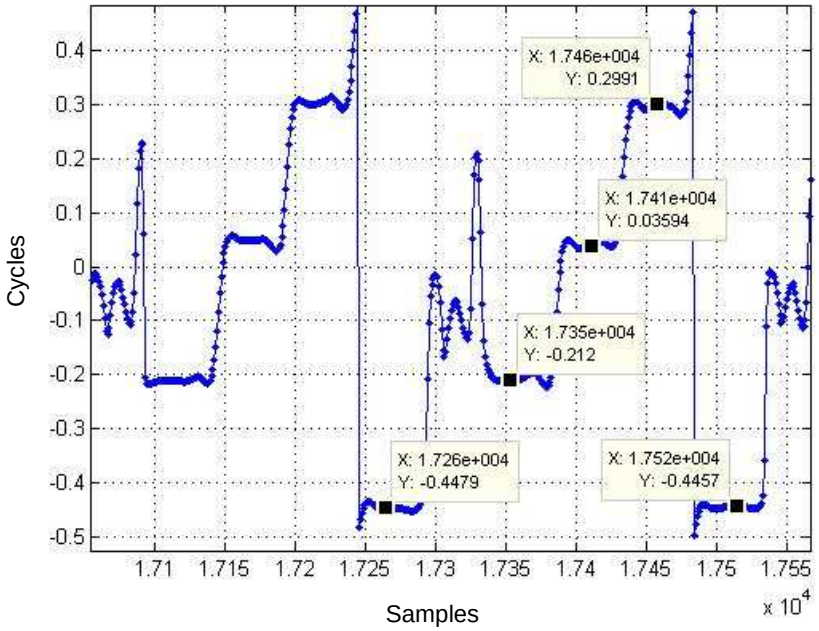

Figure 5.5 – Test for I/Q phases in I/Q Modulator 2.

To prove that the usage of PN sequences is possible, a first test has been performed.

The transmitting antennas remained on hold.

It is possible to observe the QPSK modulation in the received signal, using Audacity software (figure 5.6).

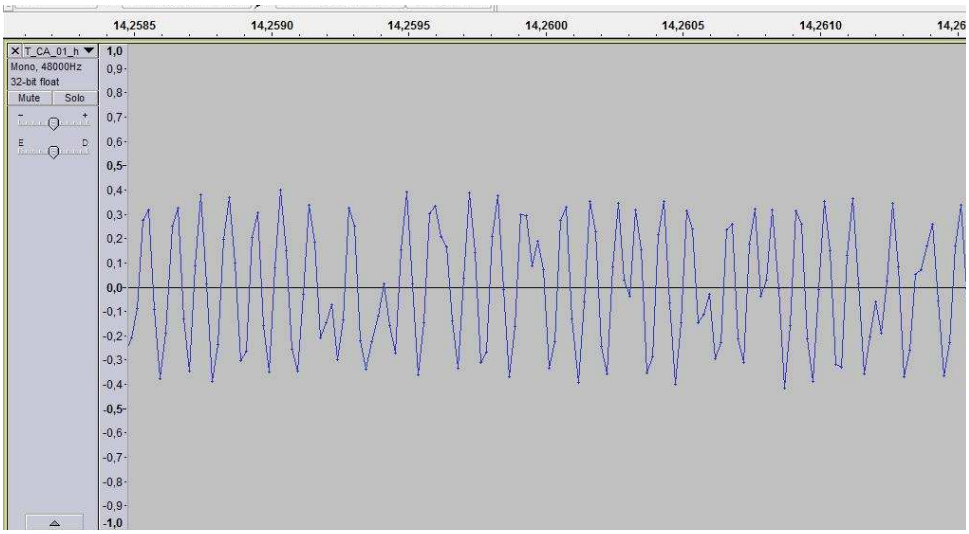

Figure 5.6 – QPSK in the received signal.

Also with Audacity, it becomes clear the central frequency of 10 kHz in baseband in the analysis of the respective spectrogram (figure 5.7).

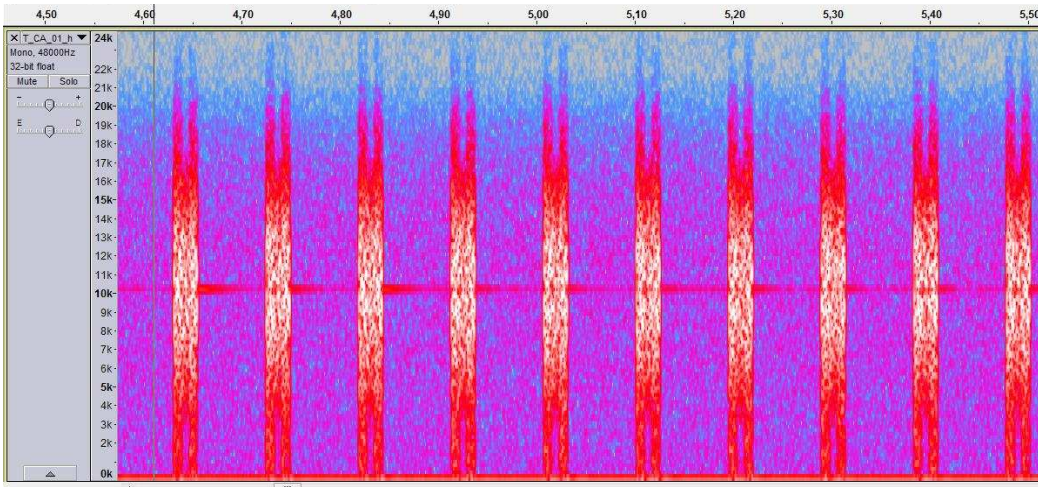

Figure 5.7 – Spectrogram of the first test.

In figure 5.8 it is shown what became clear in chapter 3, that the time lapse between the beginnings of each burst is 94.5 msec.

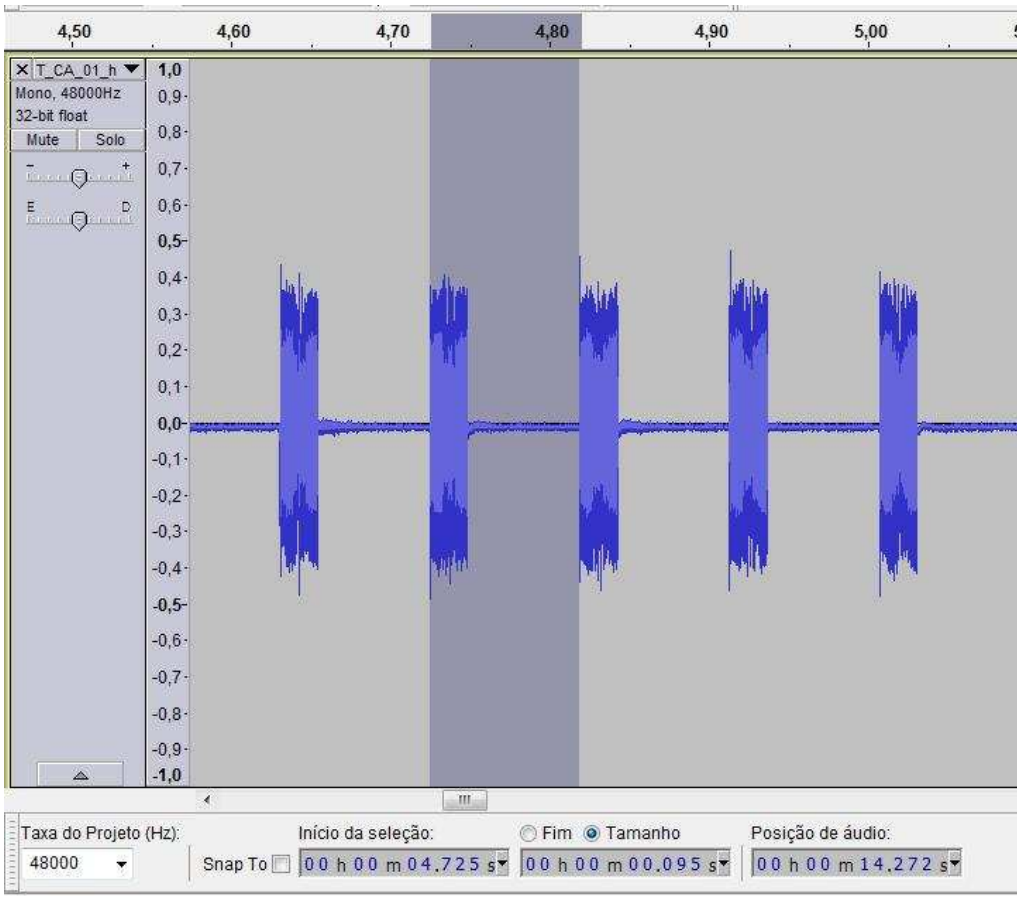

Figure 5.8 – Time in each face is visited.

Figure 5.9 shows 48 000 samples. Each burst corresponds to the transmission of one face and has 1134 samples.

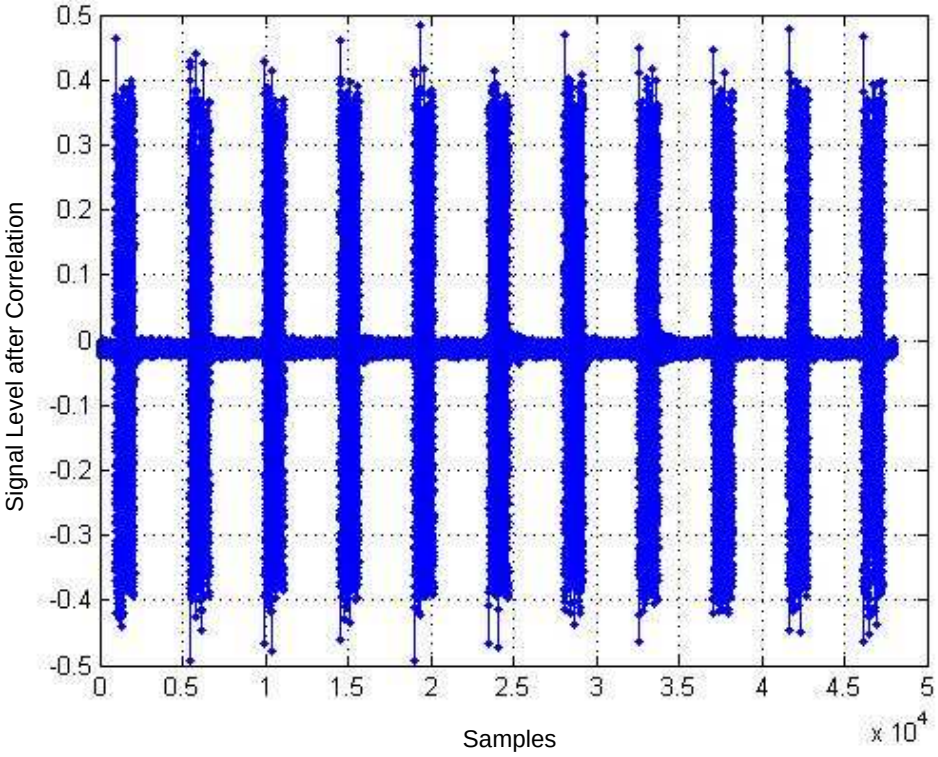

Figure 5.9 – Transmission of 1 sec, with 48 000 samples.

Zooming one burst it is possible to distinguish the transmission that corresponds to antennas 1, 2 and 3, separately (figure 5.10). Each antenna has 378 samples. It is verifiable that antenna 2 transmits in lower power..

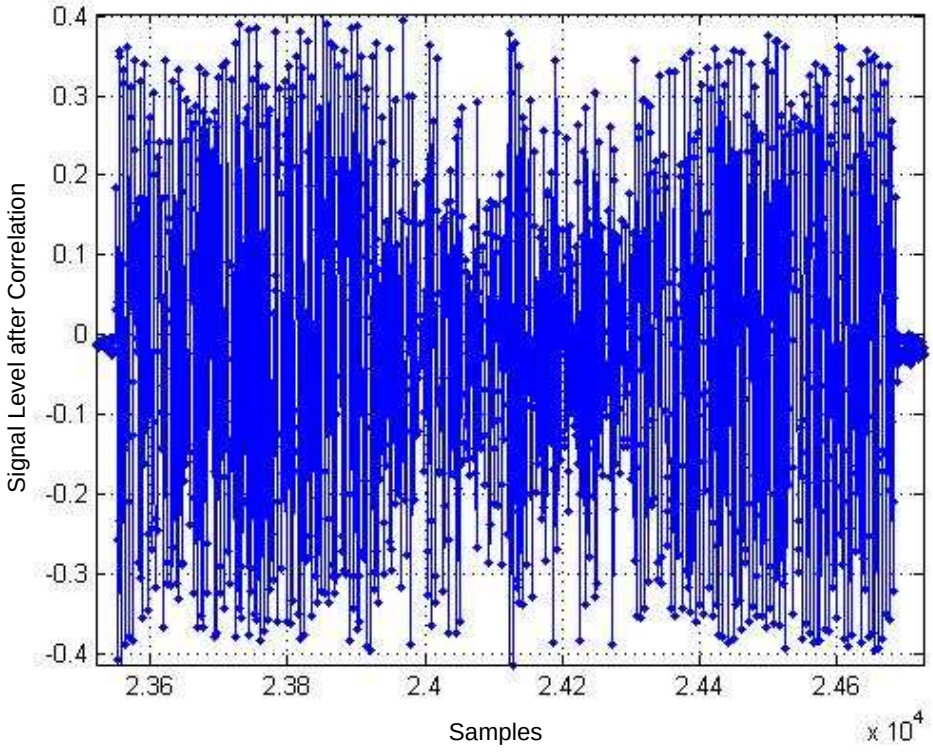

Figure 5.10 – Transmission of 3 antennas.

With more zoom it is possible to distinguish 3 peaks in each burst. This is the result of the peak definition technique developed and explained during chapter 3. These peaks correspond to one antenna each. Again, it is possible to verify that antenna 2 transmits in lower power (figure 5.11). This proves that the usage of PN sequences is valid. It also becomes clear that it is possible to achieve good peaks according to the work performed in chapter 3.

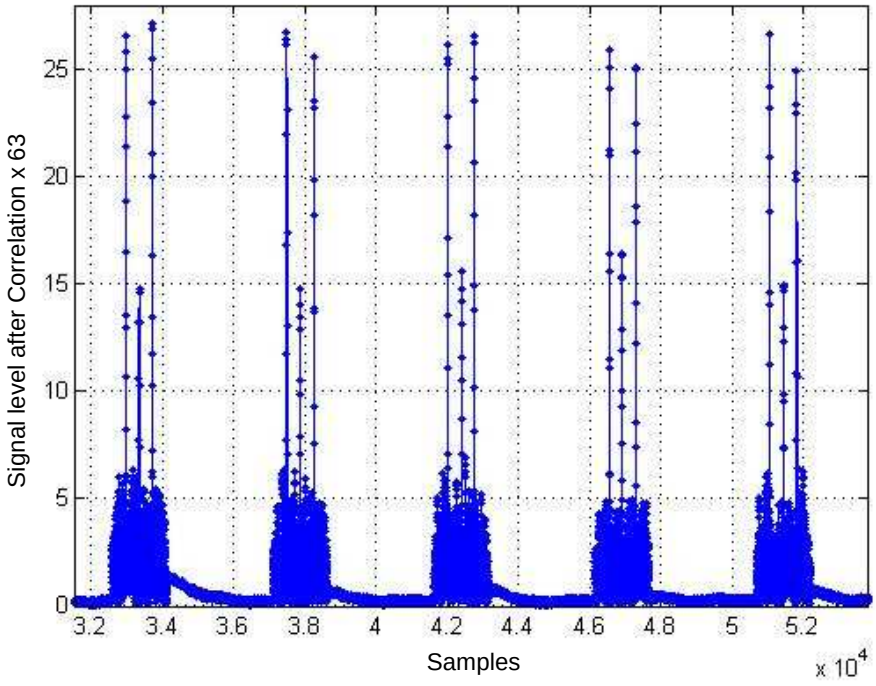

Figure 5.11 – Peak definition.

In the second test, transmitting antennas 1 and 2 have been rotated. First, 20 degrees to the right, then 40 degrees to the left, and then 20 degrees to the right so that the final position can be the initial position.

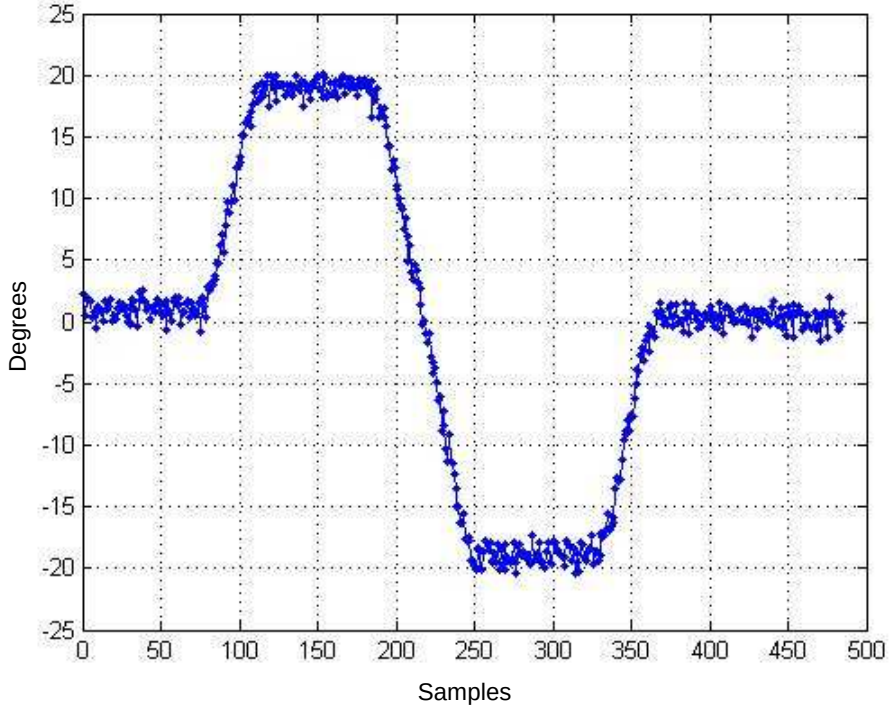

Figure 5.12 – Rotation of the antennas.

Figure 5.12 allows a more clear observation of the rotation applied to the antennas.

So that the predictable error can be calculated or, in other words, the precision of the measurement of the attitude can be determined, the standard deviation and the mean value of both extremes have been calculated.

There have been created 7 time intervals, divided according to the rotation of the antennas:

- $\Delta t_0 \rightarrow$ initial position;
- $\Delta t_1 \rightarrow$ during rotation of 20º;
- $\Delta t_2 \rightarrow$ stopped at 20º;
- $\Delta t_3 \rightarrow$ during rotation of -40º;
- $\Delta t_4 \rightarrow$ stopped at -20º;
- $\Delta t_5 \rightarrow$ during rotation of 20º:
- $\Delta t_6 \rightarrow$ final position (the same as initial position).

For calculations for Δt_1, Δt_3 and Δt_5 it has been necessary to perform the interpolation of the points, as illustrated in figure 5.13.

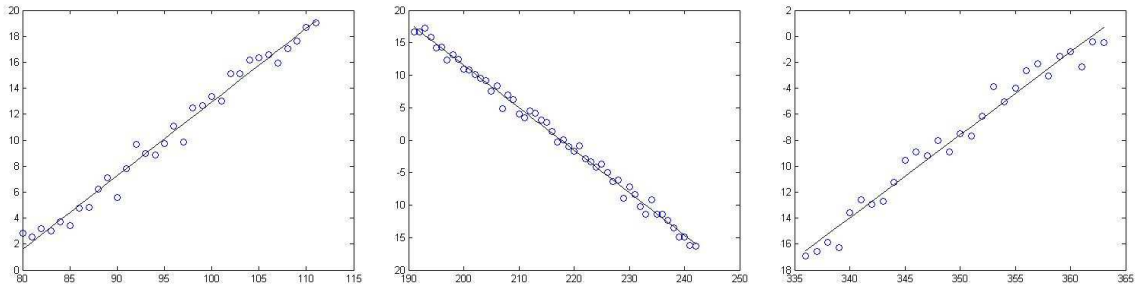

Figure 5.13 – Interpolation of data during rotation.

From the collected data, table 5.2 can be elaborated. It is important to refer that close to the shifts in rotation, when it stopped after being in movement and vice-versa, some imprecisions occur, quite probably due to the effect of inertia. This effect is more significant when passing from movement to stop. Also, when the engine starts, it suffers an acceleration that influences the measurements. Ergo, samples of data near the transitions were ignored.

Table 5.2 – Error and standard deviation for the several time intervals of the test of rotation of antennas.

TIME INTERVAL	MAX	MIN	MEAN	MAX ERR	STD
Δt0	2,5452	-0,7144	1,0449	1,7593	0,7005
Δt1	N/A	N/A	N/A	2,3329	0,7190
Δt2	20,0795	17,4062	19,0437	1,6375	0,6057
Δt3	N/A	N/A	N/A	2,1015	0,7771
Δt4	-17,2675	-20,3783	-18,9216	1,6541	0,7568
Δt5	N/A	N/A	N/A	2,39	0,8761
Δt6	1,9028	-1,5887	0,3117	1,9004	0,7012

As expected, when the antennas are stopped (Δt_0, Δt_2, Δt_4 and Δt_6), errors in detection are smaller. Even though there may be errors of nearly 1.9º, the standard deviation is approximately 0.75º, which is a very good result.

For moments of rotation (Δt_1, Δt_3 and Δt_5), maximum error detected is slightly higher, taking the value of 2.39º. However, the standard deviation is 0.8761, what allows, still, for a good accuracy in attitude determination.

The third test simulated the transmission of VORSat when it is distanced of 500 km of the ground station. It is possible to verify it is easy to distinguish the transmission of each face, even if the difference between the peaks and noise is smaller (figure 5.14).

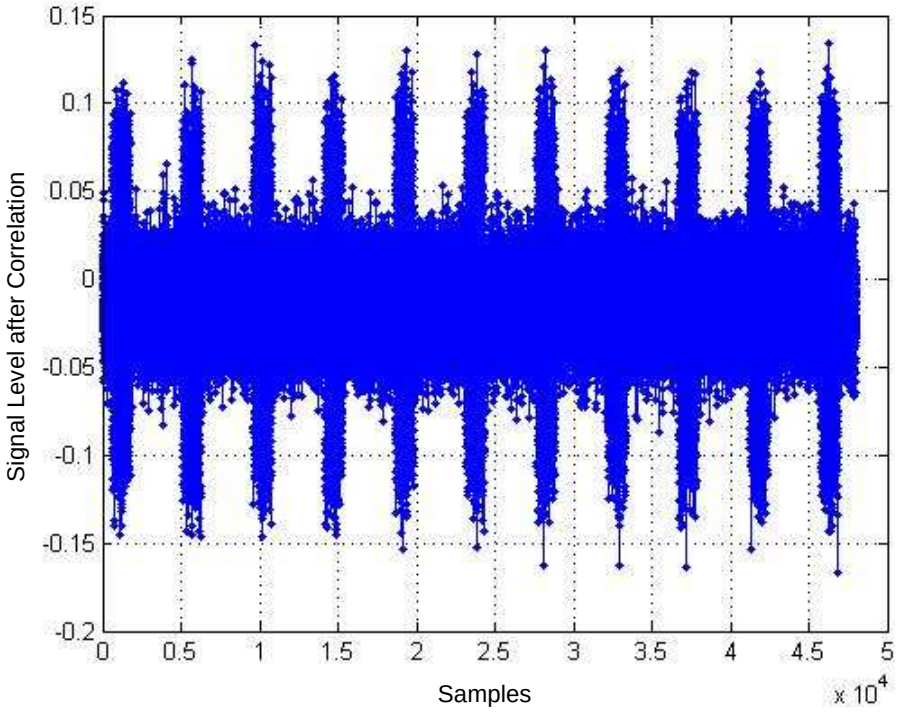

Figure 5.14 – Transmission for 500 km.

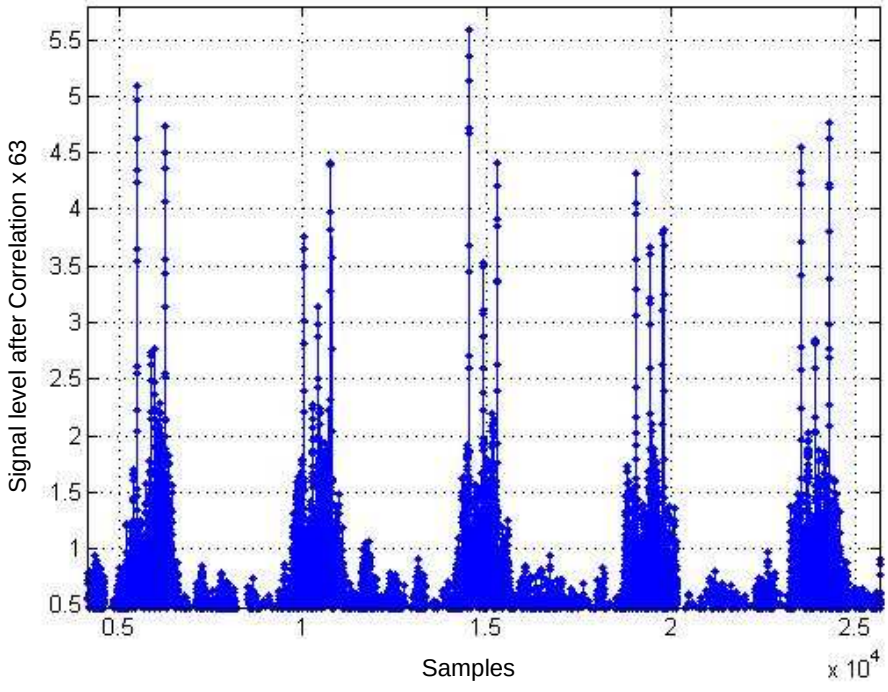

Figure 5.15 – Peak Definition at 500 km.

The same analysis performed before to verify the existence of defined peaks is repeated for this case. Sharp peaks are still visible and confirm the possibility of detection of a transmission at this distance (figure 5.15).

The last test sought for the confirmation of the possibility of good detection of signals from VORSat. That implied the worst case scenario of a transmission at an elevation angle of $\theta = 5^{o}$, what happens at a distance of 1 500 km. In order to do so, calculations to simulate increased losses due to distance had to be made.

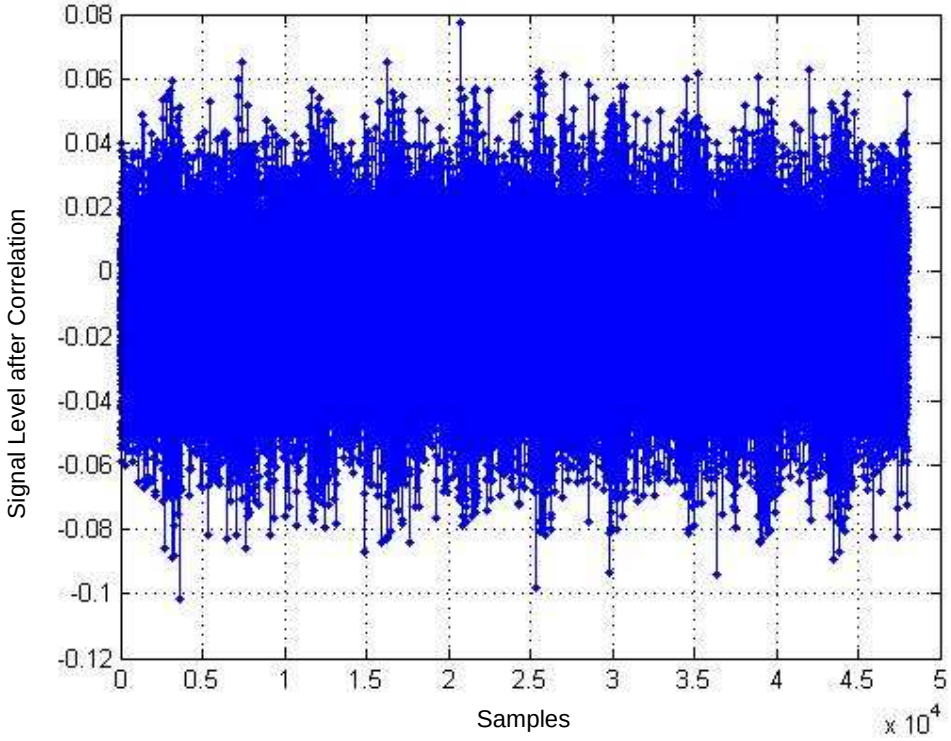

Figure 5.16 – Transmission for 1 500 km.

Figure 5.16 shows that the distinction between transmission and noise is feeble, but it is possible to be detected. A further analysis in order to get good peak definition shows that transmission at 1 500 km distance is possible (figure 5.17).

With this test becomes clear that communication between VORSat and the ground is possible for all possible distances.

Seeing this issue from another standpoint, figure 5.18 illustrates the frequency spectrum of the transmission at 500 km. This plot allows the identification of the frequencies received by the Rx antenna. With the peak near 10 kHz, it is possible to observe that in the reception all the reception is quite within the audio band.

It is possible to verify that the signal definition becomes fainter with the increase of the distance. Comparing both transmissions, it is obvious the loss of the peak that exists for 500 km. However, for 1 500 km, it can still be distinguishable the peak around 10 000 Hz, what confirms what has been proved before.

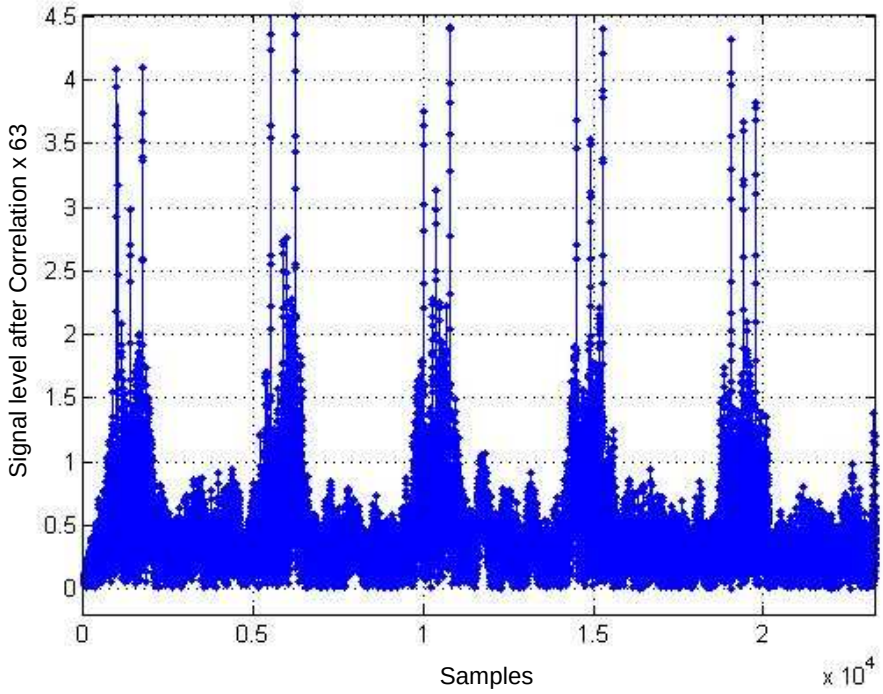

Figure 5.17 – Peak Definition at 1 500 km.

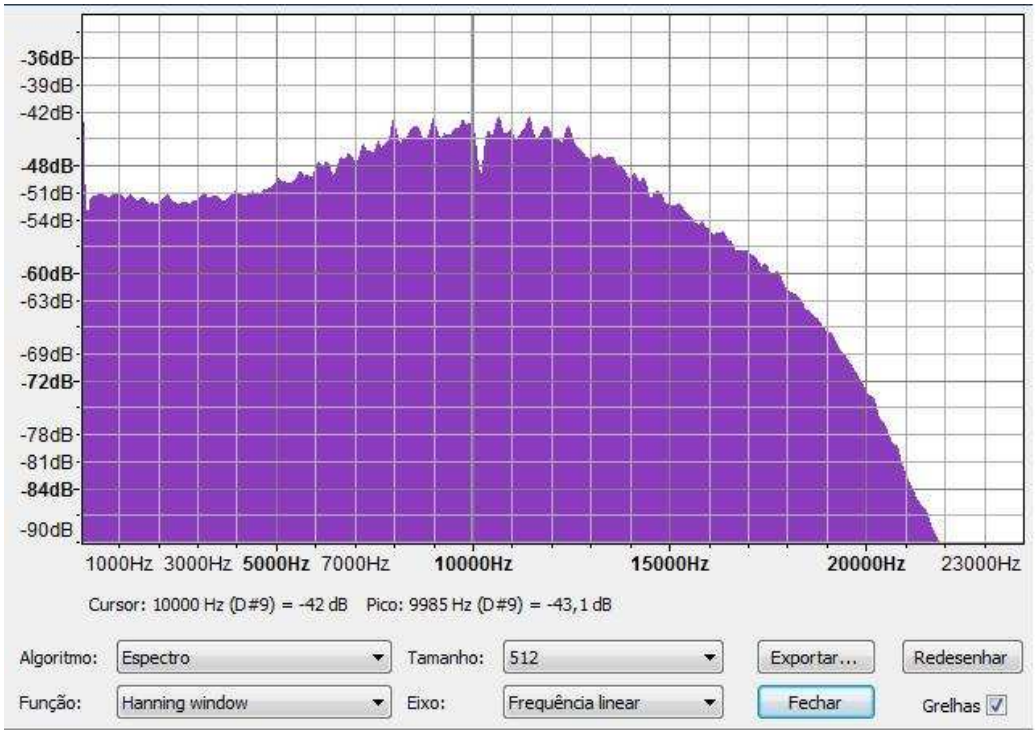

Figure 5.18 – Frequency Spectrum at the Reception.

In order to perform the mentioned tests of transmissions at different distances, in this case of 500 km and 1 500 km, some simple calculations had to be done.

The transmitted power had to be decreased so that the increased free space losses that higher distances imply could be properly compensated.

First, it has been determined the free space loss of both distances relatively to the real distance of 4 m.

$$20\log_{10}(1500km/4) = 111.48\ dB$$

$$20\log_{10}(500km/4) = 101.94\ dB$$

It is known that, obviously for both cases, G_R = 34.72 dB and $G_T \approx 4$ dB. Calculations for the Tx Antennas are being conducted so that they may reach at the least 4.5 dB, but it is used here a conservative value. It is important to leave the reminder that the Rx Antenna will be a parabolic dish antenna and the Tx Antenna will be patch antennas.

Additional losses are calculated:

$$For\ 1500\ km:\ -111.48 + 34.72 - 4 = 80.76\ dB$$

$$For\ 500\ km:\ -101.94 + 34.72 - 4 = 71.22\ dB$$

The real transmission power of 500 mW is converted in decibels. It is a common figure for both cases.

$$10\log_{10}(500) = 26.99\ dBm = -3.01\ dB$$

The power can then be calculated as:

$$For\ 1500\ km:\ -3.01 - 80.76 = -83.77\ dB$$

$$For\ 500\ km:\ -3.01 - 71.22 = -74.23\ dB$$

5.3 – Conclusions

All 4 objectives of the tests have been succeeded.

The first was to prove the feasibility of using PN sequences in this specific case. The search for a better peak definition, has explained in chapter 3, has proven to be of great utility.

Skipping the second objective, it has also been demonstrated that transmission from 1 500 km, the worst case possible, is possible. The comparison has been made with a shorter transmission and the increased losses are unambiguous. However, it is still possible to detect signal sent from VORSat at the distance of 1 500 km with the available power of 0.5 W.

The second objective, the heart of this dissertation, is also a surpassed milestone. It became clear that is possible to determine the attitude of VORSat through the receiving signals from its antennas. There are some issues that need to be taken into account so that the results may be improved and the still existing errors may be corrected, but the concept has been proved as feasible and possible.

5.4 – Summary

Chapter 5 is fully dedicated to the experiment conducted under this dissertation. First, the necessary equipment and the setup were described. The objectives of these tests were mentioned and all the most relevant steps have been explained in detail, so that it can be possible to keep up with the experiment.

As mentioned before, all goals have been accomplished.

Chapter 6

Conclusions

This chapter is dedicated to a general overview and to the conclusions of all the performed work. Some topics for future work are also outlined, in order to accomplish better results in the forthcoming months.

6.1 – Summary of the Performed Work

The full definition of the protocol of communications for VORSat was the goal of this dissertation. This encompassed several other partial objectives that had to be accomplished so that the protocol could be defined.

First of all, the main guidelines were defined and the partial objectives were outlined.

Next step was to elaborate a deep study about satellite transmission losses so that the link budget could be properly calculated. In these calculations, some specifications of VORSat have also been used, such as the frequency for the determination of free space losses and attenuation. The characteristics of LEO satellites also define an important feature. Only knowing that LEO satellites have a limited time of passage and that they appear low in the horizon, it is possible to calculate the maximum distance. In parallel, system noise had to be calculated because it is imperious to be in possession of the system noise temperature to calculate other parameters such as the figure of merit of the receiving antenna. Other important parameter could only be calculated later, because other parameters such as the bit rate and BER were not determined yet.

While link budget was calculated, a review about pseudonoise sequences and their characteristics was conducted, with the option of performing Spread Spectrum falling on Direct Sequence through Gold Sequences.

The transmission scheme was defined according to the number of available Gold sequences generated by preferred pairs. Also, the distribution of the sequences by the satellites had to obey to criteria of correlation. The number of chip delays to use from each sequence was the next step. It has been decided to use 26 from a total of 63 possible. Depending on the modulation to use, on the transmission scheme and on the number of sequences, the number of possible

combinations and therefore the number of information bits can be determined. That will influence decisively the bit rate and the number of bits per word.

Meanwhile, strategies to achieve a good peak definition have been developed. The result has been quite satisfactory.

Message structure could only be defined after a search about the TLE of a satellite. Only then it became possible to go through to message definition. The number of bits per word was an essential data, because it is the basis for all the work to be done in this field. Frame composition and word structure have been defined and link budget completed at this point.

Afterwards, tests have been made in order to confirm the defined objectives.

6.2 – Accomplishments

This dissertation had some initial objectives.

The definition of the protocol of communications of VORSat has been done. It is still necessary to perform some improvements, but the base structure already exists.

Another goal was to define the transmission scheme of the antennas it has been achieved.

It became also clear that it is possible to use PN sequences in satellite communications.

One great challenge that was overcome was to prove the detectability of signals from VORSat at its maximum distance possible. Tests showed that in despite of the quality of the signal in reception is faint, signal can be detected.

However, the greatest challenge was to prove the feasibility of attitude determination. Tests performed in the anechoic chamber revealed positive results in this field once the rotation of antennas relatively to a fixed one can be measured. Not only it is possible to determine attitude of a satellite in space from the ground, but also the accuracy is quite satisfactory.

6.3 – Future Work

Regardless of the results accomplished in this dissertation, several aspects justify an attention and future review, in order to achieve better results for the whole project.

1. Instead of Gold sequences, the small set of Kasami can be a valid option. It presents the advantage of lower crosscorrelation, quite close to the Welch lower bound. In its favour, the small set of Kasami also present the possibility of 8 sequences. That would increase the number of combinations and therefore the number of information bits that could be used. More bits per word could be used at a higher bit rate;
2. It could be studied the possibility of sending the difference between a new value of the TLE and the previous one, so that computation of the collected data on the ground could be performed afterwards. It could represent a gain of bits;
3. Synchronism has been slightly approached during this dissertation. A deeper analysis is mandatory;
4. BER could be improved if FEC was implemented. The possibility of introducing bits for error correction is a possible step to take;
5. Tests can be completed with measurements for more angles. The concept of attitude determination has been proven, but more exact values can be achieved with full rotation

of antennas, in order to determine the exact moment when signal from one face outperforms the other signal.

Even though several conclusions can be taken from this work, it is clear that this is a project with continuity, far from being completed with the development of this dissertation.

References

[1] California Polytechnic State University. *CubeSat Design Specification*. 2009

[2] QB50 web page. URL: *https://www.vki.ac.be/QB50/project.php*

[3] A. Oliveira, S. Cunha. *GAMA-Sat – Short Description and Highlights*. 2011

[4] T. Pratt, C. Bostian. *Satellite Communications*. 1986

[5] Software: *Orbitron*

[6] M. Leitão. *Sistemas de Transmissão*.

[7] CubeSat web page. URL: *http://www.cubesat.org*

[8] B. Klofas, J. Anderson. *A Survey of CubeSat Communication Systems*. 2008

[9] Space Track web page. URL: *https://www.space-track.org*

[10] G. Maral, M. Bousquet. *Satellite Communications Systems – Systems, Techniques and Technologies*, 5th edition. 2009

[11] D. Roddy. *Satellite Communications*, 3rd edition. 2001

[12] Software: *Satmaster Pro*

[13] *http://www.phys.hawaii.edu/~anita/new/papers/militaryHandbook/polariza.pdf*

[14] R. L. Freeman. *Reference Manual for Telecommunications Engineering*, 2nd edition. 1994

[15] J. M. de Naer. *Spread Spectrum*. 1999

[16] *http://webhome.idirect.com/~griffith/tdoafig1.gif*

[17] S. Ghuffar. *Design and Implementation of Attitude Determination Algorithm for the Cubesat UWE-3*. 2009

[18] S. Lan, J. Lin, D. Ye, X. Cao, G. Xu. *Attitude Measurement for Small Satellite Using Multiple-Plane X-Ray Pulsars Vector Observation* – The 4S Symposium. 2010

[19] *http://www.physik.uni-wuerzburg.de/~praktiku/Anleitung/Fremde/ANO14.pdf*

[20] K. M. Aludaat and M. T. Alodat. *A Note on Approximating the Normal Distribution Function. Applied Mathematical Sciences*, Vol. 2, 2008

[21] Recommendation ITU-R P.676-8. *Attenuation by Atmospheric Gases*. 2009